Optimization of CUBIC tissue clearing and cellular labeling methods applied to the cerebral cortex of rodents

Deepthi David Thommana

Master of Engineering

Department of Biological and Biomedical Engineering

McGill University

Montreal, Quebec, Canada

December 2021

A thesis submitted to the Faulty of Graduate Studies and Research in partial fulfillment of the degree of Master of Engineering.

TABLE OF CONTENTS

LIST OF TABLES

LIST OF FIGURES

Abstract (English)

The development of tissue clearing and whole-brain imaging with single-cell resolution opens the way for comprehensive analysis of neuronal circuits. Aqueous-based tissue clearing protocols have been improved to generate translucent samples that can be further processed with histology methods and/or labeled with immunohistochemistry antibodies. The two major protocols - CUBIC and CLARITY - have achieved multi-label imaging of proteins in sub-cellular structures including axons and dendritic spines, by labeling with fluorescent or immunohistochemical stains in adult brain samples. These protocols offer a cost-effective and reliable method to acquire three-dimensional structural details in rodent models with multi-spectral high-resolution microscopy. Here we optimized the CUBIC protocol for labeling cell bodies of the cerebral cortex. We varied (1) the post-fixation duration, (2) the thickness of the brain coronal slab used for clearing and labeling, (3) the temperature during the de-lipidation stage, and (4) the dilution of the staining solution. We also tested the effect of the animal's age on the clearing process. Lastly, we performed clearing and labeling with X-Clarity, for comparison with the CUBIC methods. We imaged the samples using an Opera Phenix confocal microscope that enables efficient comparison of multiple samples imaged simultaneously. We verified that thicker samples take longer to clear. We report that with increasing post-fixation duration, it takes longer to delipidate the brains tissue. However, adequate post-fixation is necessary for preventing fragility of the sample, and delipidation at 37°C is significantly shorter than at room temperature. We therefore recommend post-fixation for 24 hours and delipidation at 37°C. We quantified the signal to background ratio of fluorescent Nissl, and show that it increases with increasing concentration. Whereas X-CLARITY is compatible with labeling with both fluorescent Nissl and MAP2, CUBIC labeling with MAP2 was restricted to the edge of the sample. The protocol we optimized can be the basis for future studies that use CUBIC for labeling the micro-structure of the cerebral cortex.

Abstract (French)

Le développement de techniques de nettoyage des tissus et de l'imagerie médicale du cerveau entier avec une résolution cellulaire, ouvrent la voie à une analyse exhaustive des circuits neuronaux. Les protocoles d'épuration à base aqueuse des tissus ont été améliorés pour générer des échantillons translucides qui peuvent ensuite être traités avec des méthodes d'histologie et/ou marqués avec des anticorps d'immunohistochimie. Les deux protocoles majeurs - CUBIC et CLARITY - ont permis d'obtenir une imagerie multicolore des protéines dans les structures sous-cellulaires dont les axones et épines dendritiques, avec des marqueurs fluorochromes ou immunohistochimiques dans des échantillons de cerveau adulte. Ces protocoles offrent une méthode rentable et fiable pour acquérir des détails structurels en trois dimensions dans des modèles animaux murins en utilisant une microscopie multispectrale à haute résolution. Ici, nous avons optimisé le protocole CUBIC pour le marquage des corps cellulaires du cortex cérébral. Nous avons fait varier (1) la durée post-fixation, (2) l'épaisseur de la tranche de cortex cérébral utilisée pendant le nettoyage et le marquage, (3) la température pendant la phase de délipidation et (4) la dilution de la solution de coloration. Nous avons également testé l'effet de l'âge de l'animal sur le processus de nettoyage. Enfin, nous avons effectué un nettoyage et marquage avec X-Clarity, à des fins de comparaison avec les méthodes CUBIC. Nous avons visualisé les échantillons à l'aide d'un microscope confocal Opera Phenix qui permet une comparaison efficace de plusieurs échantillons en même temps. Nous avons vérifié que les échantillons plus épais mettent plus de temps à devenir transparents. Nous rapportons aussi que l'accroissement de la durée de post-fixation du tissu augmente le temps nécessaire pour délipider les tissus cérébraux. Cependant, une post-fixation adéquate est nécessaire pour prévenir la fragilité de l'échantillon, et la délipidation accomplie à 37°C est significativement plus rapide que celle faite à la température ambiante. Nous préconisons donc une post-fixation de 24h et une délipidation à 37°C. Nous avons aussi quantifié le rapport signal/bruit de fond de l'histologie fluorescente de Nissl, et montré qu'il augmente avec la concentration de la solution. Enfin, alors que X-CLARITY est compatible avec la coloration histologique fluorescente de Nissl et MAP2, le marquage CUBIC avec MAP2 a été limité au bord de l'échantillon. Le protocole que nous avons optimisé peut servir de base à de futures études utilisant CUBIC pour marquer la microstructure du cortex cérébral.

ACKNOWLEDGEMENTS

I would like to thank Dr. Mihai Victor Mocanu, Dr. Archita Rajasekharan, and Prof. Amir Shmuel for proofreading this thesis and providing feedback. I would like to thank my friends Maria Matossian and Sethu K Boopathy Jegathambal for their important inputs in image analysis. I thank Dr. Aleksandra Beata Bortel, Barbara Borelli, and Tiago André Antunes David for performing excellent perfusion experiments of rodents which was part of this work. I thank Abby Jia for capturing the images of delipidated rodent brains. I thank Barbara Borelli for hands-on training on microtome and cryostat. I would like to thank Victor Mocanu for his valuable inputs on how to select primary antibody and secondary antibody for immunolabeling of the brain thick slabs and hands-on training for standard IHC using mouse brain thin slices from mounting on microscopic slides to imaging. I would like to thank the ABIF microscope facility and Neuro microscopy core facility. Dr. Anne and Dr. Michael for giving in-person training on Light Sheet Microscopy and Opera Phenix Microscopy respectively. I would like to thank Dr. Robert Funnel for his guidance by serving as the Graduate Program Director. I would like to thank the steadfast support of my husband - Joseph Davis, parents, and family members during my research work. I thank Dr. Amir Shmuel, my academic supervisor, for his support and guidance, teaching me the importance of planning and organization in research.

CONTRIBUTION OF AUTHORS

The candidate (DDT) served as the main researcher for this project. The candidate also performed a thorough review of the literature of aqueous methods in tissue clearing. She optimized the tissue clearing protocols including CUBIC and X-CLARITY - for 2-3 mm thick slabs of rodent brains, to enable the visualization of the brain using high resolution confocal and light-sheet microscopes. The candidate also evaluated the reproducibility of the proposed methods.

Tiago David performed the animal procedures for obtaining the brain samples.

Maria Matossian participated in obtaining part of the data, and advised on microscopy and image analysis procedures.

Dr. Amir Shmuel initiated the research project, advised on how to plan and perform the procedures, evaluated and gave feedback on the results, and edited the thesis manuscript.

CONTRIBUTIONS TO SPECIFIC CHAPTERS

The abstract was written by the candidate (DDT), edited by Dr. Shmuel, and was translated to French by Victor M. Mocanu.

Chapter I was conceptualized and written by the candidate and edited by Dr. Shmuel.

Chapter II – The review of existing methods for tissue clearing using CUBIC and X-CLARITY methods was written by the candidate and edited by Dr. Shmuel.

Chapter III: The description of methodology was written by the candidate and edited by Dr. Shmuel.

Chapter IV: The images and results were analyzed by the candidate. Maria Matossian contributed software for quantitative analysis. Dr. Shmuel commented and edited this chapter.

Chapter V: The discussion was written by the candidate and edited by Dr. Shmuel.

1. CHAPTER I - INTRODUCTION

1.1. Tissue Clearing

The three-dimensional (3D) visualization of intact brains with their inherent complexity is highly desirable in neuroscience (Rocha et al., 2019). The biological tissues are complex with hundreds of millions of cells intertwining locally and projecting to distant regions (Rocha et al., 2019). As the cell is the basic unit of living organisms, tissue-clearing techniques in combination with optical microscopy have attracted attention in recent years, to answer the challenging 3D visualization task. This enables the analysis of various cells concurrently in thick sections ranging from 100 µm to a few centimeters of tissue, besides preserving the molecular and structural information with minimal distortion of the sample (Hao et al., 2018; Susaki et al., 2015; Lee et al., 2016; Ariel, 2017). The focus of the tissue clearing methods is to make a thick sample transparent following a series of chemical processing steps (Ariel, 2017). Scattering of light by the lipids is substantially decreased while keeping the proteins largely intact. Imaging is pursued using fluorescent three-dimensional (3D) microscopy, making it possible to image the interior of the thick sample (Reveles Jensen and Berg, 2017). In this way, the need for mechanical slicing into thin slices, staining each slice separately, and the commonly imprecise 3D reconstruction of the 2D slices can be replaced by staining and imaging thick tissue 3D samples (Rocha et al., 2019).

Most biological samples are non-transparent due to the presence of lipids and proteins in the cell structures and each having different refractive indexes. Hence, transparency is achieved by eliminating, substituting, and modifying these components (Ariel, 2017) which then helps in permitting imaging deep structures within the tissues (Hao et al., 2018). Hence, the de-lipidation and dehydration/hyperhydration steps in tissue-clearing techniques followed by refractive index (RI) matching have a vital role in homogenizing the scattering of light and imaging (Seo, Jinyoung et al., 2016). Tissue clearing techniques preserve the details of composition, structure, and morphology with minimal damage to the biomolecules in the specimens (Hao et al., 2018).

The decision on which tissue-clearing method to use depends on the rapidity, expense, the toxicity of reagents, complexity in implementation, preservation of proteins and incorporated

fluorescence, compatibility with immunohistochemistry (IHC), the critical concentration of primary and secondary antibodies, and so on (Ariel, 2017; Reveles Jensen and Berg, 2017). Finally, the efficiency of the tissue clearing is directly linked with the percentage of transparency achieved by the sample (Reveles Jensen and Berg, 2017). In the transparent sample, the extent of residual lipids residual is unknown (Reveles Jensen and Berg, 2017) but the degree of protein loss can be quantified (Reveles Jensen and Berg, 2017).

The visualization of the entire neuronal network at the resolution of single cells is not achievable with existing macroscopy techniques such as computer tomography, MRI, positron emission tomography, and microscopic techniques. However, it is achievable with the confocal and two-photon microscopy platforms. Practically, the highest resolution is attainable with standard 2D histological sections for macroscopic specimens. But the three-dimensional (3D) reconstruction of tissue from adjacent slices is extremely laborious (Ariel, 2017) and susceptible to errors (Lee et al., 2016). Besides this, the mechanical deformations lead to inaccuracies (Dodt et al., 2007) and complications in drawing mapping reference points (Lee et al., 2016).

Another major challenge arises from the usage of conventional microscopy. In the conventional confocal and single-/multi-photon microscopy, a large area of the cleared sample is illuminated, causing photobleaching of fluorophores (Reveles Jensen and Berg, 2017). For this reason, we must consider using an innovative imaging technology that selectively and sequentially illuminates a single thin plane of the sample using single-photon excitation microscopy (Susaki et al., 2014; Reveles Jensen and Berg, 2017). Major known examples are spinning disc Opera Phenix microscope and the light-sheet fluorescence microscopy which enables obtaining optical sectioning of macroscopic specimens with microscopic resolution (Dodt et al., 2007; Reveles Jensen and Berg, 2017; Du et al., 2018). In addition, these techniques allow substantially faster imaging relative to a confocal microscope, supporting a high rate of data acquisition. For instance, the 'UltraMicroscope' - a variant of light-sheet microscopy where low phototoxicity is one of the highlighted features (LaVision BioTec 2017) allows depth imaging with very low photo-damage and associated bleaching effects (Ultramicroscope II brochure, see the bibliography). It allows fast imaging of the labeled sample which is illuminated in a single plane perpendicularly to the direction of detection

(Ultramicroscope II brochure, see the bibliography) as shown in **Figure 1** (Dodt et al., 2007; Du et al., 2018). Thus, multiple images can be captured and then stitched together to a final image. Moreover, using the UltraMicroscope allows flexibility in using all tissue-clearing protocols, including the 3DISCO (3D Imaging of Solvent Cleared Organs), iDISCO (Immunolabeling-enabled 3D Imaging of Solvent-Cleared Organs), CLARITY, and CUBIC (LaVision BioTec 2017).

The image quality can be optimized for small and large samples. For the large samples, it is recommended to select a high refractive index matching solution and low numerical aperture (NA) illumination. Thus, the combination of tissue-clearing protocols, spinning disc and light sheet technology opens a promising platform to obtain 3D reconstructions of intact specimens by excluding the incorrect results that stem from the mechanical cutting and reconstruction of 2D slices into a 3D structure (LaVision BioTec 2017). Still, two main criteria must be considered in the development of tissue-clearing technique: efficacy and transparency in preserving the fluorescence of proteins, and reproducibility, especially required for comparing multiple samples (Renier et al., 2014; Susaki et al., 2015).

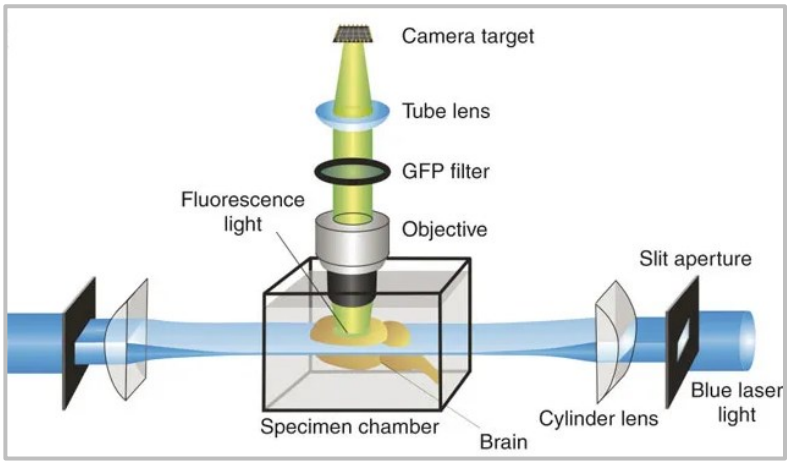

Figure 1. Principle of Ultramicroscope (Image courtesy of (Dodt et al., 2007))

According to the mode of action of the chemicals, tissue-clearing techniques are classified into three major categories, including solvent-based, aqueous-based, and tissue-gel hybridization-based clearing (Seo, Jinyoung et al., 2016) (**Figure 2**). This review mainly focuses on aqueous-

based and hydrogel-embedding-based tissue-clearing techniques for thick slabs, especially in rodent brain samples (Seo, Jinyoung et al., 2016).

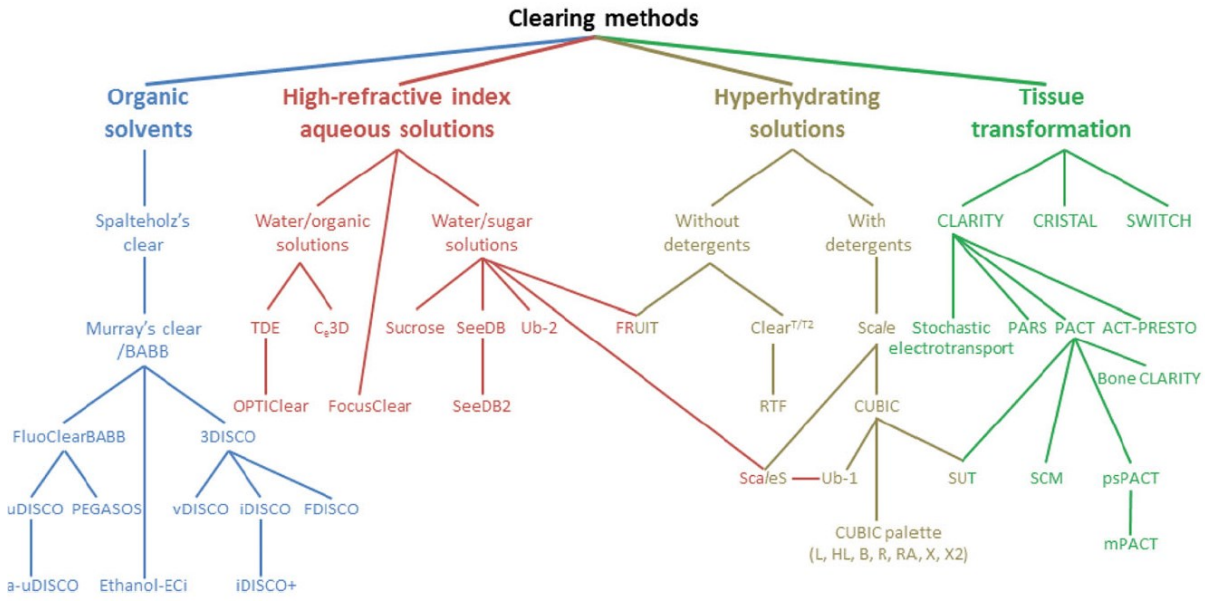

Figure 2. Different protocols used in larger biological tissue clearing
(Image courtesy of (Matryba et al., 2019))

In the second and third chapters, we will elaborately review these two tissue-clearing techniques (chapter 2), conventional histology and IHC labeling of 2D sections (chapter 3) and optimized IHC labeling for cleared thick samples (chapter 3) along with validated antibody specific for cleared-brain tissues. We will also present details on fluorescent nuclear staining for cleared thick brain samples and imaging of cleared samples using a spinning disc Opera Phenix microscope.

In the following section, I present the rationale and objectives of my research.

1.1.1 Rationale

Tissue clearing methods offer the promise of studying neuronal cellular structures and their distribution in large samples of the brain, by reducing light scattering to address the challenges related to the specimen thickness (Pan et al., 2016).

The main aim of my research is to optimize aqueous based tissue clearing methods (CUBIC and CLARITY) and optical microscopy for visualization of somas in 3D volumes of the cerebral cortex.

1.1.2 Objectives

a) Optimize both CUBIC (and, if time permits, X-CLARITY) tissue clearing protocols for application to the mouse brain.
b) Optimize CUBIC tissue clearing protocols for application to the rat brain.
c) Visualize the distribution of neuronal cell Nissl bodies in the cerebral cortex of the rodent brain using nuclear fluorescent Nissl stain.
d) Visualize the distribution of dendritic structures in the cerebral cortex of the rodent brain using IHC with the MAP2 primary antibody, thereby evaluating the compatibility both CUBIC and X-CLARITY for labeling with MAP2.

2. CHAPTER II - REVIEW & BACKGROUND

2.1 Aqueous-based tissue clearing

The main goal of all tissue clearing methods is to make the biological thick samples transparent (Ariel, 2017). The thickness is ranging from 100 µm to centimetres (Ariel, 2017). Traditionally, we slice the thick biological samples into thin sections (4 – 60 µm) and analyze them under the visible wavelength of light using microscopy (Ariel, 2017). This extreme labor-intensive and time-consuming approach can be replaced by tissue clearing methods (Ariel, 2017). These clearing procedures represent an alternative approach that renders thick samples composed of lipids, proteins, and water transparent through a series of chemical treatments (Ariel, 2017). In tissue clearing, the differing refractive index (RI) of biological components are homogenized to achieve transparency (Ariel, 2017). It is critical for obtaining high-quality images with super-resolution microscopy (Tainaka et al., 2018).

In 2014, Susaki, E. A. *et al.*, developed the tissue clearing technique known as CUBIC (*clear, unobstructed brain imaging cocktails and computational analysis*) as an efficient method where brain samples were treated with chemicals comprised of aminoalcohols (Susaki et al., 2014). The CUBIC method facilitates whole-brain 3D imaging of immunohistochemistry (IHC) labeled adult brain samples along with cell-nuclear staining. It enables a single-cell and subcellular structures imaging, including axons and dendritic spines (Susaki et al., 2014), without cutting thin sections of the specimens (Gómez-Gaviro et al., 2017; Tainaka et al., 2018). This is because the light penetration depth is increased by CUBIC tissue clearing (Gómez-Gaviro et al., 2017; Tainaka et al., 2018). In addition, it reduces the time required for primary and secondary antibody labeling of the slabs (Gómez-Gaviro et al., 2017; Tainaka et al., 2018). Positive counterstained nuclei signals were obtained throughout the depth of the z-plane. This tissue transparentizing method is technically simple and does not require expensive equipment (Ariel, 2017).

In 2018, Ueda's lab reported four different CUBIC protocols after chemical profiling of > 1,600 hydrophilic chemicals (Tainaka et al., 2018). They include protocol 1 for mouse organ and body clearing, protocol 2 for tissues including bone clearing, protocol 3 for aggressive organ clearing, and protocol 4 for human brain clearing (Tainaka et al., 2018). The paper announced chemical

cocktail upgrades for existing ScaleCUBIC-1 and ScaleCUBIC-2 (Tainaka et al., 2018). As a result, ScaleCUBIC-1 was upgraded as 'CUBIC-L' (N-butyldiethanolamine and Triton X-100) and 'CUBIC-HL' (1,3-bis(aminomethyl) cyclohexane is along with sodium dodecylbenzenesulfonate) (Tainaka et al., 2018).

Similarly, the RI-matching medium - ScaleCUBIC-2 was upgraded as 'CUBIC-RA' (30 wt% N-methylnicotinamide and 45 wt% antipyrine) and 'CUBIC-R' (nicotinamide in combination with antipyrine) (Tainaka et al., 2018). Compared to Histodenz, these reagents are cost-effective (Tainaka et al., 2018). Ueda et al., (2018) found that the RI values of the mounting medium alone have no direct correlation with tissue transparency but with the chemical properties of the constituent. Due to the presence of the amide group in antipyrine and N-methylnicotinamide, these compounds are considered promising RI-matching candidates where the former caused tissue swelling and the latter demonstrated the highest clearing performance (Tainaka et al., 2018). The CUBIC tissue clearing using CUBIC-L and CUBIC-R reagents are remarkably effective for thick biological samples (Ariel, 2017; Tainaka et al., 2018).

However, the CUBIC method required weeks for completing sample de-lipidation compared to another tissue clearing method called as X-CLARITY (Susaki et al., 2014). Still, CUBIC-L and -R medicated tissue clearing faster than ScaleA2 and ScaleU2 (Susaki et al., 2014; Tainaka et al., 2018). CUBIC clearing caused swelling of the sample; the swelling was reduced following the refractive index matching step (Gómez-Gaviro et al., 2017; Tainaka et al., 2018). It can be monitored by measuring the volume of the sample while in the de-lipidation stage (Gómez-Gaviro et al., 2017). While the BABB (benzyl alcohol and benzyl benzoate) tissue clearing protocol decreases the weight of the sample by approximately 30%, CUBIC clearing increases the average weight by less than 10%. This weight change correlates with the brain volumetric increase of ~3-10 % which was observed in microscopy (Gómez-Gaviro et al., 2017). The subcellular microstructures and antigenicity were preserved in a CUBIC cleared mouse brain samples (Tainaka et al., 2018). Likewise, X-CLARITY preserves the tissue architecture and is compatible with standard immunolabeling methods.

A minor disadvantage of CUBIC is the lack of image contrast in CUBIC cleared samples (due to the lack of lipids) during microscopy acquisition (Gómez-Gaviro et al., 2017). This was demonstrated by Susaki et al., (2014) using osmium tetroxide which specifically binds to lipids to improve image contrast under TEM staining (Gómez-Gaviro et al., 2017). Ueda et al. showcased the protocol for registering volumetric images of the CUBIC protocol-1 cleared brain sample treated with a nuclear staining RedDot2 dye to that of the reference brain (Tainaka et al., 2018). The impact of CUBIC clearing can be assessed based on sample transparency rate, and cellular and subcellular tissue integrity using computed tomography (CT) imaging and confocal microscopy, light-sheet microscopy, and Opera Phenix high content screening (HCS) (Opera_Phenix, see the bibliography**;** Gómez-Gaviro et al., 2017).

2.2 Hydrogel-embedding based tissue clearing

In 2013, Tomer, Chung, and Colleagues introduced a hydrogel-embedding tissue clearing technique called CLARITY (Clear Lipid-exchanged Acrylamide-hybridized Rigid Imaging/Immunostaining/*In situ* hybridization-compatible Tissue-hYdrogel) (Ariel, 2017; Ueda et al., 2020). It permits multiple rounds of IHC staining and de-staining in a thick tissue sample (non-sectioned tissue) following the clearing step (Chung et al., 2013) and achieves an optically transparent (although fragile) samples (Epp et al., 2015; Du et al., 2018) for 3D reconstruction by establishing a hydrogel cross-linked with acrylamide (Reveles Jensen and Berg, 2017). Additionally, it permits antibody labeling and intact-tissue *in situ* hybridization in the adult mouse brain (Chung et al., 2013). Initially, it was time-consuming and expensive. The tissue transparency depended on electrophoresis (Reveles Jensen and Berg, 2017) and was unobtainable with passive clearing alone (Epp et al., 2015). Since then, various improvements were reported from different research labs such as PACT (Passive clarity technique), EDC-CLARITY and others (Reveles Jensen and Berg, 2017).

An overview of the steps in the original CLARITY protocol is shown in **Figure 3** (Tomer et al., 2014). The main steps include fixation of the tissue, infusion of the hydrogel monomer, hybridization of hydrogel-tissue, extraction of lipids, molecular labeling (if required), refractive index matching of the sample, and finally imaging. Even before the removal of lipids, macromolecules and nucleic acids (DNA and RNA) were polymerized using acrylamide in fixed tissues and created tissue-

hydrogel hybrid (Reveles Jensen and Berg, 2017). The proteins and parts of the DNA and RNA are bound with tissue-hydrogel hybrid and constitute the skeletal structure (Chung et al., 2013; Reveles Jensen and Berg, 2017). While the de-lipidation step uses detergent (sodium dodecyl sulfate, SDS), the lipids are encapsulated into negatively charged micelles (Reveles Jensen and Berg, 2017). In an applied electrical field, these electrically charged micelles were easily eluted out through the pores in the acrylamide-based hydrogel (Reveles Jensen and Berg, 2017). This step is based on the ionic extraction technique and results in tissue expansion which reverted to its original size after the refractive index matching step (Chung et al., 2013). Hence, it transforms the tissue into a highly transparent sample without severe deformities (Du et al., 2018). Based on the porosity of the hydrogel hybrid, the antibodies can also diffuse and result in the labeling of fixed membrane proteins (Reveles Jensen and Berg, 2017). As a result, this technique is widely applied in the field of neuroscience to image brains; it is also used in a variety of other tissues and organs, including whole-body clearing (Du et al., 2018).

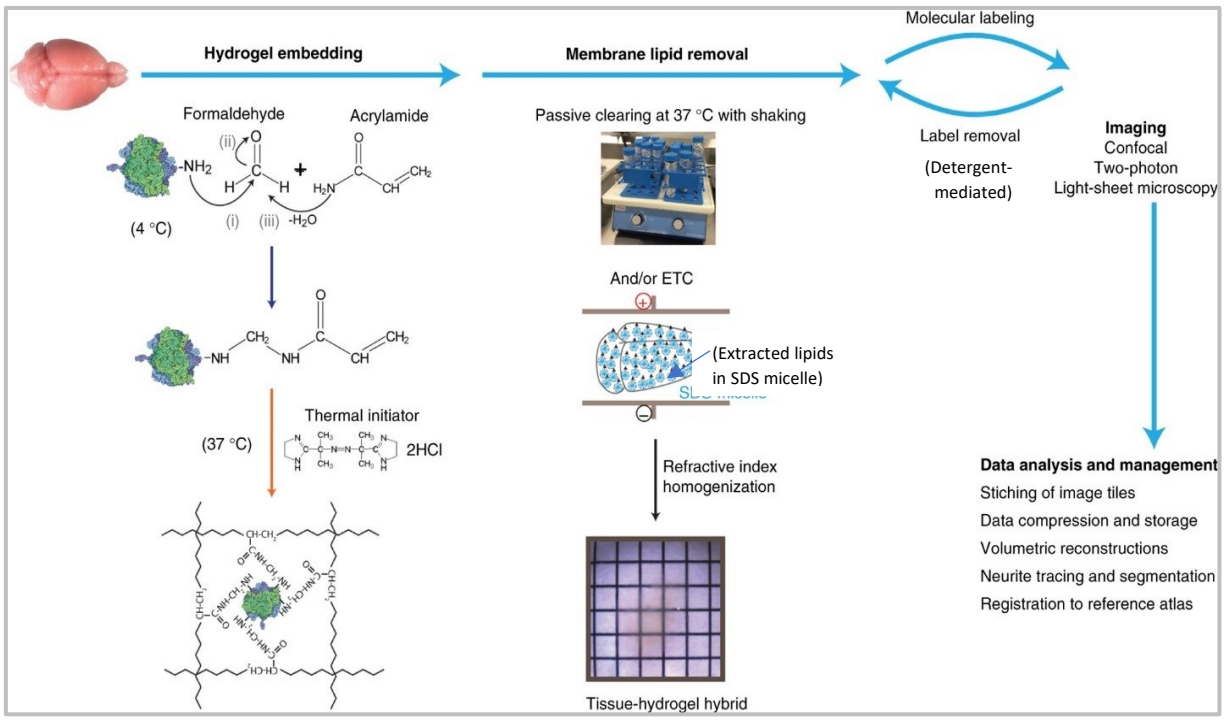

Figure 3. The CLARITY protocol's major steps for creating tissue-hydrogel hybrid
(Image courtesy of (Tomer et al., 2014))

In biological tissue samples, lipid bilayers are responsible for preventing the macromolecules (e.g., antibodies) from penetrating into the cells. They also cause light scattering that may

interfere with imaging. The first goal in conducting this method is to achieve a non-destructive removal of lipid, facilitating the 3D imaging and IHC staining but extending a physical framework by infusing hydrogel monomers (acrylamide and bis-acrylamide) and formaldehyde to ensure structural and molecular integrity (Chung et al., 2013; Lee et al., 2016). These hydrogel monomers covalently link the tissues as well as biomolecules comprising proteins, small molecules, and nucleic acids (Logos XP1710-01, see the bibliography; Hao et al., 2018; Lee et al., 2016; Ariel, 2017). This permits multiple rounds of molecular labeling and elution (Du et al., 2018) due to its compatibility with fluorophores based on proteins (Ariel, 2017). All fluorescent proteins such as green fluorescent proteins (GFP), yellow fluorescent proteins (YFP), and red fluorescent proteins (RFP) are compatible with tissue-hydrogel hybrid (Chung et al., 2013).

Under anaerobic conditions, the hydrogel polymerization occurs at 37^0C for 3 hours (hrs) where the thermal initiator decays into free radicals and reacts with monomers (Logos XP1710-01, see the bibliography). Further, this hydrogel-tissue hybrid is cleared by collecting lipids by passively diffusing SDS-micelle in and out of the sample (Logos XP1710-01, see the bibliography) and would require many months to complete this extraction of lipids (Chung et al., 2013). An ultimate expedition in tissue clearing can be attained by electrophoresis, collectively by active transport organ-electrophoresis approach, which is beneficial for thick samples (Logos XP1710-01, see the bibliography; Chung et al., 2013). The samples can be stored for weeks to months after the tissue clearing steps (Du et al., 2018). Still, the most preferred duration is one week (Logos XP1710-01, see the bibliography).

However, there are reports on key disadvantages with passive- and active- CLARITY protocols. The slow-lipid clearing requires weeks to months for clearing the lipids from the sample, in accordance with the specimen thickness (Tomer et al., 2014; Du et al., 2018). While the passive CLARITY involves slow-lipid clearing, the active CLARITY showed fast-lipid clearing (Ariel, 2017). However, active CLARITY requires custom-made electrophoretic equipment in order to maintain a steady perfusion rate of SDS detergent solution to accomplish transparency, and temperature exchange to protect the sample from browning (Tomer et al., 2014; Ariel, 2017; Ueda et al., 2020). The next disadvantage is the need of highly expensive commercially available refractive index (RI)-matching solutions (Ariel, 2017; Reveles Jensen and Berg, 2017; Du et al., 2018). Based

on the hydrogel-tissue hybridization, several other techniques have emerged to address the above limitations such as PACT, PARS (Perfusion-assisted Agent Release in Situ), and ACT-PRESTO (Du et al., 2018).

Consequently, the active CLARITY was proposed as a novel tissue-clearing method that allows the chemical transformation of biological tissues into a hybrid of nanoporous hydrogel-tissue networks (Tomer et al., 2014; Ariel, 2017; Reveles Jensen and Berg, 2017), demonstrating optical transparency and macromolecular permeability (Hao et al., 2018; Lee et al., 2016; Seo, Jinyoung et al., 2016; Ariel, 2017; Reveles Jensen and Berg, 2017; Ueda et al., 2020). Thus, active CLARITY preserves anatomical fine information along with minimum damage / disassembly of native biological proteins and nucleic acids after the intensive de-lipidation by strong ionic-detergents, sodium dodecyl sulfate (SDS) (Hao et al., 2018; Seo, Jinyoung et al., 2016; Ariel, 2017; Reveles Jensen and Berg, 2017; Ueda et al., 2020). During the de-lipidation step in the CLARITY protocol, only 10% of proteins are lost compared to 65-70% of protein loss reported in formaldehyde-fixed tissues (Reveles Jensen and Berg, 2017; Ueda et al., 2020).

The main characteristics, including transparency, preservation of ultrastructures such as neural circuitry, and fluorescence of biological tissue are achieved with stable hydrophilic non-toxic chemicals (Logos XP1710-01, see the bibliography; Tomer et al., 2014; Seo, Jinyoung et al., 2016). It is clear that this CLARITY protocol is considered relevant in the field of neuroscience, because it retains the native cytoarchitecture intact in adult mouse brains (Tomer et al., 2014), and imaging of long-range projections, subcellular structures, protein complexes and neurotransmitters (Chung et al., 2013). Besides, the hydrogel-tissue hybrid is stable with optical transparency and chemical accessibility for molecular phenotyping such as macromolecular antibody staining and oligonucleotide probe labeling (Tomer et al., 2014; Reveles Jensen and Berg, 2017; Ueda et al., 2020).

2.2.1 Classifications based on hydrogel-tissue hybridization

Based on hydrogel-tissue hybridization, the tissue-clearing methods can be classified into four main classes. These are electrophoresis-assisted de-lipidation, passive de-lipidation along with low-density tissue-gel hybrid formulations, thermally facilitated de-lipidation (SWITCH) with

high-density glyceraldehyde-tissue-gel formation, and stochastic electro-transport (Seo, Jinyoung et al., 2016).

A. <u>Current-assisted clearing & macromolecule diffusion</u>

The first category constitutes particularly the original CLARITY, SE-CLARITY, and ACT-PRESTO (*active clarity technique-pressure related efficient and stable transfer of macromolecules into organs*)(Seo, Jinyoung et al., 2016). The highlighted feature of ACT-PRESTO is that the electric current increases tissue-clearing efficiency with a continuous exchange of SDS solution (Reveles Jensen and Berg, 2017) and overall speed (Logos XP1710-01, see the bibliography) (a minimum of 2 – 3 days for mouse brain)(Seo, Jinyoung et al., 2016).

The original CLARITY protocol was developed by Chung *et al*., demonstrating the tissue clearing protocol on rodent brains, mainly on adult mouse whole brains. An outline of his protocol is as given below:

1) Tissue fixation: The adult mouse is transcardially perfused with a cocktail of 4% paraformaldehyde (PFA), 4% acrylamide, 0.05% bis-acrylamide, 0.25% VA-044 in phosphate-buffered saline (PBS). The brain is then removed and incubated in the same cocktail for 3 days (Reveles Jensen and Berg, 2017).
2) Tissue-hydrogel hybrid formation: The polymerization of the acrylamide and bis-acrylamide is initiated by the thermal initiator VA-044 at 37°C during a 3 hr heat activation cycle applied to the PFA-fixed tissue sample (Reveles Jensen and Berg, 2017).
3) Tissue clearing: In an applied electric field, the sodium borate buffer (0.2 M, pH 8.5) containing 4% weight per volume (w/v) SDS results in the removal of negatively charged lipids through the porous hydrogel at a varying temperature from 37 - 50^0C for two days (Reveles Jensen and Berg, 2017).
4) Refractive index matching: Prior to the refractive index matching, the complete removal of SDS is accomplished by washing the tissue for two days in PBS. Then the tissue was incubated in the preferred refractive index matching solutions (RIMS) until the tissue achieved complete transparency before (Reveles Jensen and Berg, 2017).

Because of the tissue-hydrogel formation, this method is different and advantageous relative to other existing clearing techniques. The reason is that the hydrogel reduces the loss of proteins and damage of antigens from 65% down to 10% during the tissue clearing, in spite of using the harsh 4% SDS buffer (Reveles Jensen and Berg, 2017). Due to this novelty, repeated cycles of antibody staining are also possible. However, some major limitations associated with the original CLARITY need to be overcome (Reveles Jensen and Berg, 2017). These include the slow-lipid clearing, design of the electrophoretic chamber, provision for unceasing exchange of SDS buffer, and the expensive RIMS medium (Reveles Jensen and Berg, 2017).

The limitations of the original CLARITY were overcome by the ACT-PRESTO technique using X-CLARITY tissue clearing system by Logos Biosystems (Logos VX1901-01, see the bibliography; Lee et al., 2016). In ACT-PRESTO, custom-made electrophoretic equipment set-up allows faster clearing while preserving the tissue structure and fluorescence signals (Lee et al., 2016; Ariel, 2017). A two-step fixation protocol is followed (Lee et al., 2016). The initial step is paraformaldehyde-based fixation, and then the acrylamide infusion is free of bis-acrylamide, thus causing less protein-acrylamide cross-linking (Lee et al., 2016). As a result, the porosity of the hydrogel is high. It allows fast removal of lipids and rapid diffusion of macromolecules. Lee et al. (2016) designed a long electrophoretic tissue clearing (ETC) chamber with a cooling system, that can produce a dense current in a steady-state. It overcomes the issues of varying temperature, pH, and discontinuous flow of current caused by bubbles (Lee et al., 2016). In addition, the long ETC chamber allows the air bubbles to float and eliminate through the top outlet. The ETC control tower maintains the temperature inside the chamber. Thus, the tissue is protected from surface burning and protein degradation (Logos VX1901-01, see the bibliography; Lee et al., 2016).

Six hrs of ETC is adequate to transform 2-mm thick slab from an adult mouse brain to transparency while preserving the proteins (**Figure 4.(A)**). In addition, the tissue integrity is not significantly reduced after 12 hrs of ETC (Lee et al., 2016). During the initial clearing process, the tissues swell up. They recover to their original size while being immersed in RIMS (refer to **Figure 4.(B)**). In addition, the method supports standard immuno-labeling procedures and accelerates the penetration of macromolecules with applied pressure (Lee et al., 2016). This was confirmed by testing 82 commercially available antibodies, with successful labeling with 91.5 % these

antibodies. Thus, this technology supports the delivery of reagents to the deep interior of thick tissue samples to acquisition of single-cell resolution imaging in a short duration (Lee et al., 2016).

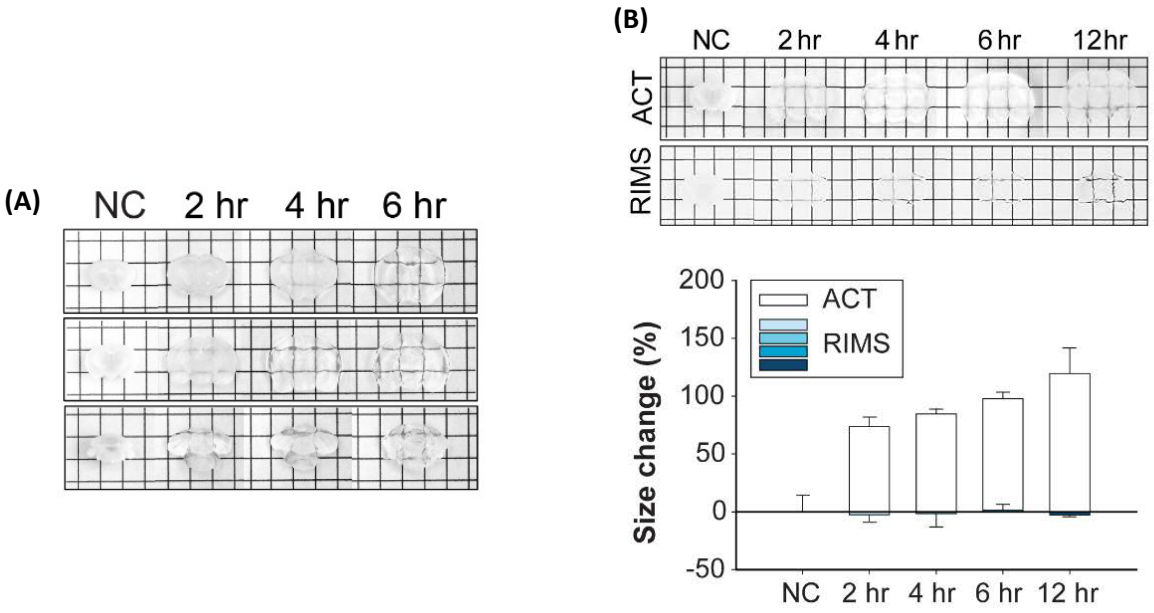

Figure 4. (A) The clearing efficiency versus tissue clearing time for a 2-mm thick adult mouse brain cleared with ACT. **(B) The expansion of 1 mm thick slabs from the mouse brain at varying time points and recovery stages in RIMS**. (Image courtesy of (Ariel, 2017)).

Furthermore, the detection of various macromolecules such as nucleic acids and proteins is possible in ACT-processed tissue hydrogel. The ACT tissue clearing is rapid compared with other clearing techniques, including CUBIC, BABB, iDISCO, original CLARITY, and PACT. Two hours of clearing of ACT is sufficient for obtaining complete transparency of a 1 mm thick slab of a mouse brain whereas in other methods 1-3 days is required to achieve the same level of transparency **(Figure 5)** (Lee et al., 2016).

Thick tissue samples were also cleared, with a longer tissue clearing. **Table 1** shows the clearing conditions for different species. This study reported an approximate linear relationship between tissue clearing time and tissue thickness, where one hour is sufficient for the clearing of 0.5-1 mm thick sample. The weight of the rat brain is 2 grams, four times heavier than the adult mouse brain. One hemisphere of a rabbit weighs 45 grams. Using the ACT custom-designed ETC chamber for mouse brain clearing, this study achieved nearly complete transparency with prolonged tissue

clearing step (Lee et al., 2016). ACT is scalable across various species, including humans; however, the efficacy of the clearing depends on several factors, including lipid and connective tissue contents along with the tissue fixation conditions (Lee et al., 2016). Using custom designed ETC chamber specifically designed for mouse brain clearance by ACT, the rabbit hemi-sectioned brain achieved nearly complete transparency with 50 hours of ACT clearing step (Lee et al., 2016).

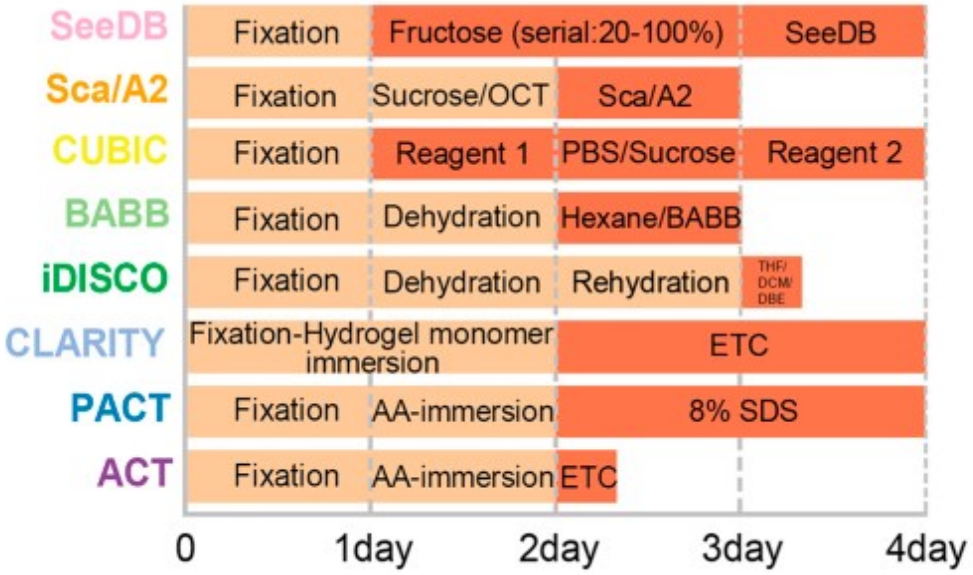

Figure 5. A comparison between various tissue-clearing procedures and associated time requirement. (Image courtesy of (Lee et al., 2016))

Peripheral organ clearing, too, was achieved with ACT (Lee et al., 2016). The peripheral organs comprise the thymus, testis, intestine, liver, lung, spleen, and kidney. The clearing and acquired transparency differed among these organs based on the thickness and content of the extracellular matrix (ECM) (**Figure 6**). The organs with ECM remained opaque after prolonged clearing. This opaqueness was solved by the using of CUBIC cocktail RIMS solution called CUBIC-mount where aminoalcohol caused decolorization of the tissue by liberating the heme group from blood throughout the sample (Lee et al., 2016).

B. Passive diffusion-assisted clearing

The second category compromises PACT, PARS, and EDC-CLARITY (Seo, Jinyoung et al., 2016). SDS incubation relies on passive diffusion; it takes over a month for a mouse brain. Passive diffusion-assisted clearing techniques are intended for large samples, achieving efficient clearing

performance within weeks instead of months. They create low-density tissue-gel hybrid formation (Tomer et al., 2014; Seo, Jinyoung et al., 2016) and reduce the crosslinking strength (e.g.: PACT)(Ueda et al., 2020). The increased porosity in the hybrid network enables the penetration of macromolecular probes for labeling (Seo, Jinyoung et al., 2016). However, the process causes damage to the structural and molecular integrity of the sample. As a result, an optimization needs to be carried out with fixative concentration, hydrogel monomers composition (acrylamide and bis-acrylamide), and clearing condition with respect to the thickness of the sample that needs to be cleared (Seo, Jinyoung et al., 2016).

Table 1: Comparison study between species

Sl. No.	Animal and organ of interest	Dimension (x: y: z)	Weight (Grams)	ETC (Hrs)	Size comparison with adult mouse brain
1	Rat; Whole Brain	1.6 mm: 3.3 mm: 1.3 mm	2	15	4 X
2	Rabbit; brain hemisphere	3.6 mm: 5.5 mm: 2.9 mm	10	50	45 X
3	Human; spinal cord	1.3 cm diameter		100	--

Data from (Lee et al., 2016)

C. SWITCH

In the third category, namely 'SWITCH', a bifunctional crosslinker called glutaraldehyde (GA) chemically transforms the density of a biological tissue sample. An associated high temperature of 70-80^{0}C results in rapid clearing of samples without impairing the molecular and structural integrity (12h is sufficient to clear an adult mouse hemisphere at 80^{0}C) wherein quenching the fluorescence is an associated drawback (Seo, Jinyoung et al., 2016; Ariel, 2017).

D. Stochastic electrotransport

The fourth category is termed 'stochastic electro-transport' (Seo, Jinyoung et al., 2016). It uses a rotational electric field that selectively facilitates the SDS micelles dispersion and achieves approximately 10 times faster clearing compared to the original CLARITY method without

damaging the sample or compromising its fluorescence (Seo, Jinyoung et al., 2016). However, this technique has been successful only with a custom-made complex electrophoresis device, significantly more expensive than the equipment required for ACT (Seo, Jinyoung et al., 2016).

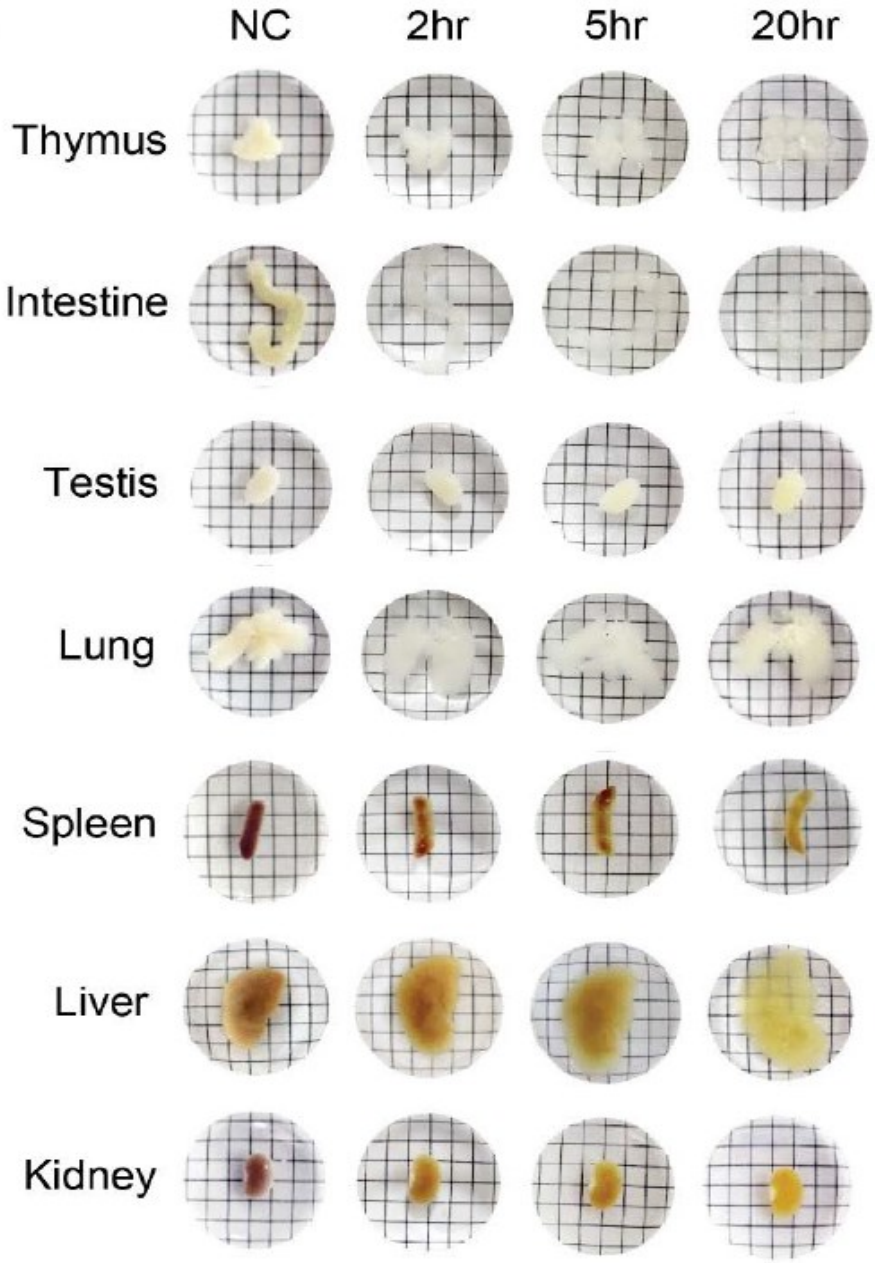

Figure 6. A typical image of peripheral organs of adult mouse obtained during ACT.
(Image courtesy of (Lee et al., 2016)).

2.2.2 Immunolabeling for cleared-thick samples:

The exploration of fine details at the cellular level is achievable with antibody labeling (Lee and Sun, 2016). The three major difficulties of conventional labeling techniques include: (1) Accessing intracellular targets via permeabilization results in the loss of native molecules, (2) time-consuming laborious tissue sectioning followed with imprecise 3D reconstruction, and (3) the harsh probe-removal process after each round of labeling damages the tissues (Chung et al., 2013). These difficulties were majorly overcome with intact-tissue clearing protocols such as BIC and CLARITY (Chung et al., 2013). Depending upon the thickness of the tissues, ECM contents in peripheral organs, and tissue-hybrid porosity generated, antibody staining mainly depends on passive diffusion with different incubation periods. It may vary from 3 - 10 days or even more (Tomer et al., 2014; Lee et al., 2016; Ueda et al., 2020). However, a rapid antibody staining can be obtained with stochastic electro-transport and ACT-PRESTO approaches (Lee et al., 2016; Ariel, 2017). Thus, the existing fundamental challenges in antibody labeling can be resolved to some extent with a minimum time requirement.

ACT-PRESTO ensures the preservation of native antigens in the hydrogel-hybridization process (Chung et al., 2013). This was confirmed by comparing protein loss in cleared mouse brains against conventional methods (Chung et al., 2013). The outcome is shown in **Figure 7**. (Chung et al., 2013). The paraformaldehyde (PFA)-fixed tissue blocks that were treated with 4% SDS for one week suffered 65% protein loss. Scale, a clearing technique that uses 4M urea, resulted in ~41% loss of protein (Chung et al., 2013). A conventionally PFA-fixed tissue sample treated with 0.1% Triton X-100, known as permeabilization agent, permitted ~24% protein loss (Chung et al., 2013). But tissue blocks clarified with CLARITY demonstrated only ~8% loss of protein (Chung et al., 2013). The CLARITY technique provides the replacement of the lipid bilayer with nanoporous hydrogels which expedite diffusion of molecular probes into the center of the intact tissue without sectioning (Chung et al., 2013). This has been affirmed using 1-mm thick clarified coronal mouse brain block of Thy1–eYFP immunostained for GFP (Chung et al., 2013). The brain block was ETC-cleared for 1 day, immunostained for 3 days and then, imaged under single-photon excitation (**Figure 8**)(Chung et al., 2013). Later on, IHC was performed using tyrosine hydroxylase labeling in clarified intact mouse brain (Chung et al., 2013). In this experiment, the primary and

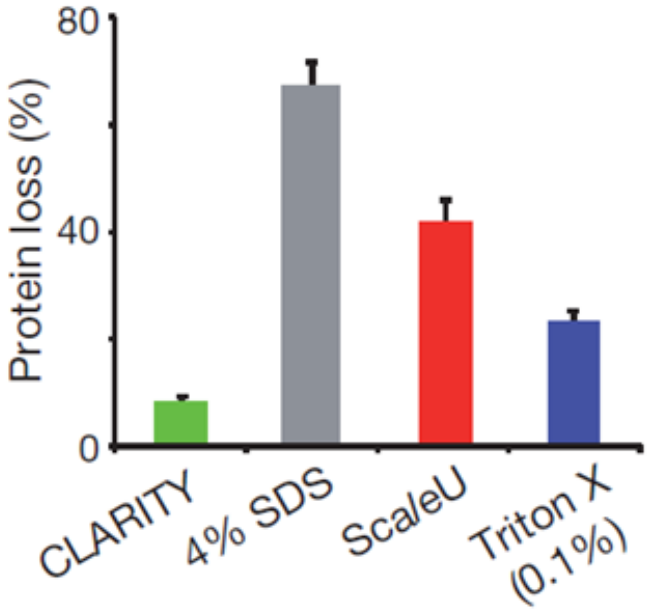

Figure 7. A comparison of protein loss by conventional clearing techniques applies to mouse brain blocks. (Image courtesy of (Chung et al., 2013)).

secondary antibodies were incubated for two weeks, allowing the demonstration of the penetration of antibodies into 2.5 mm from each surface, i.e., immunolabeling of the 5-mm thick brain. Thus, the analysis of subcellular molecular architecture in intact brain tissues can be achieved in thick samples clearing and using high-resolution imaging (Chung et al., 2013).

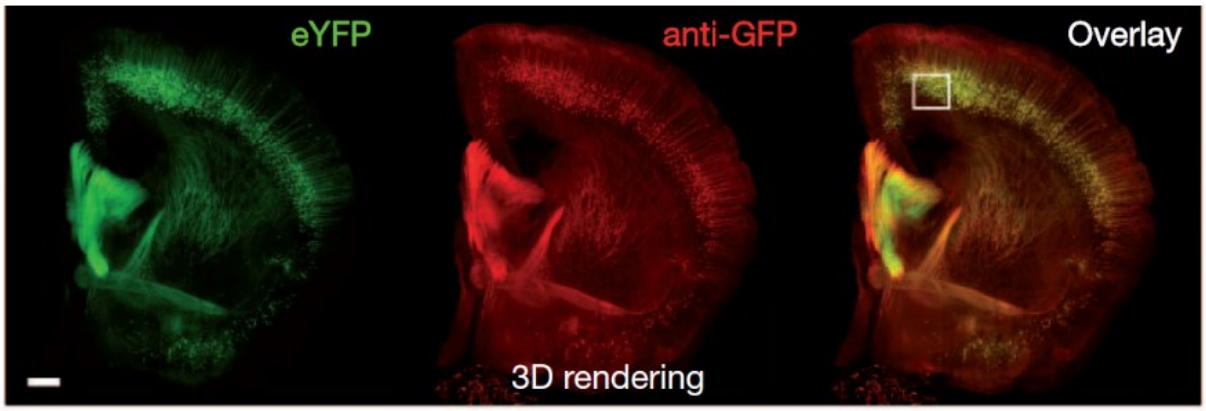

Figure 8. Clarified 1-mm slab from a mouse brain after immunostaining and 3D rendering. Scale bar, 500 µm. (Image courtesy of (Chung et al., 2013)).

Indeed, this approach is an improved solution relative to conventional mechanical slicing that may involve deformation of tissue and imprecise registration across sections. In addition, multiple rounds of antibody staining are possible with nanoporous hydrogel-tissue hybrid due to its structural and chemical stability (Chung et al., 2013). The ionic detergent, namely - 4% SDS/neutral-pH buffer makes it possible to denature antibodies and upset existing binding, thus assisting antibody exchange. This feature was confirmed in mouse brain using tyrosine hydroxylase where the antigenicity remained the same throughout three rounds of staining and elution (Chung et al., 2013). Moreover, CLARITY preserves continuity in the tracing of neurites and offers three-dimensional and topological morphology details (Chung et al., 2013).

PRESTO (*pressure related efficient and stable transfer of macromolecules into organs*) can be used to infuse the macromolecules into dense structures actively by applying pressure (Lee and Sun, 2016; Lee et al., 2016). Depending upon the nature of the organ such as soft (e.g. Brain) or hard (e.g. Kidney), two variants of PRESTO protocols are available (Lee et al., 2016): syringe PRESTO (*s-PRESTO*) and centrifugal PRESTO (*c-PRESTO*) (Lee et al., 2016). The former is designed to immune-stain thick and soft samples, for example, brain, where conventional flow with a syringe pump is used (Lee and Sun, 2016; Lee et al., 2016). The pump executes the infusion of the labeling reagent into the sample under the pressure (Lee and Sun, 2016; Lee et al., 2016). The latter is for peripheral organs including kidney, testis, and lung. It applies centrifugal force using standard, table-top centrifuge apparatus (600rcf) (Lee and Sun, 2016; Lee et al., 2016). This speedy and consistent protocol accelerates the achievement of 3D histological research and volume-based sample diagnoses (Lee and Sun, 2016; Lee et al., 2016). Following de-lipidation and immunolabeling and/or counter nuclear staining steps, the samples are immersed in commercially available refractive index (RI)-matching solutions (between 1.38 – 1.45) to gain complete optical clearing (Seo, Jinyoung et al., 2016; Ariel, 2017).

CHAPTER 3 – MATERIALS AND METHODS

3.1 Animal model

Mice: Twenty-three adult wild-type C57BL/6 mice (16 males and 7 females) were used. The age range was 10 weeks to 30 weeks.

Rat: Adult male Sprague-Dawley rats (4 males) weighing 250–300 g were used. The rats were 8 weeks to 10 weeks old.

3.2 Specimen Preparation

All procedures were approved by the animal care committees of the Montreal Neurological Institute and McGill University and were carried out in accordance with the guidelines of the Canadian Council on Animal Care. Mice and rats were housed under controlled environmental conditions at 22 ±·2^{0}C with a 12 h light/12 h dark cycle (lights on from 7:00 a.m. to 7:00 p.m.) and received food and water *ad libitum*.

Procedures applied in mice: The mice were anesthetized with anesthetic cocktail consisting of ketamine 100 mg/kg, xylazine 10 mg/kg, and acepromazine 3 mg/kg (Mouse Anesthesia, 2021, see the bibliography) through intraperitoneal injections (i.p.). They were then transcardially perfused with 15 ml of cold PBS to flush out the blood, followed by perfusion with 20 ml of 4% paraformaldehyde (PFA) used for fixing the brain (Murakami et al., 2018; Xu et al., 2019). The rate of perfusion was set at 3 ml/min in all mice experiments (Cahill et al., 2012). Finally, the brains were extracted and post-fixed in 4% PFA at 4°C for 2 - 24 hours. The duration was varied depending on the experiment design, in order to test the effect of post-fixation duration on the sample's structure and clearing results.

Procedures applied in rats: Adult rats were anesthetized with ketamine 50 mg/kg, xylazine 5 mg/kg, and acepromazine 1 mg/kg (Rat Anesthesia, 2021, see the bibliography). Within the next 5 min, we checked the pedal withdrawal reflex to monitor the depth of anesthesia. The animals were transcardially perfused with 150 ml of cold PBS to flush out the blood, followed by perfusion with 150 ml of paraformaldehyde for the fixing the brains. The perfusion flow rate was set at 10 ml/min in all rat experiments. The brains were extracted and post-fixed in 4% PFA at 4°C for 2 -

24 hours. The duration was varied depending on the experiment design, in order to test the effect of post-fixation duration on the sample's structure and clearing results.

3.3 Methods for Tissue Clearing

a. CUBIC Protocol

The duration for post-fixation in 4% PFA depended on the clearing protocol, namely (a) 'CUBIC-P' or (b) 'CUBIC-L and CUBIC-R' (Brochure_LL060, see the bibliography). In the CUBIC-P protocol, the intra-cardiac perfusion included an extra round of PBS washing followed by 100 ml of CUBIC-P reagent perfusion. This extra-round was performed following the initial PBS and 4% PFA perfusion steps. Subsequently, there was no post PFA fixation step after the extraction of the brain. Instead, the sample was directly immersed in 100% of CUBIC-L reagent solution at RT (Tainaka et al., 2018). In the CUBIC-L and -R protocol, PBS and 4% PFA perfusions were conducted initially. The extracted brain was post fixed with PFA, for a duration ranging from 2 to 24 hrs to examine the structural stability and integrity of the brain sample during and after the de-lipidation, antibody labeling, (if applicable as per experimental design) and nuclear staining steps (Brochure_LL060, see the bibliography). Prior to the de-lipidation step, the fixed organs were washed thoroughly using PBS for 1 day (**Figure 9**).

b. X-CLARITY Protocol

After the extraction of the brain, the sample was thoroughly rinsed with PBS, then post-fixation was performed with PFA for 24 hrs. Following this stage, the mouse brain samples were incubated in X-CLARITY Hydrogel Solution Kit (from the Logosbio company) at 4^0C for 24 hrs (Logos XP1710-01, see the bibliography; Lee et al., 2016). This solution consists of X-CLARITY polymerization Initiator and X-CLARITY Hydrogel Solution where one part 25% (w/v) X-CLARITY polymerization Initiator (VA-044) was mixed thoroughly with 100 parts X-CLARITY Hydrogel Solution before use. This solution was used right after its preparation or it was divided into small aliquots and frozen at -20^0C for future use (Epp et al., 2015). Hydrogel-infused samples were polymerized for 3 hrs at 37^0C with an X-CLARITY Polymerization System at -90kPa (Epp et al., 2015). The X-CLARITY polymerization initiator (VA-044) is triggered by the 37^0C temperature generated inside the polymerization system. Following the polymerization step, the samples were shaken gently for one minute to ensure homogenous spreading of the sticky hydrogel

solution over the sample. Then, we rinsed the polymerized brain samples with 1X PBS for multiple times to remove excess hydrogel. Subsequently, we transferred the brain sample into the clearing solution (Epp et al., 2015).

3.4 Tissue Clearing Reagents

a) Reagents for CUBIC clearing

i. CUBIC – P

The perfusion cocktail includes CUBIC-P. It is expected to result in faster clearing of the tissues in adult mouse brains (Susaki et al., 2015). This perfusion cocktail is expected to provide rapid decolorization effect due to the presence of amino alcohol in 1-methylimidazole(Susaki et al., 2015). The CUBIC-P reagent was prepared as a mixture of 5 wt% 1-methylimidazole (Aldrich Chemical Co LLC, CAS No. 616477, USA), 10 wt% N-butyldiethanolamine (Aldrich Chemical Co LLC, CAS No. 102794, USA), and 5 wt% Triton X-100 (Aldrich Chemical Co LLC, CAS No. 9002931, USA) (Tainaka et al., 2018). For example, to prepare 100 g of CUBIC-P reagent solution, we mixed 1.67 g of 1-methylimidazole, 3.33 g of N-butyldiethanolamine, and 1.67 g of Triton X-100 in 93.33 g of distilled water (DW) with a magnetic stirrer for one hour in RT. Following the complete dissolution, we degassed the reagent with a vacuum desiccator (~ 30 minutes). This reagent can be stored up to six months at RT.

ii. CUBIC – L

It was reported that the CUBIC-L reagent has decolorizing properties and high capacity to dissolve lipids, which reduces light scattering inside the tissue. It is responsible for the degree of transparency achieved in the tissue samples (Susaki et al., 2015). The CUBIC-L reagent was prepared as a mixture of 10 wt% N-butyldiethanolamine (Aldrich Chemical Co LLC, CAS No. 102794, USA) and 10 wt% Triton X-100 (Aldrich Chemical Co LLC, CAS No. 9002931, USA) in DW (Tainaka et al., 2018; Matsumoto et al., 2019). For instance, to prepare 200 ml of CUBIC-L reagent solution, we had 10 g of N-butyldiethanolamine in a beaker and added 10 g of Triton X-100 to it.

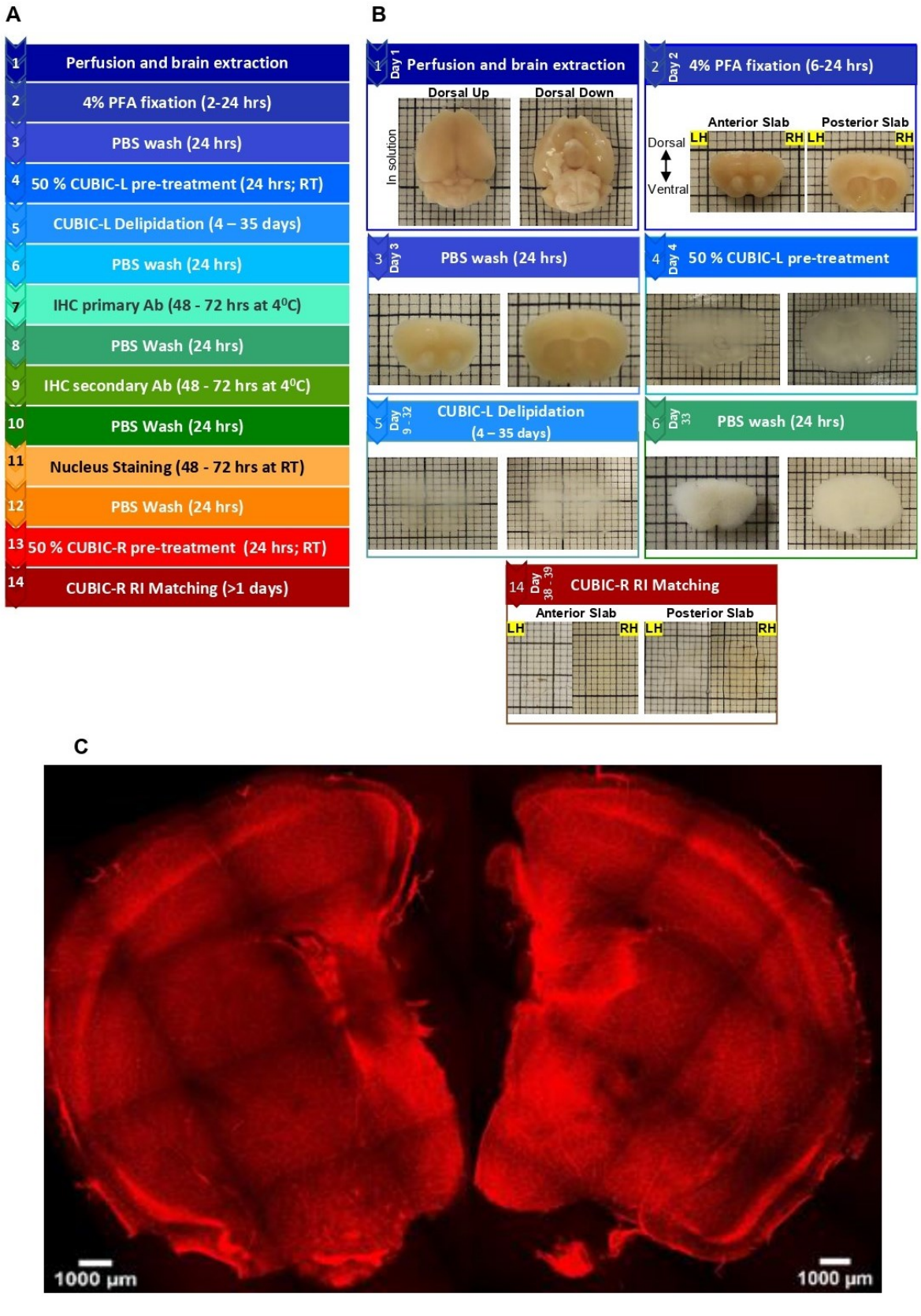
A
1 Perfusion and brain extraction
2 4% PFA fixation (2-24 hrs)
3 PBS wash (24 hrs)
4 50 % CUBIC-L pre-treatment (24 hrs; RT)
5 CUBIC-L Delipidation (4 – 35 days)
6 PBS wash (24 hrs)
7 IHC primary Ab (48 - 72 hrs at 4⁰C)
8 PBS Wash (24 hrs)
9 IHC secondary Ab (48 - 72 hrs at 4⁰C)
10 PBS Wash (24 hrs)
11 Nucleus Staining (48 - 72 hrs at RT)
12 PBS Wash (24 hrs)
13 50 % CUBIC-R pre-treatment (24 hrs; RT)
14 CUBIC-R RI Matching (>1 days)
B
1 Day 1 Perfusion and brain extraction
Dorsal Up
Dorsal Down
In solution
2 Day 2 4% PFA fixation (6-24 hrs)
Anterior Slab
Posterior Slab
Dorsal
Ventral
LH
RH
3 Day 3 PBS wash (24 hrs)
4 Day 4 50 % CUBIC-L pre-treatment
5 Day 9 - 32 CUBIC-L Delipidation (4 – 35 days)
6 Day 33 PBS wash (24 hrs)
14 Day 38 - 39 CUBIC-R RI Matching
Anterior Slab
Posterior Slab
LH
RH
C
1000 µm
1000 µm

Figure 9. Mouse brain clearing using the CUBIC-L and CUBIC-R protocol. (A) Timeline for mouse brain clearing and immunostaining or nucleus staining followed by refractive index matching. (B) The appearance of mouse brain after each step. The post-fixation was carried out for 2 hours at 4^0C followed by PBS washing for 1 day. We used coronal slabs cut from each hemisphere separately, in order to make direct comparisons of contra-lateral slabs that have similar vasculature and microstructure. This was followed by the clearing of the brain slabs from day 4 to day 32 using the CUBIC-L reagent, and by nucleus staining. Following the nucleus staining, the brain slabs were washed using PBS and immersed into CUBIC-R for refractive index matching (1-2 days). (C) Images of Nissl-stained cell nuclei of the left and right hemispheres of the slab cut posteriorily relative to bregma, obtained using an Opera Phenix spinning confocal microscope at 5X magnification. *Red, fluorescence of Nissl bodies. RI, Refractive index; LH, Left hemisphere; RH, Right hemisphere.* Scale bar: 3 mm slab thickness in B, and 1000 µm in C.

We then mixed thoroughly using a magnetic stirrer for 10 minutes, added 180 g of DW, and continued stirring for one hour at RT for complete dissolution. Lastly, we degassed the CUBIC-L reagent with a vacuum desiccator (~ 30 minutes). The CUBIC-L reagent should not be prepared with PBS. Using PBS causes salt contamination and decreases the clearing efficiency (Susaki et al., 2015).For starting the de-lipidation, initially the samples were incubated in 50% CUBIC-L reagent. To prepare the 50% CUBIC-L reagent, we mixed the reagent and DW at a ratio of 1:1 prior to use. It is recommended to prepare half diluted CUBIC-L just before the experiment (Matsumoto et al., 2019). If prepared before hand, it can be stored at RT for up to six months; storing at 4^0C is expected to form crystals.

b) Reagents for X-CLARITY clearing

i. **Electrophoretic Clearing Solution (SDS Solution)**

The SDS clearing solution was prepared as a mixture of 61.83 g of boric acid and 200 g of SDS (4% SDS in 0.2 M Borate buffer) in 4.5 L of DW wherein the final pH needs to be adjusted to 8.5 using 10 N NaOH solution (Logos XP1710-01, see the bibliography). In the CLARITY clearing, a strong detergent - namely SDS – is used to remove lipids actively from the tissue under the electrophoretic current. Therefore, this solution is also known as electrophoretic clearing solution (Logos XP1710-01, see the bibliography). Hence, those lipid molecules that are not linked with hydrogel scaffolding are removed by the SDS clearing solution with the aid of electric current (Logos XP1710-01, see the bibliography). To eliminate residual SDS, the cleared samples were washed using PBS overnight with gentle shaking at RT (Lee et al., 2016).

3.5 Refractive Index Matching Solutions (RIMS)

a) CUBIC-R

It was reported that antipyrine has high clearing performance which reduced the light scattering of the tissue (Susaki et al., 2015); it also prevents tissue shrinkage (Tainaka et al., 2018). The CUBIC-R reagent was prepared as a mixture of 45 wt% antipyrine (Aldrich Chemical Co LLC, CAS No. 60800, USA) and 30 wt% nicotinamide (Aldrich Chemical Co LLC, CAS No. 98920, USA) in DW. For example, to prepare 100 ml of CUBIC-R reagent solution, we mixed 45 g of antipyrine, 30 g of nicotinamide and 36 ml of DW thoroughly using a magnetic stirrer for one hour at RT to complete dissolution. Following the complete dissolution, we added 1400 µl of N-butyldiethanolamine so that the pH of this reagent lies between 8 and 9 and the RI is 1.522 (Tainaka et al., 2018; Matsumoto et al., 2019). Lastly, we degassed the CUBIC-R reagent with a vacuum desiccator (~ 30 minutes). This reagent can be stored up to six months at RT.

b) CUBIC-R2

The CUBIC-R2 reagent was prepared as a mixture of 25 wt% urea (Sigma-Aldrich Canada Co., CAS No. 57-13-6, Canada), 50% wt sucrose (Sigma-Aldrich Canada Co., CAS No. 57-50-1, Canada), and 10 wt% triethanolamine (CAS No. 102-71-5) in DW (Susaki et al., 2015). For instance, to prepare 10 g of CUBIC-R2 solution, we dissolved 2.5 g of urea and 5 g of sucrose in 1.5 g of in DW. If this reagent is prepared with PBS instead of DW, its clearing performance is reduced because of salt contamination. For complete dissolution, we placed this mixture on a hot pot with magnetic stirrer for 20 mins. The degradation of the urea due to excess heating during preparation is ascertained by the acrid ammonia smell. However, the user must avoid over heating of the hot pot and boiling of the solution, because the boiling the evaporates the water and results in a highly concentrated reagent. Once it cooled down at RT, we added 1 g of triethanolamine and continued stirring for 5 more mins. Lastly, we degassed the highly viscous CUBIC-R2 with a vacuum desiccator (~ 30 minutes). This reagent can be stored up to two weeks at RT. Before use, we checked the presence of any precipitation. The precipitation in the reagent – if present - can be dissolved by mild heating and stirring. During the CUBIC-R2 treatment, we inspected the sample to check for bubbles around and inside the sample which indicated that the degassing was insufficient.

c) CUBIC-mount Solution

The CUBIC-mount reagent was prepared as a mixture of 50% (w/v) sucrose (Sigma-Aldrich Canada Co., CAS No. 57-50-1, Canada), 25% (w/v) urea (Sigma-Aldrich Canada Co., CAS No. 57-13-6, Canada), and 25% (w/v) N,N,N',N'-tetrakis (2-hydroxypropyl) ethylenediamine (Millipore Sigma Canada Ltd, CAS No.102-60-3, Canada) (Lee et al., 2016). For example, to prepare 500 ml of CUBIC-mount reagent, we dissolved 250 g of sucrose, 125 g of urea, and 125 g of N,N,N',N'-tetrakis (2-hydroxypropyl) ethylenediamine in 150 ml of DW and brought up the volume to 500 ml (Lee et al., 2016). The aminoalcohols in this mounting cocktail take part in the bleaching by releasing the heme group from hemoglobin; the sucrose and urea take part in adjusting the RI (Lee et al., 2016). The RI value of this solution was 1.43 – 1.48; it rendered the sample transparent (Lee et al., 2016).

d) Fructose-Glycerol Solution

Fructose-glycerol solution was prepared as a mixture of 60 % (v/v) glycerol and 2.5 M fructose. It has high viscosity. For instance, to prepare 660 ml of this reagent, we dissolved 330 ml of glycerol and 297.2 g of fructose in DW using a magnetic stirrer (Dekkers et al., 2019). The RI of this solution is 1.4688 at RT. Finally, we degassed the reagent with a vacuum desiccator (~30 minutes). Otherwise, bubbles are expected to surround the sample and cause interference while imaging. Hence, we transferred this reagent to the vial containing the sample slowly and carefully to reduce the possibility of generating new air bubbles. It can be stored in darkness at 4^0C for one month.

3.6 Transparency Estimation

The post-fixed mouse brains were cut along the mid-sagittal plane; then, 2-3 mm-thick coronal slabs were cut. The slabs were imaged with a conventional Canon camera pre- and post-clearing every three days. We observed and documented the process in which the tissue slabs became progressively transparent, along with an increase in the size of the slabs. Our criterion for determining that a tissue slab became transparent was based on the visibility of a millimetric grid under the jar with the tissue. We determined the status of the sample as 'cleared' following the CUBIC-L-mediated clearing or the electrophoretic clearing buffer-mediated tissue clearing subjectively, according to the visibility of the grid through the tissue. To reduce variability of

estimation, the same person evaluated the transparency levels for all sample. While the slabs became transparent, we observed an increase in the size of the slabs. Once the delipidation completed, then PBS washing of the samples started (Lee and Sun, 2016).

3.7 Solutions for immunostaining and neuronal cell staining protocols

For uncleared frozen brain slices (Shi et al., 2008)**:** 30 - 60 µm thin slices were washed using PBS for 30 minutes. To improve the permeability of slices, the slices were then moved into 0.3% PBST and incubated at RT for 1 hr with gentle shaking. Then, we transferred the slices into 1% blocking buffer and incubated for 30 min at RT. The blocking buffer was made of 1% bovine serum albumin in 0.3% PBST solution. Next, the slices were immersed in a MAP2 primary antibody solution (1:1000) and incubated at 4^0C overnight with gentle shaking. Next, we performed PBST washing, of 10 min immersion in 2 ml PBST, repeated 3 times. Then, the incubation of the slices continued in the secondary antibody solution (Goat anti-Chicken IgG (H+L) secondary antibody, 1:1000) in darkness at RT for 2 hrs. Subsequently, the slices were rinsed with PBST solution and were ready for fluorescent Nissl body counterstaining.

For cleared brain slabs: To perform the immunostaining, the 2-3 mm thick cleared brain slabs were incubated in the primary antibody and secondary antibody solutions respectively (Tomer et al., 2014) for 2-3 days. The primary MAP2 antibody solution contained a primary antibody in PBS in addition to 0.1 % (vol/vol) Triton X-100 buffer (Tomer et al., 2014). Similarly, the secondary antibody solution consisted of a secondary antibody in PBS in addition to 0.1 % (vol/vol) Triton X-100 buffer (Tomer et al., 2014). The optimized fluorescent immunostaining and neuronal cell staining protocol for CUBIC-cleared cleared rodent brain sample is presented in **Figure 9.** Following the de-lipidation and PBS washing steps, the thick brain slabs were incubated in a primary antibody solution (anti-MAP2) and left on a shaker (with 80 rpm) for 2-3 days at 4^0C (Lee et al., 2016). Following the washes, the sample was immersed in the fluorescent secondary antibody (Alexa 488) solution (1:300) and was left on a shaker (80 rpm) for additional 2-3 days at RT in darkness (Lee et al., 2016).

3.8 Counter Staining

The counterstaining with fluorescent Nissl enables the precise extraction of particular anatomical structures and alignment of different samples for evaluating signal intensities (Susaki et al., 2015). The quality of imaging of cleared tissue samples is directly linked with the fluorescence wavelength. The red wavelength is recommended for thicker tissue samples as it can penetrate the tissue deeper than green fluorescence (Susaki et al., 2015). The NeuroTrace 530/615 red fluorescent Nissl stain is selective for visualizing Nissl substance in neurons with improved sensitivity compared to Cresyl violet-based traditional histological dyes (Fluorescent tracers, see the bibliography; Thermofisher Manuals Fmp21480, see the bibliography).

For uncleared thin brain slices (Shi et al., 2008)**:** Immediately after the secondary antibody labeling, the slices were transferred into Nissl fluorescent solution at (1:1000) dilution and incubated at RT for 1 – 2 hours in darkness. Then, these slices were mounted on gelatin-coated microscope slides and were dried overnight at RT. Lastly, antifade mounting medium was applied on the microscope slide. We placed the coverslip over this mounting medium and slowly lowered it. We applied slight pressure to squeeze away air bubbles, and then dried it overnight. On the next day, it was ready for microscopic imaging.

For Cleared thick brain slabs: After completing the immunostaining labeling step (if required per the experimental design), the brain slabs were thoroughly washed in PBS. Then to counterstain cells, the slabs were transferred into Nissl fluorescent (530/615 nm) stain diluted in PBS solution (e.g., 1: 50 is the optimized concentration for 2-3 mm thick mice brain slabs) for 2-3 days at RT with gentle shaking(Yang et al., 2014). Thereafter, the brain slabs were ready for refractive index matching and subsequent imaging.

3.9 Opera Phenix Microscopy

Immunostained and Nissl labeled 2-3 mm thick brain slabs were imaged using an opera phenix high-content screening (HCS) fluorescent confocal spinning disk microscope. It has fully integrated hardware and software system for automatic acquisition of multiple samples. The spinning disc feature captures the field of view of each sample, while permitting different wavelength of light from 4 different laser sources. Thus, simultaneous imaging of 4 channels can be achieved with minimum crosstalk. At 5X and 10X image acquisition, 60% and 80% of laser power was utilized for Alexa 488 and fluorescent Nissl stain (530/615 nm), respectively. The exposure time was 200 ms and the binning factor 1. When imaging at 5X, we used '2 peaks', to make automatic detection of both the bottom surface (peak # 1) and the top surface (peak # 2) of the well's glass. Since our solution and cleared samples have a high RI value, similar to the RI value of the well plate's cover glass, the 2 peak selection no longer works at 10X. Therefore, when imaging with the 10X objective, we selected 1 peak.

3.10 Image Analysis

The Opera phenix images were acquired using the Harmony software. The confocal microscope images were acquired using the Zen software (Zeiss). Image processing was then performed using a combination of software packages including Imaris (Bitplane) and ImageJ for 2D stitching and automatic adjustments of brightness and contrast. The Imaris software package was mainly used for the conversion of harmony files into (.ims), followed by stitching. ITKSNAP was used for delineating the microscopy images (ITK-SNAP 2021). Custom-written scripts in Matlab were used for estimating signal-to-background ratio from microscopy images

3.11 Quantitative estimation of signal to background

An important feature to evaluate for estimating the detectability of neurons is the Signal to Background Ratio (SBR) (**Figure 10**). To estimate the SBR, we used a custom-written code in Matlab. It allowed us to present an image of a 2D plane parallel to the slab, and sample the signal in the center of identified labeled neurons. Following the sampling of the intensity in a specific neuron, we sampled the background intensity close to the neuron but clearly outside of it. For

the sampling, neurons were selected from each of several ROIs and dilutions. The selected neurons were distributed approximately homogeneously across the cortical depth. **Figure 10** presents the sampling of the signal (in green) from inside two neurons, and the matching background (in yellow) adjacent to these two neurons.

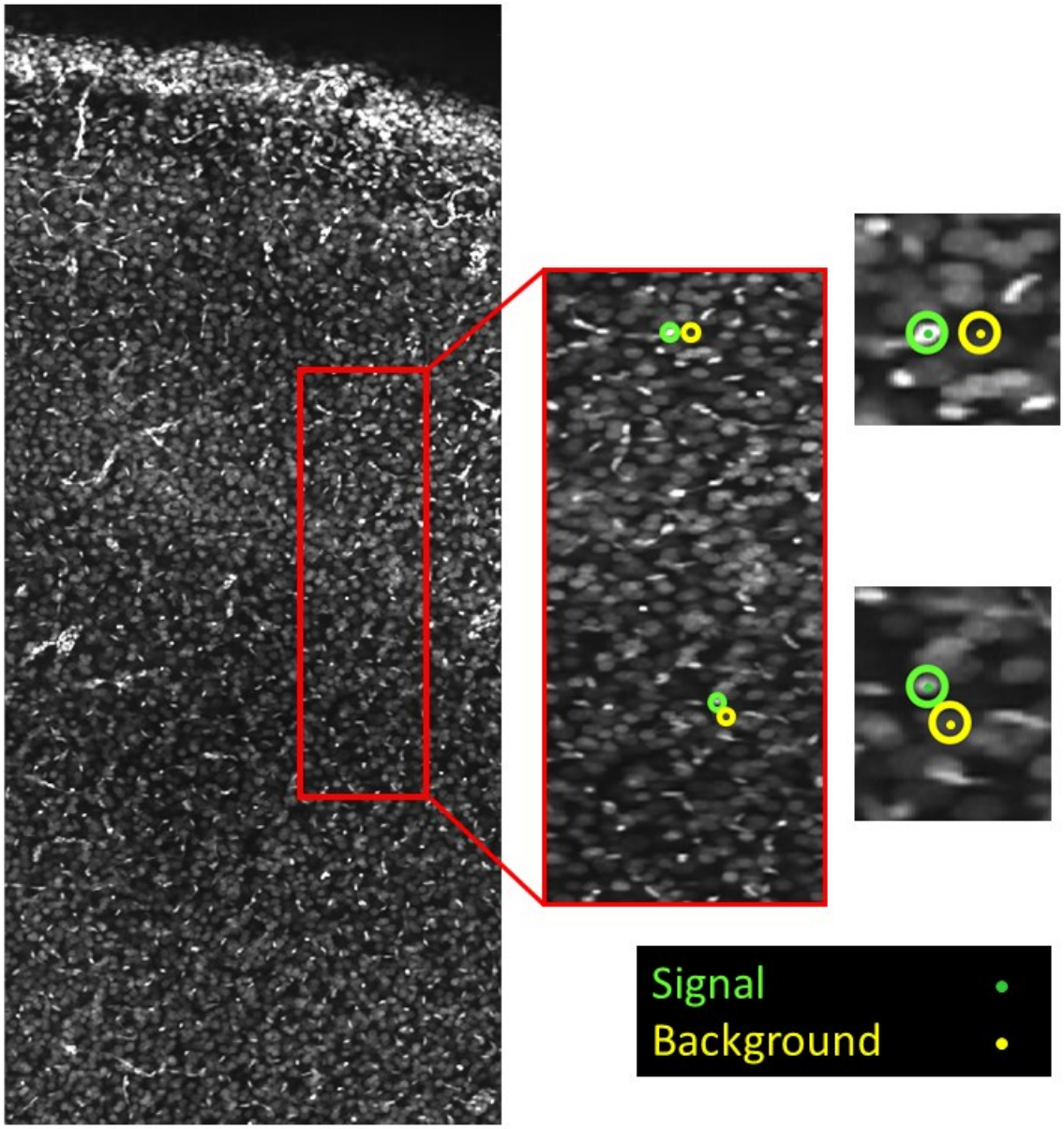

Figure 10. A demonstration of the sampling of the signal (in green) from inside two neurons, and the matching background (in yellow) adjacent to these two neurons.

CHAPTER 4 – RESULTS: EVALUATION OF THE METHODOLOGY

4.1. CUBIC-L & R

4.1.1. Effect of varying the duration of post-fixation on the duration required for the de-lipidation of mouse brain slabs at room temperature

This section demonstrates the application of the CUBIC-L reagent on mouse brain slabs, in experiments where we varied the duration of post-fixation periods.

Figure 11 provides the outline of the cutting pattern of 2-mm-thick and 3-mm-thick slabs with respect to bregma, and incubation of the mouse brain slabs in the lipid removal CUBIC-L reagent. The names of the slabs are given with reference to the bregma. Anterior and adjacent to bregma is named '1st anterior slab' and posterior and adjacent to bregma is '1st posterior slab'. With 3-mm thickness, we obtained 4 coronal slabs using the mouse brain matrix. Among the 4 coronal slabs, we used the first anterior, first-posterior and second-posterior slabs for our experiments. The third-posterior slab from bregma was discarded as it consists of the cerebellum and brain stem. Likewise, when testing with 2-mm thick slabs, five 2-mm-thick coronal slabs were obtained. We used the first 4 slabs from the anterior part of the mouse brain.

The processing of the 3-mm thick brain slabs from the time of the transcardial perfusion until sufficient transparency was achieved is demonstrated in **Figure 12**. The post-fixation was carried out for 2 hrs. **Figure 13** presents the rate of delipidation of 3-mm brain slabs post-fixed for 24 hrs. The corresponding graphical representations of the mean and S.D. durations is presented in **Figure 14** for the data presented in **Figure 12** and **Figure 13**. These graphs indicate the average number of days taken by the CUBIC-L reagent to achieve transparency. These graphs included data from 4 and 9 mice brains with samples post-fixed for 2 hrs and 24 hrs, respectively. **The results show two clear trends. First, slabs cut posteriorly to bregma took significantly more time to clear than slabs cut anteriorly to bregma.** The mean time it took to delipidate 3-mm thick '1st anterior slabs' at RT (62±8.8 days) was shorter than the time it took to delipidate the 'posterior 1st slabs' (102.4±15.5 days; $p<4.2\times10^{-6}$, two-tail t test). It was also shorter than the time it took to delipidate the 'posterior 2nd slabs' (123.0±10.7 days; $p<5.0\times10^{-10}$, two-tail t test). **Second, slabs post-fixed for 24 hours took significantly more time to clear than slabs post-fixed**

for 2 hours (See below a statistical test for the difference between delipidation of slabs post-fixed for 6 hrs and 24 hrs).

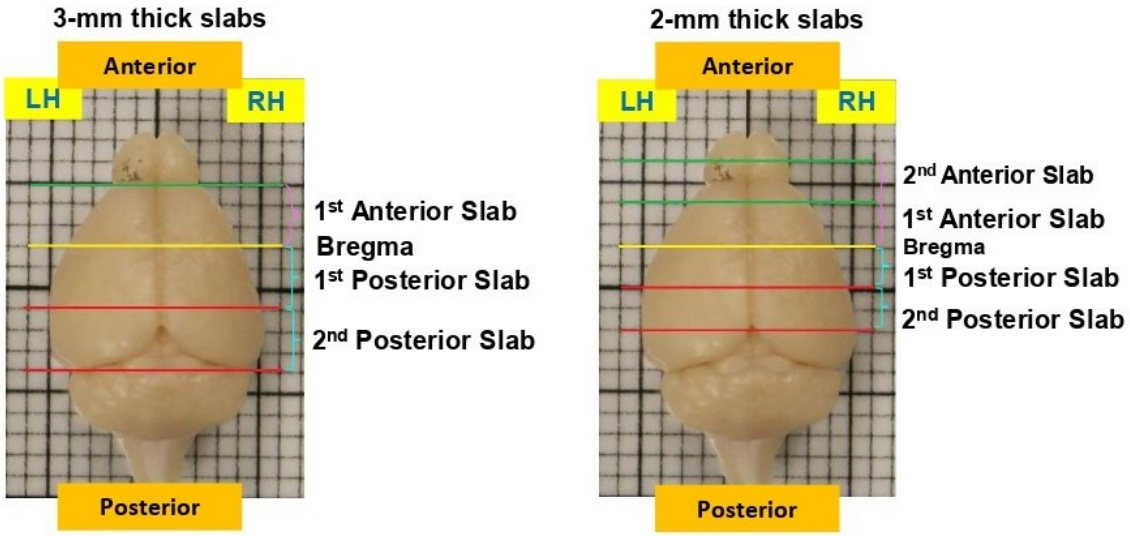

Figure 11. An overview of the mouse brain cutting pattern for CUBIC-L based de-lipidation. For 3-mm (left) and 2-mm (right) thick slabs. The coronal cuts were made at the green, yellow, and red markings. The yellow line indicates the position of bregma. The region between the yellow and green markings represents the 1st anterior slab. The region between the two green markings represents the 2nd anterior slab. Similarly, the region between the yellow and red markings represents the 1st posterior slab, and the region between red markings represents the 2nd posterior slab.

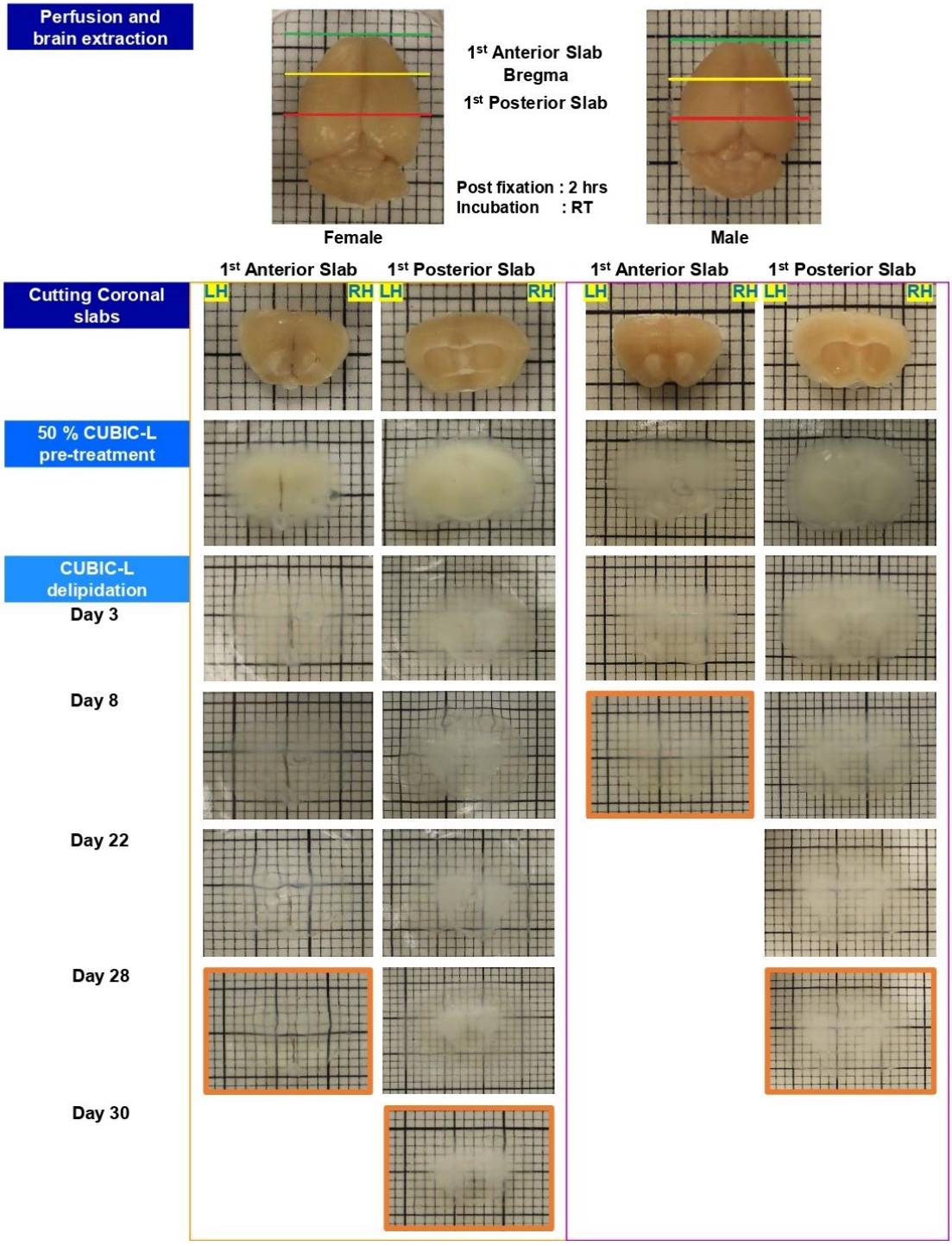

Figure 12. The rate of delipidation of 3 mm thick mouse brain slabs from the time of extraction of the brain following perfusion until completing the tissue clearing. We used the CUBIC-L reagent. We present data from two mice. All slabs were post-fixed for 2 hours. An orange frame indicates that the clearing completed.

A.

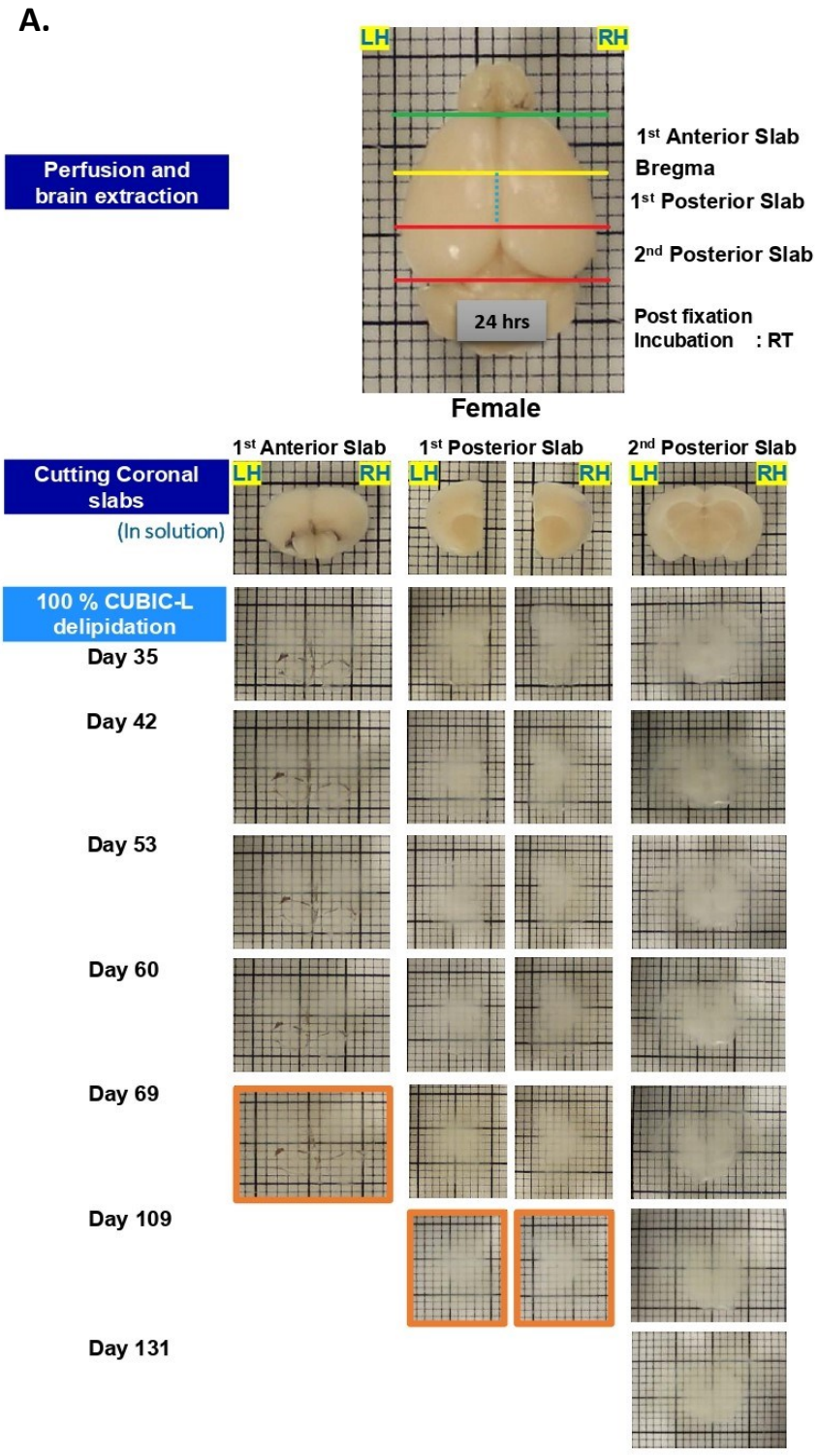
Perfusion and brain extraction
LH
RH
1st Anterior Slab
Bregma
1st Posterior Slab
2nd Posterior Slab
24 hrs
Post fixation
Incubation : RT
Female
1st Anterior Slab
1st Posterior Slab
2nd Posterior Slab
Cutting Coronal slabs
(In solution)
100 % CUBIC-L delipidation
Day 35
Day 42
Day 53
Day 60
Day 69
Day 109
Day 131

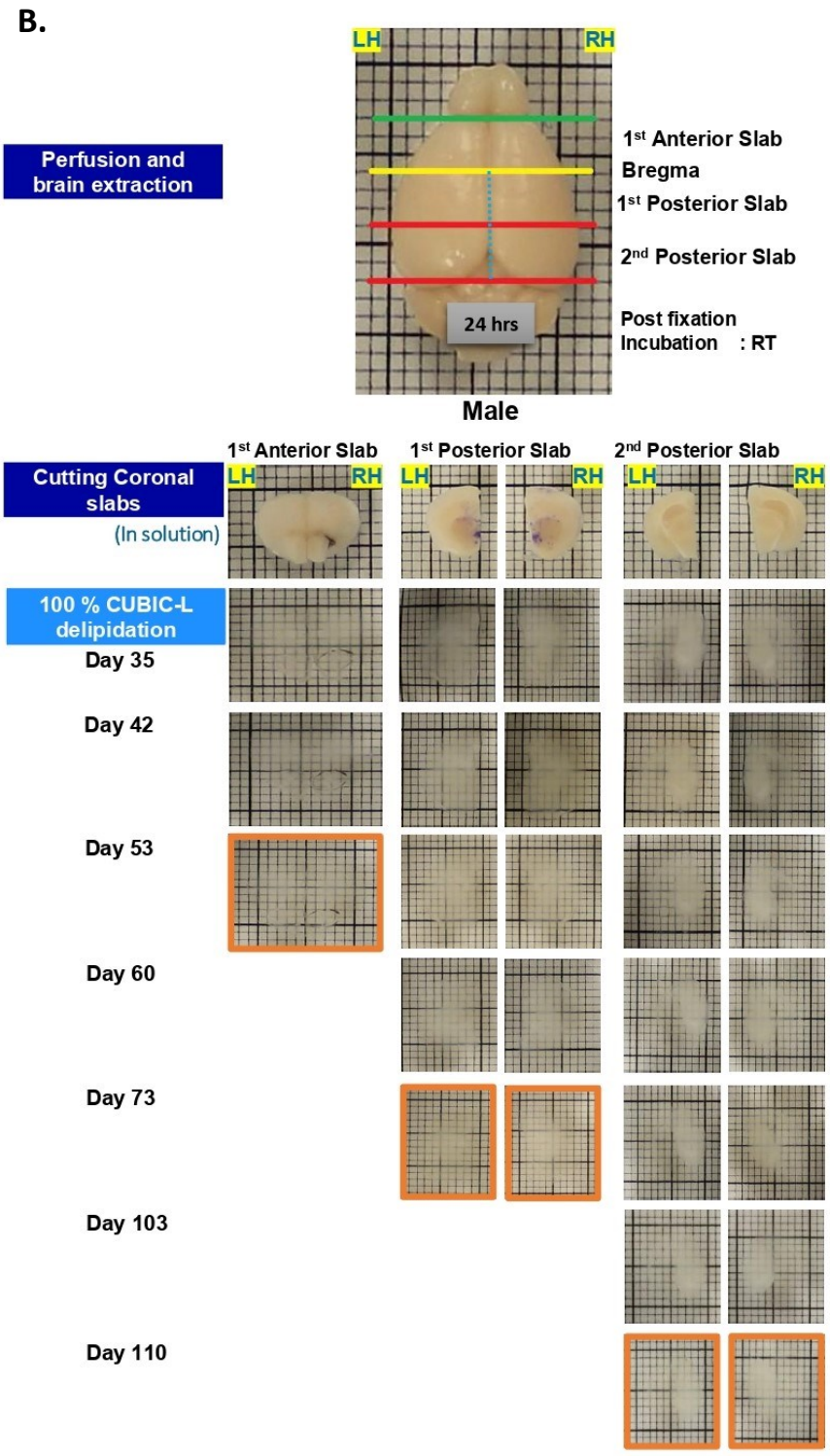

Figure 13. The rate of delipidation of 3 mm thick mouse brain slabs. The Figure presents slabs from 2 brains that were post-fixed for 24 hours. A de-lipidation completion status is denoted by an orange frame.

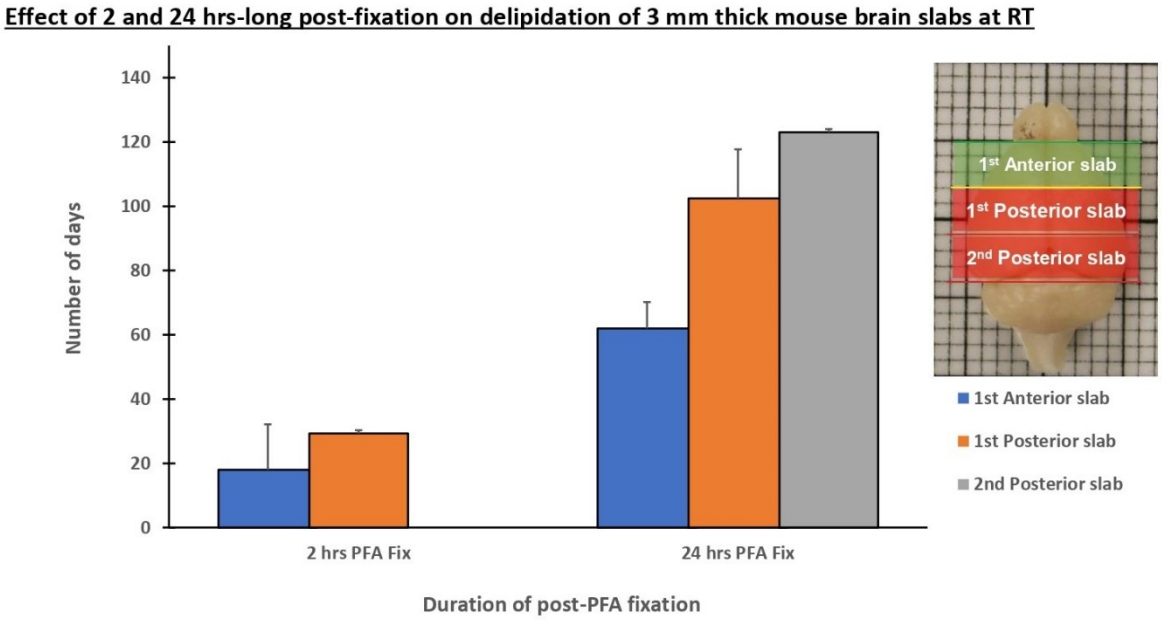

Figure 14. The average number of days required for CUBIC-L reagent-based clearing of slabs post-fixed for 2 hours and for 24 hours.

To further test the effect of post-fixation duration on the delipidation rate and to test whether slabs thinner than 3 mm will clear faster, the brain slab thickness was reduced from 3- to 2-mm. Following the perfusion, the brain hemispheres were separated with a cut along the mid-sagittal plane. Then the left- and right- hemispheres were post-fixed for 24 hrs and 6 hrs, respectively. Following the post-fixation, four 2-mm thick coronal slabs were cut using a mouse brain matrix, and were immersed CUBIC–L. **Figure 15** presents the 2-mm brain samples clearing process from two animals. The average number of days required for the CUBIC–L clearing is illustrated by **Figure 16**. As already observed with 3-mm thick slabs, there was a clear trend of **slabs cut posteriorly to bregma taking significantly more time to clear than slabs cut anteriorly to bregma.** Also, as already observed with 3-mm thick slabs, **there was a clear trend of increasing delipidation duration with increasing post-fixation duration**. The mean delipidation duration (at RT) of 3 mm slabs post-fixed for 24 hours (14.7±9.9 days) was longer than the mean time it took to delipidate slabs that were post-fixed for 6 hours (7.7±4.8 days; ($p < 0.009$ two tail t test).

Lastly, comparing the delipidation duration at RT required for 3-mm thick slabs (95.8±28.3 days, mean±SD; **Fig. 14**) and 2-mm thick slabs (14.7±9.9 days; **Fig. 16**) post-fixed for 24 hours, we

A.

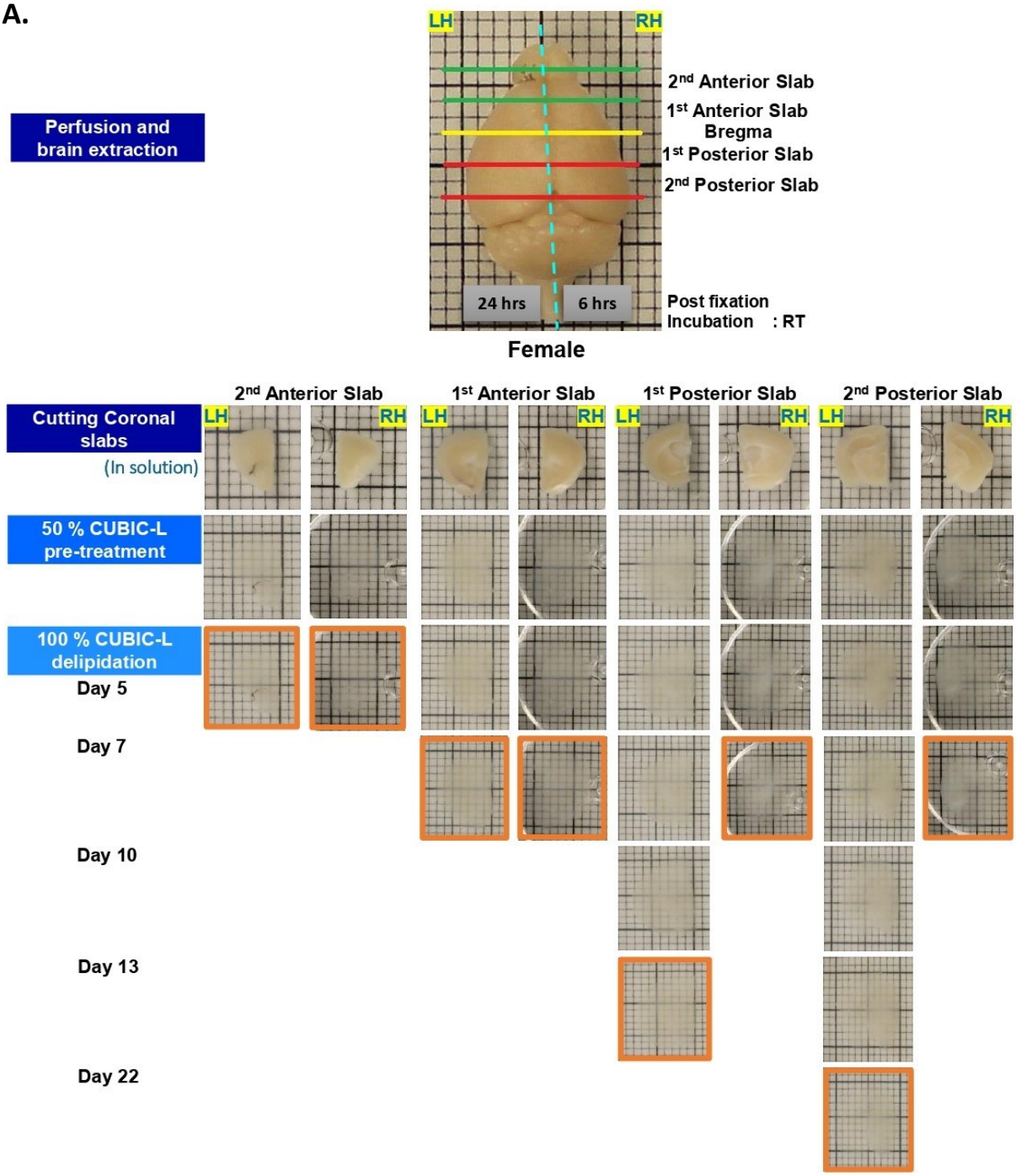
Perfusion and brain extraction
LH
RH
2nd Anterior Slab
1st Anterior Slab
Bregma
1st Posterior Slab
2nd Posterior Slab
24 hrs
6 hrs
Post fixation Incubation : RT
Female
2nd Anterior Slab
1st Anterior Slab
1st Posterior Slab
2nd Posterior Slab
Cutting Coronal slabs
(In solution)
50 % CUBIC-L pre-treatment
100 % CUBIC-L delipidation
Day 5
Day 7
Day 10
Day 13
Day 22

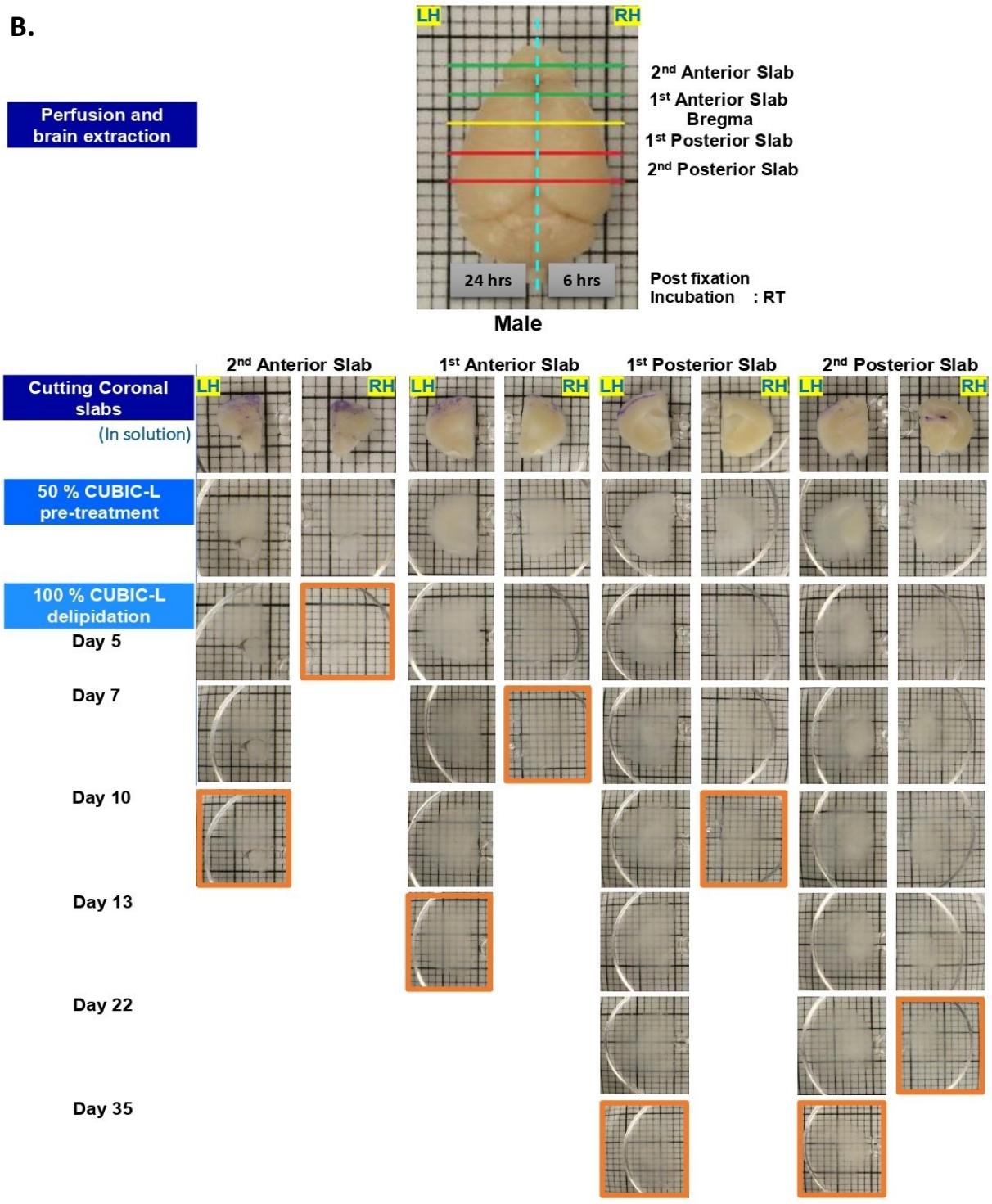

Figure 15. The effect of post-fixation duration on the delipidation of 2-mm thick slabs at RT. Panels A and B present data from two different mice. The left and right brain hemispheres of each mouse were post-fixed for 24 hrs and 6 hrs, respectively. A de-lipidation completion status is denoted by an orange frame.

observed **a clear statistically significant increase in delipidation duration (at RT) with an increase in slab thickness** ($p < 7.6\times10^{-14}$; two tail t test).

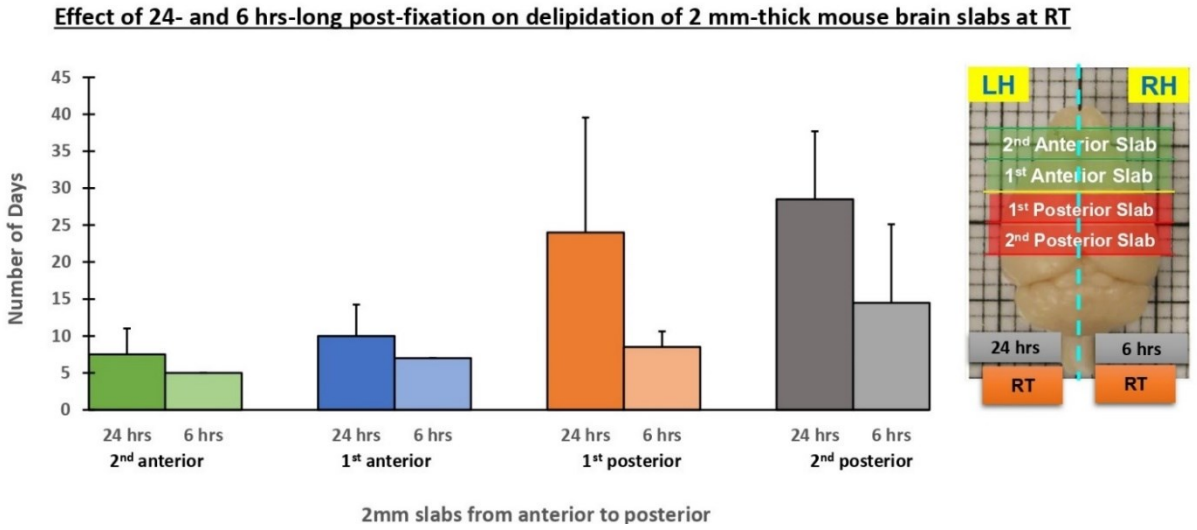

Figure 16. The effect of post-fixation duration on delipidation of 2-mm thick mouse brain slabs. The figure presents the number of days taken for CUBIC-L mediated delipidation for each slab. The post-fixation was performed for 24 and 6 hrs on the left hemisphere (LH) and right hemisphere (RH), respectively. The cutting plan is outlined on the image to the right.

4.1.2. The effect of incubation temperature on the duration required for clearing rodent brain slabs

Mice experiments:

To test the effect of incubation temperature on CUBIC clearing, we carried out additional experiments at 37^0C and room temperature (RT) and compared the duration required for clearing. We separated the hemispheres by cutting along the mid-sagittal plane. Each hemisphere was post-fixed for 24 hrs or 6 hrs. Then, we incubated the samples at RT or 37^0C (**Figure 17**).

In each analysis, two mouse brains were used. Initially, the brain hemispheres were separated along the midline, and then were post-PFA fixed for 24 hrs and 6 hrs, respectively. Following the post-fixation, four 2-mm thick coronal slabs were cut using a mouse brain matrix. Contralateral

slabs were immersed in CUBIC–L solution at 37^{0}C or RT. The clearing process, from the time of extraction to clearing of 4 mouse brains is shown in **Figure. 18**. **Figure 19** presents the average duration of delipidation. A strong trend can be observed, of **shorter duration of clearing at 37^{0}C relative to RT.** For slabs post-fixed for 24 hours. The mean duration it took to delipidate 2 mm-thick slabs post-fixed for 24 hours at 37^{0}C was 7±3.6 days, compared to 14.7±9.9 days it took on average to delipidate similar slabs in RT slabs' ($p<0.017$, two-tail t test). In contrast, we found no statistically significant difference between the delipidation durations at 37^{0}C and RT for 2 mm slabs post-fixed for 6 hours ($p = 0.22$).

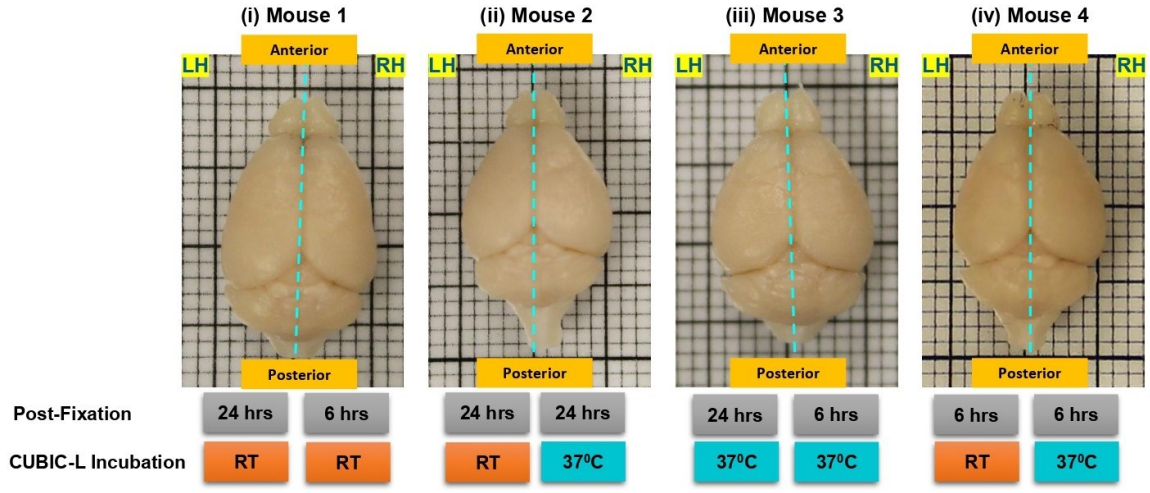

Figure 17. The experimental plan for evaluating the effect of the temperature and duration of post-fixation on the delipidation. RT, room temperature.

A.

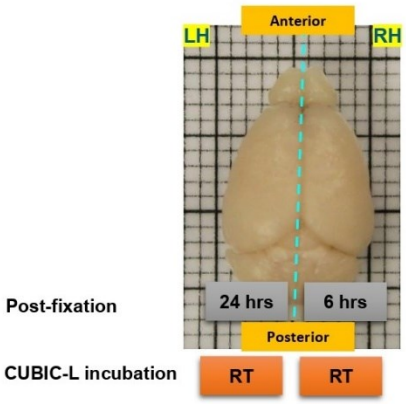

100 % CUBIC-L delipidation	Day 5	Day 7	Day 13	Day 16	Day 21
LH, 2nd Anterior Slab					
RH, 2nd Anterior Slab					
LH, 1st Anterior Slab					
RH, 1st Anterior Slab					
LH, 1st Posterior Slab					
RH, 1st Posterior Slab					
LH, 2nd Posterior Slab					
RH, 2nd Posterior Slab					

B.

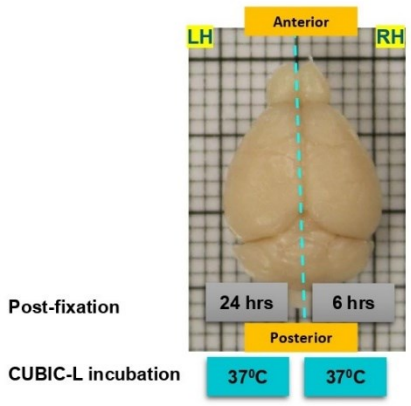

100 % CUBIC-L delipidation	Day 5	Day 7	Day 13	Day 16	Day 21
LH, 2nd Anterior Slab					
RH, 2nd Anterior Slab					
LH, 1st Anterior Slab					
RH, 1st Anterior Slab					
LH, 1st Posterior Slab					
RH, 1st Posterior Slab					
LH, 2nd Posterior Slab					
RH, 2nd Posterior Slab					

C.

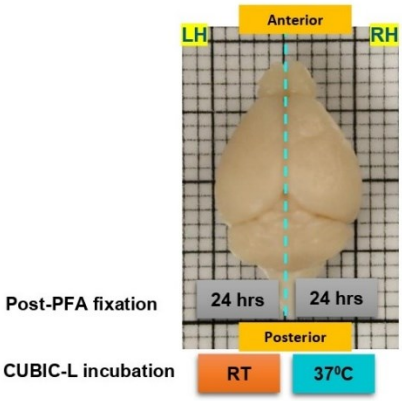

100 % CUBIC-L delipidation	Day 5	Day 7	Day 13	Day 16	Day 21
LH, 2nd Anterior Slab					
RH, 2nd Anterior Slab					
LH, 1st Anterior Slab					
RH, 1st Anterior Slab					
LH, 1st Posterior Slab					
RH, 1st Posterior Slab					
LH, 2nd Posterior Slab					
RH, 2nd Posterior Slab					

D.

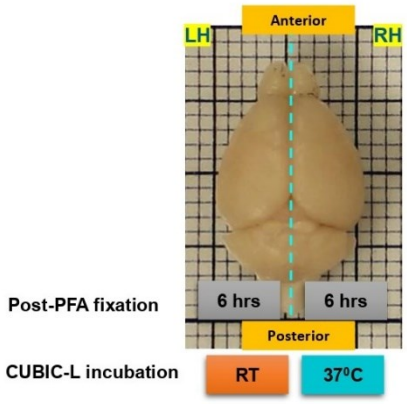

100 % CUBIC-L delipidation	Day 5	Day 7	Day 13	Day 16	Day 21
LH, 2nd Anterior Slab					
RH, 2nd Anterior Slab					
LH, 1st Anterior Slab					
RH, 1st Anterior Slab					
LH, 1st Posterior Slab					
RH, 1st Posterior Slab					
LH, 2nd Posterior Slab					
RH, 2nd Posterior Slab					

Figure 18. The effect of temperature used during the delipidation on the rate of delipidation of 2-mm thick mouse brain slabs. A, B, C, and D present data from four different rats. The left and right hemispheres in A were delipidated in RT; in B, in 37^{0}C; The left and right hemispheres in C (and D) were delipidated in RT and 37^{0}C, respectively.

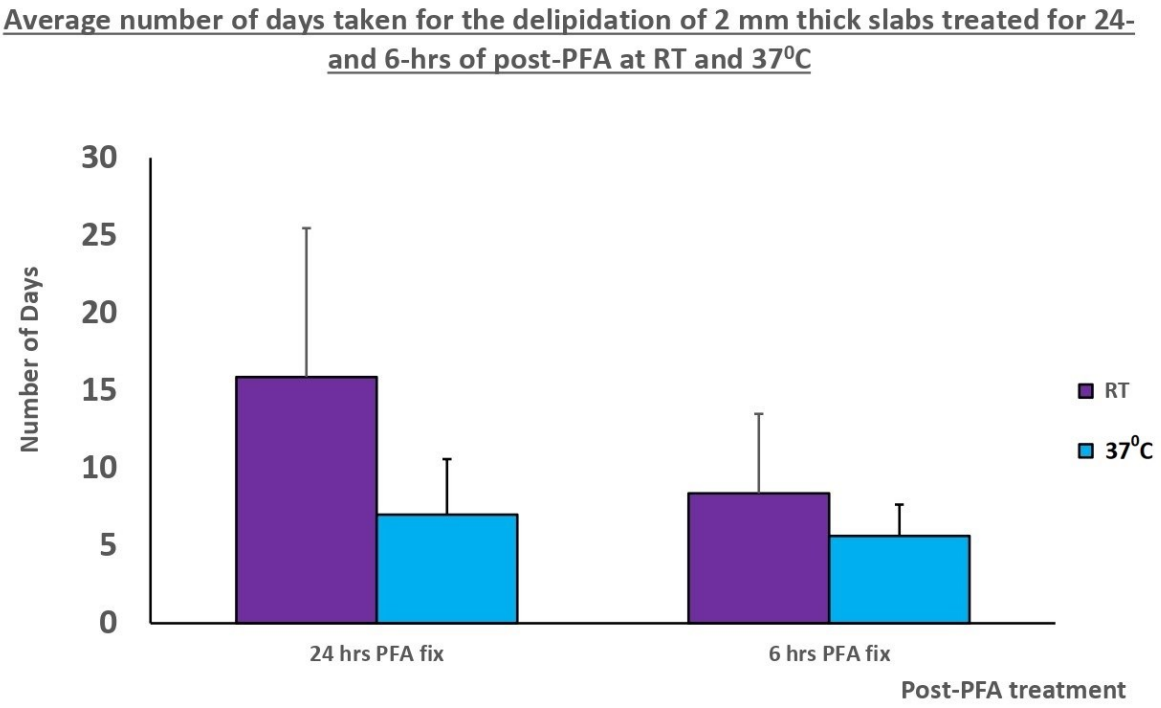

Figure 19. The effect of temperature during delipidation on the duration of CUBIC - L delipidation. Note that the figure presents data of varying the temperature and the post-fixation duration. Each bar represents the mean and SD obtained from 4 hemispheres.

Rat experiments:

To test the effect of post-fixation duration on the duration of CUBIC clearing, we carried out similar experiments in rats. Following the perfusion, the two hemispheres were separated by performing a cut along the mid-sagittal plane. Each hemisphere was post-fixed separately, for 6 or 24 hours. Then, eight 2-mm thick coronal slabs were cut from each hemisphere using a rat brain matrix. **Figure 20** presents the cutting pattern and naming for each slab. Then, each slab was immersed in CUBIC-L at 37^{0}C. The clearing timeline is shown in **Figure 21. Figure 22** presents the average delipidation rate computed from four-rat brain experiments.

As already observed in mice, also in rats the duration of delipidation was longer for posterior slabs relative to anterior slabs. The average duration of delipidation of slabs post-fixed for 24 hours was longer than the duration required for delipidation of slabs post-fixed for 6 hours, although this trend was not statistically significant.

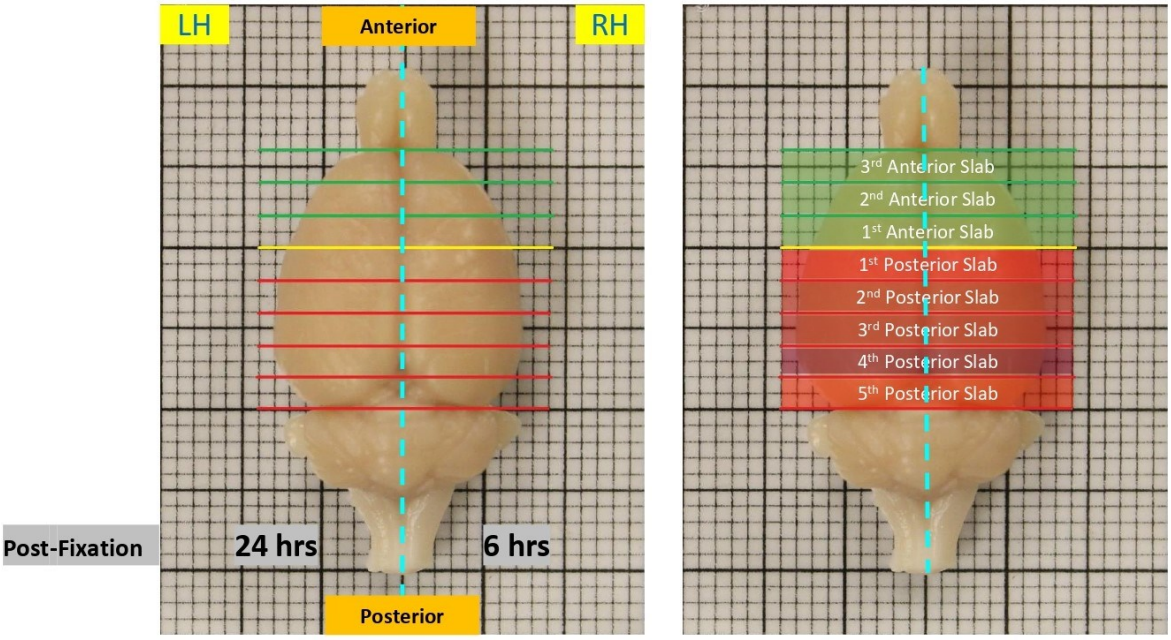

Figure 20. The cutting pattern of a rat brain for evaluating the effect of varying post-fixation durations. For cutting 2-mm-thick slabs (4.1.10, left), an initial sagittal cut was made along the midline (marked in cyan). Following the post-fixation, coronal slabs were cut (cuts are marked in green, yellow, and red lines). The yellow line indicates the bregma. The region between the yellow and green lines, and regions between green lines represent the anterior slabs. Similarly, the region between the yellow and red lines and those between red lines mark the posterior slabs.

A.

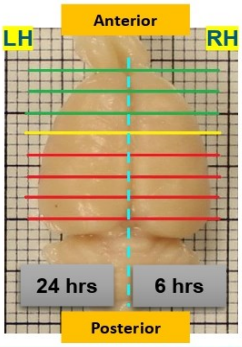

	After post-PFA fixation	100 % CUBIC-L delipidation					
		Day 4	Day 5	Day 7	Day 9	Day 10	Day 23
LH, 3rd Anterior Slab RH, 3rd Anterior Slab							
LH, 2nd Anterior Slab RH, 2nd Anterior Slab							
LH, 1st Anterior Slab RH, 1st Anterior Slab							
LH, 1st Posterior Slab RH, 1st Posterior Slab							
LH, 2nd Posterior Slab RH, 2nd Posterior Slab	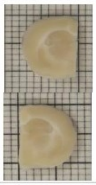						
LH, 3rd Posterior Slab RH, 3rd Posterior Slab							
LH, 4th Posterior Slab RH, 4th Posterior Slab							

B.

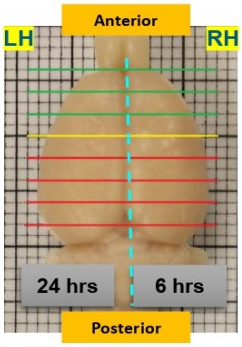

Post fixation

	After post-PFA fixation	100 % CUBIC-L delipidation					
		Day 4	Day 5	Day 7	Day 9	Day 10	Day 23
LH, 3rd Anterior Slab RH, 3rd Anterior Slab							
LH, 2nd Anterior Slab RH, 2nd Anterior Slab							
LH, 1st Anterior Slab RH, 1st Anterior Slab							
LH, 1st Posterior Slab RH, 1st Posterior Slab							
LH, 2nd Posterior Slab RH, 2nd Posterior Slab							
LH, 3rd Posterior Slab RH, 3rd Posterior Slab							
LH, 4th Posterior Slab RH, 4th Posterior Slab							

Figure 21. The effect of post-fixation durations on the delipidation rate of 2-mm thick rat brain slabs at 37^{0}C. The left and right brain hemispheres were post-fixed for 24 hrs and 6 hrs, respectively. Delipidation completion status is denoted by an orange frame.

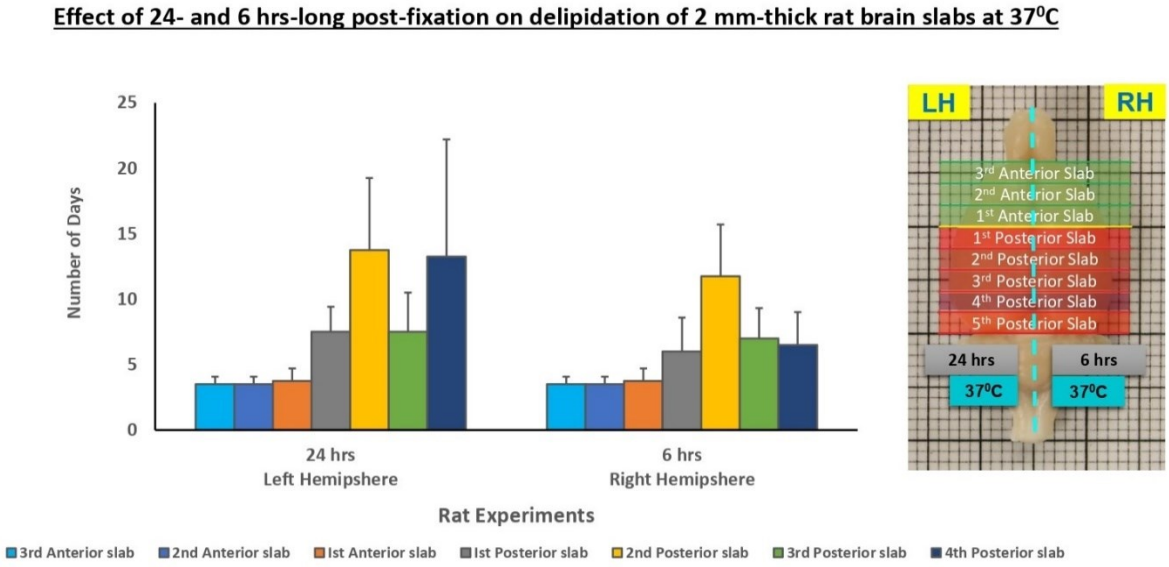

Figure 22. The average number of days taken for CUBIC - L delipidation of different slabs and post-fixation duration. Note the color code at the bottom, used for presenting data from different slabs.

..

4.1.3. The effect of age on the duration of CUBIC-L delipidation

To validate the effectiveness of the CUBIC-L reagent in clearing tissue across a range of ages, we used mice with age ranging from 2 to 7 months old. Following the brain extraction, all samples were post-fixed for 24 hrs, then cut into 2- and 3-mm thick slabs, then went through tissue clearing at RT. A total of four coronal slabs were obtained from each of 5 brain. The first group consisted of 2-, 5-, and 7- months old mice. The second group consisted of 3- and 6- months old mice. **Figure 23** provides the cutting pattern and naming for each slab, including 2- and 3- mm thick slabs with respect to bregma. We selected this plan in order to balance the number of 2- and 3- mm-thick Anterior and Posterior slabs in each animal and across the left and right hemispheres. The rates of delipidation for the anterior and posterior slabs are presented in **Figure 24.** As expected, there was a clear trend of increased clearing duration for 3 mm-thick slabs relative to 2 mm-thick slabs.

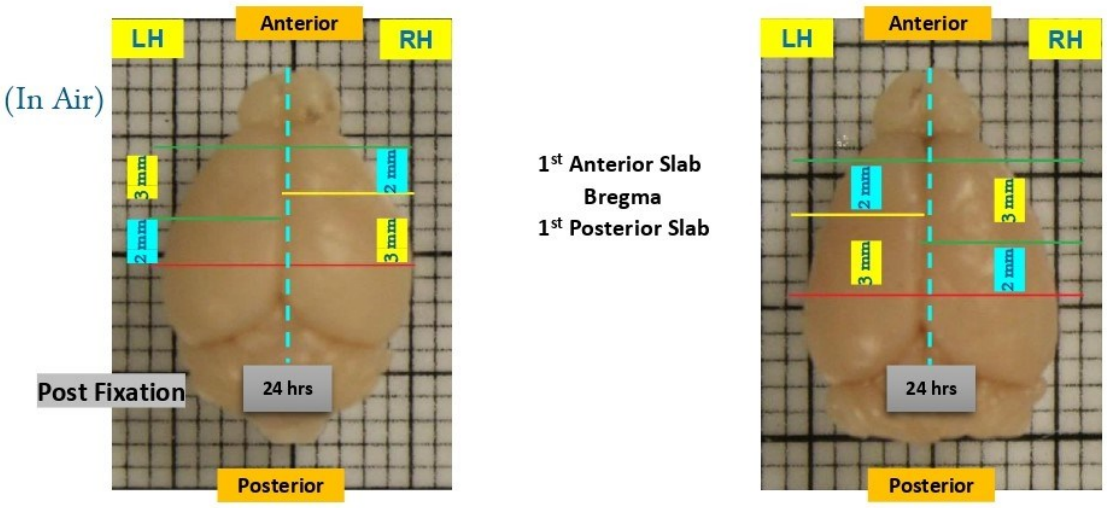

Figure 23. The mouse brain cutting patterns for group 1 (left) and group 2 (right) experiments. The dashed cyan line marks an initial mid-sagittal cut. Following 24 hours-long of post-fixation, coronal cuts were made along the green, yellow, and red lines. The yellow line indicates the bregma. The regions between the yellow and green lines (2-mm thick slabs) & green and green lines (3-mm thick slabs) represent the slab we term '1st anterior slab'. Similarly, the regions between the yellow and red lines (3-mm thick slabs) & the green and red lines (2-mm thick slabs) represent the 1stposterior slab.

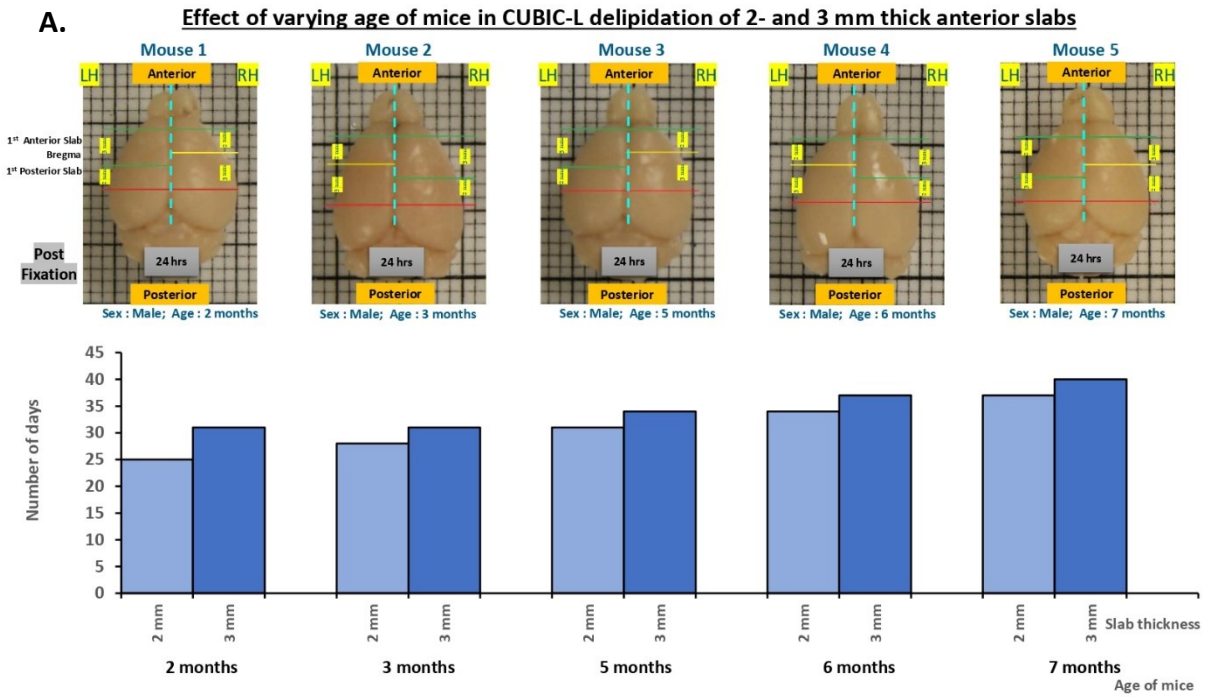

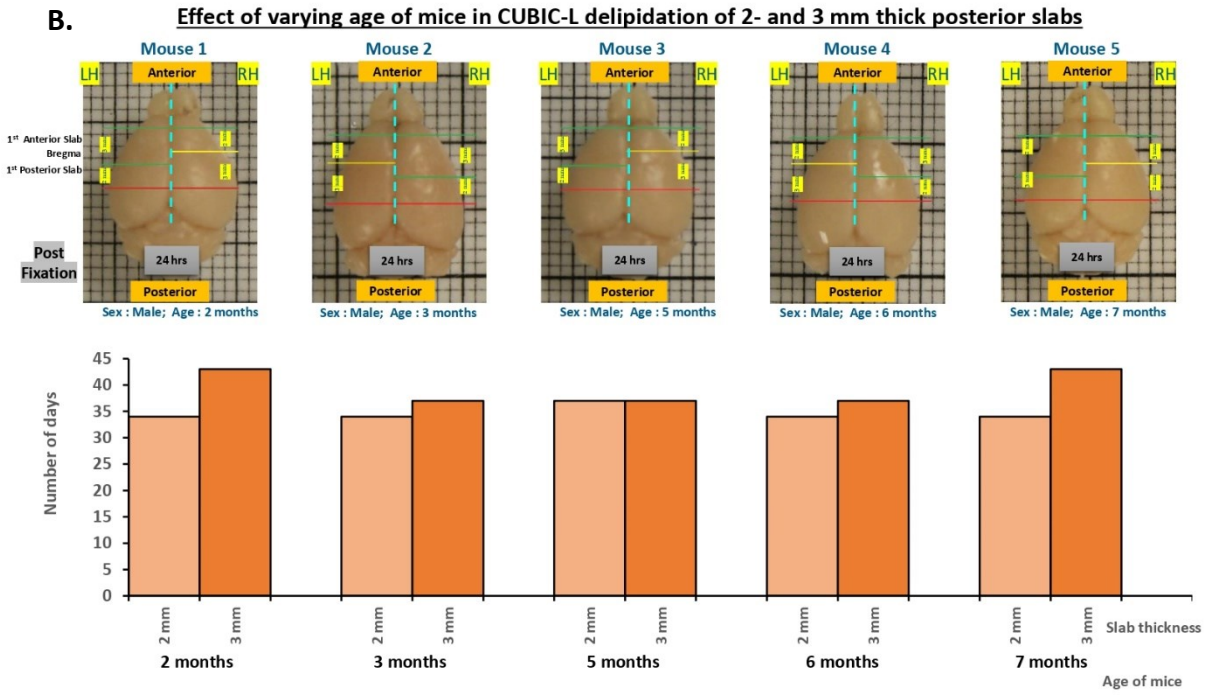

Figure 24. Effect of age on CUBIC-L mediated delipidation of 2- and 3 mm thick anterior (A) and posterior (B) slabs.

In addition, the anterior slabs showed a clear trend of increasing clearing duration with increasing age (**Fig. 24A**). This trend was less clear in the posterior slabs (**Fig. 24B**). **Figure 25** presents the mean and SD of clearing durations for 2 mm- and 3 mm-thick anterior and posterior slabs, confirming the trends observed in **Figure 24**.

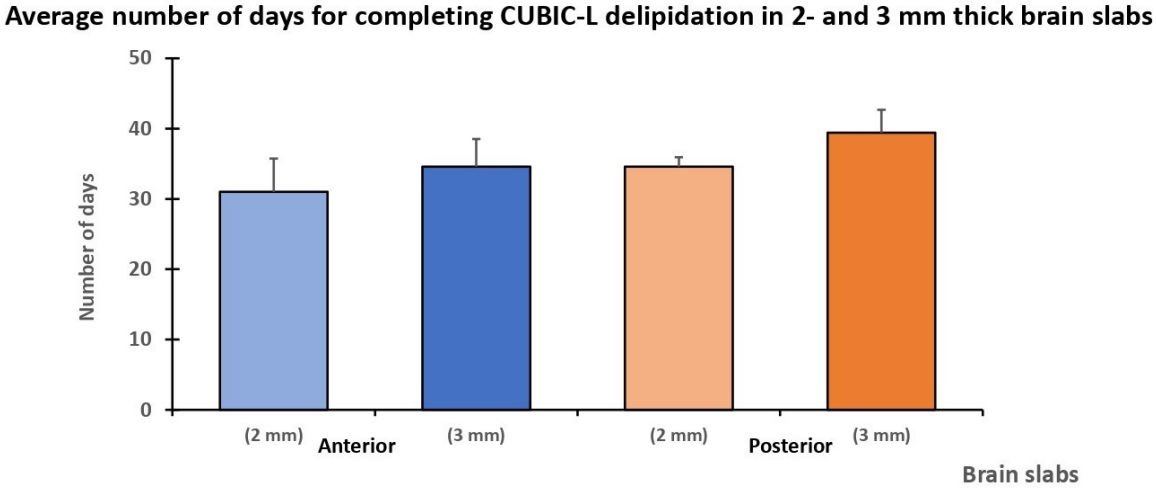

Figure 25. The effect of slab thickness and position on the duration of CUBIC-L delipidation in mice.

4.1.4. Optimization of Fluorescent Nissl stain (530/615 nm) concentration in rodent thick brain slabs

Mouse experiments:

To optimize the concentration of fluorescent Nissl stain (530/615 nm) for 3-mm thick mouse brain slabs, we used CUBIC-L cleared slabs. Following the tissue clearing, these slabs were thoroughly washed using PBS. As a result, the transparency of the slabs was lost and turned into non-transparent. The lost transparency was recovered during the CUBIC-R treatment step. We applied 6 different dilutions of the Nissl-Fluorescence stain, including (1:12.5), (1:25), (1:50), (1:75), (1:100), and (1:125). The fluorescent Nissl staining plan is given in **Figure 26**. This experiment plan was repeated in two mouse brains. For imaging, we used an Opera Phenix HCS fluorescent confocal spinning disk microscope. At 10X magnification, it produced images with sufficient resolution to identify distinct single labeled cells in brain slabs (Gómez-Gaviro et al., 2017). **Figure 27** presents the mean fluorescent Nissl stain intensity obtained from cortical ROIs in a mouse brain as a function of dilution. Except for one dilution (1:25), there was **a trend of increasing intensity with increasing concentration**. However, the differences within the dilution range of 1:12.5 to 1:75 were not large.

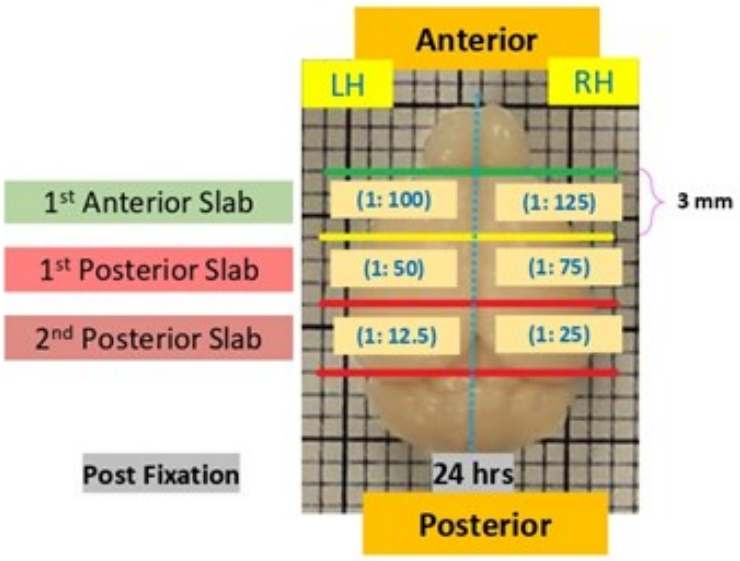

Figure 26. A presentation of the slabs used for applying fluorescent Nissl stain (530/615 nm) of different dilution in mouse brains. We used six different dilutions of Nissl stain, as denoted in the yellow rectangular boxes.

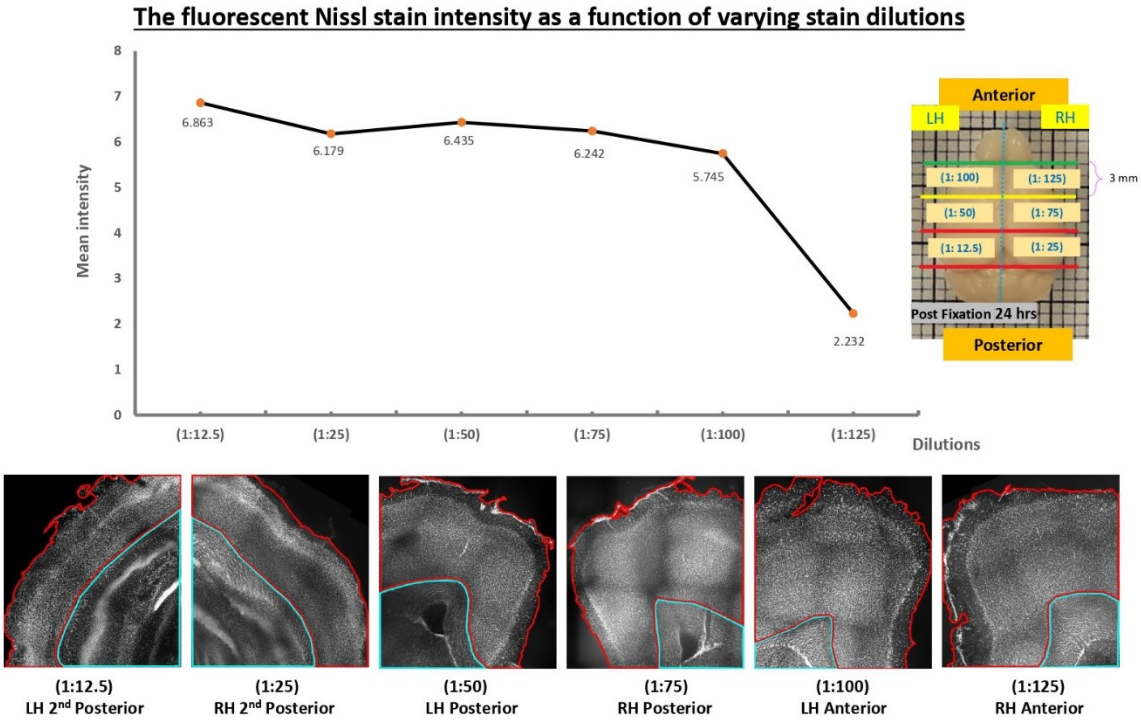

Figure 27. Fluorescent Nissl stain (530/615 nm) intensity as a function of dilutions in a mouse experiment. The intensity was averaged in cortex, delineated here in blue color.

As expected, we obtained increased intensity averaged over the slab with increasing concentration of the Nissl fluorescence. However, another feature is important for the detectability of neurons: the Signal to Background Ratio (SBR). To estimate the SBR, we sample the signal in the center of identified labeled neurons. Following the sampling of the intensity in a specific neuron, we sampled the background intensity close to the neuron but clearly outside of it. For the sampling. fifty neurons were selected from each of 5 ROIs and 6 dilutions. The selected neurons were distributed approximately homogeneously across the cortical depth. **Figure 28** presents the results in a format of the mean and SD of the SBR in each specific ROI presented by one bar. While the dilution of 1:75 presents an outlier SBR, all other 5 dilutions show **a trend of increased SBR with increasing concentration**.

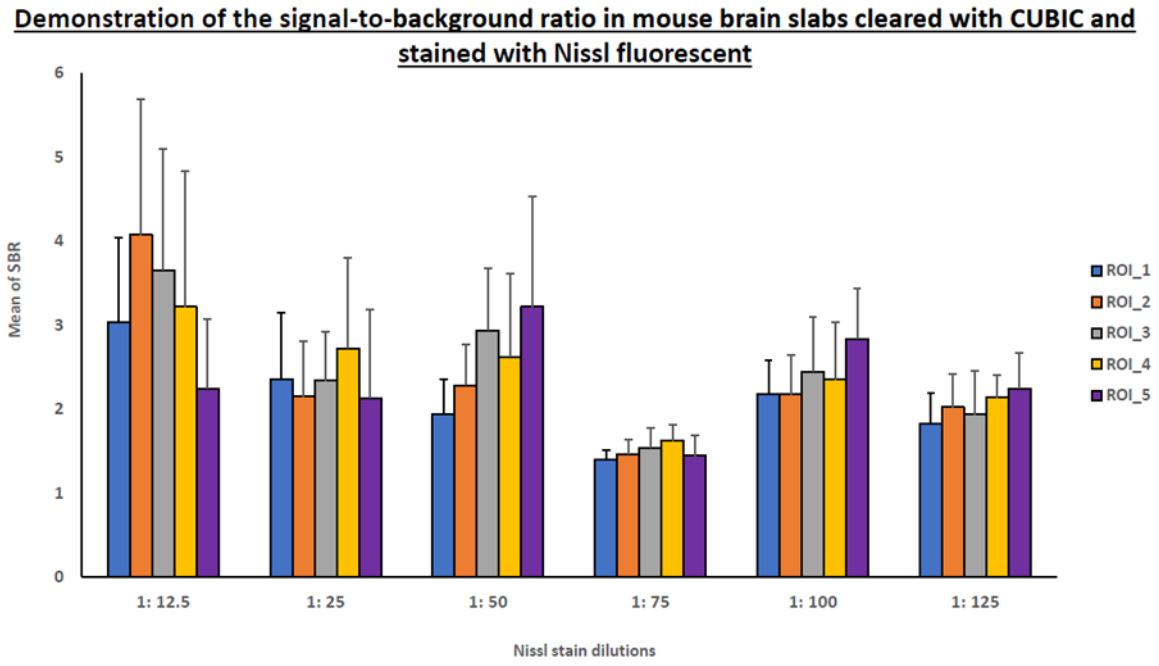

Figure 28. Signal-to-background (SNR) ratio of labeled neurons in mouse brain slabs cleared with CUBIC and stained with Nissl fluorescent.

Rat experiments:

We next optimized the concentration of fluorescent Nissl stain (530/615 nm) for 2-mm thick rat brain slabs cleared with CUBIC-L. Before starting Nissl staining, these cleared slabs were washed thoroughly by PBS. We employed 6 different dilutions including (1:12.5), (1:25), (1:50), (1:75), (1:100), and (1:125). The fluorescent Nissl staining plan is given in **Figure 29.**

The image acquisition was performed by an Opera Phenix HCS fluorescent confocal spinning disk microscope. At 10X magnification, single somas were clearly visible and identifiable. **Figure 30** presents the ROIs from the slabs extracted from the cerebral cortex of right hemisphere (note that we excluded the slab with dilution of 1:100, because it broke during the processing). We selected ROIs from the dorsal part of the hemisphere. All ROIs were approximately at the same distance from the midline. We delineated 10 rectangles in each slab's ROI, exclusively in cortex and arranged according to cortical depth. The upper panel in. **Figure 31** presents the mean and SD of the sampled signal to background as a function of dilution. For each dilution, the data are arranged according to the 5 ranges of cortical depth. Similar to the results obtained in mice, also in rats the mean SBR shows a strong trend of increase with increasing concentration.

Note that the dilution of 1:50 is an outlier to this trend. We hypothesized that this could be due to outliers in the data. We therefore plotted the scatter plot of all data points in the lower panel of Fig. 4.1.23. The lower panel, that presents the scatter plot of all sampled data points, shows that the SBR of the 1:50 dilution was pulled up by outliers. The SBR showed a string linear relationship with the inverse of the dilution (Correlation coefficient ® = 0.53; $p < 4.0 \times 10^{-23}$).

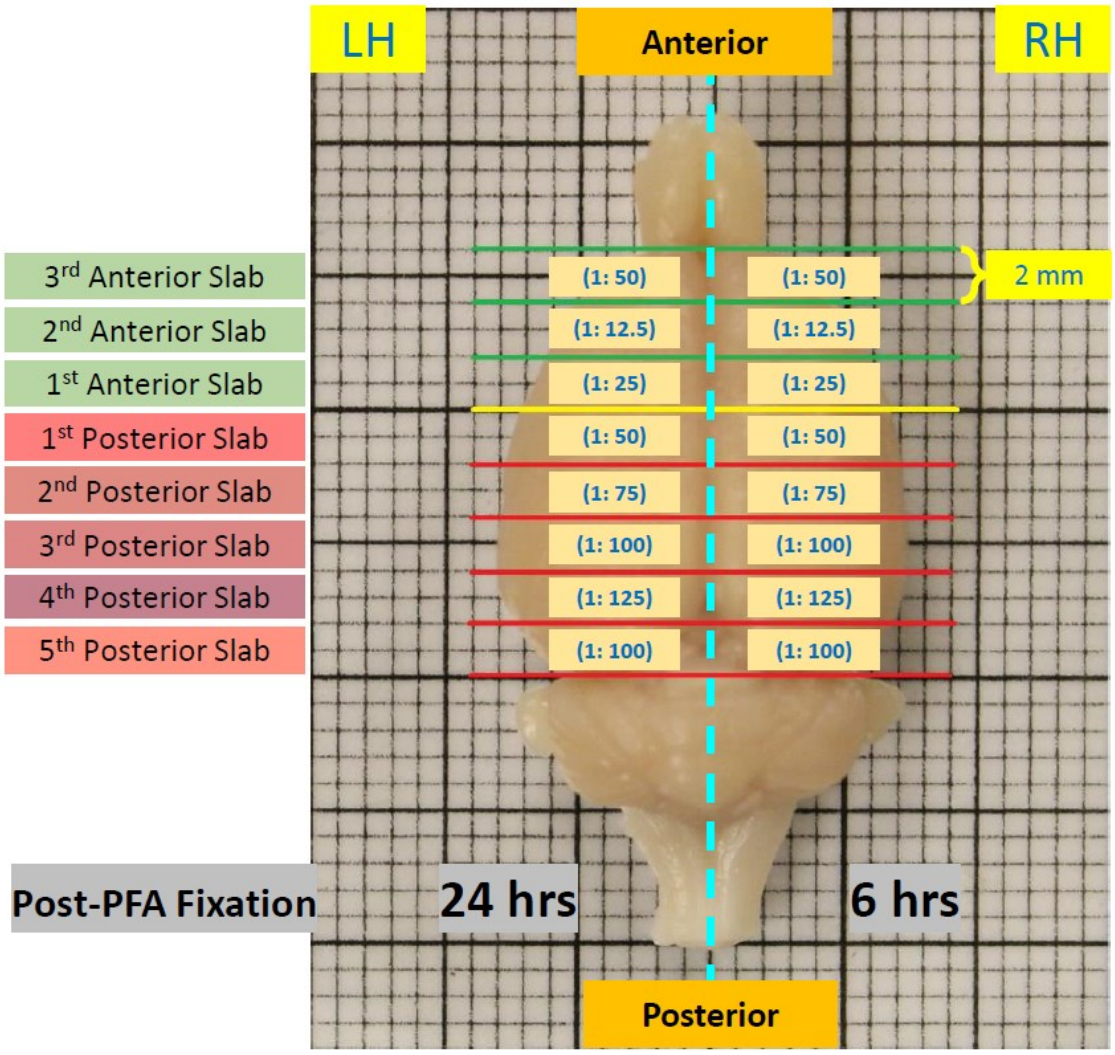

Figure 29. Staining with fluorescent Nissl stain (530/615 nm) in a rat brain. Six different dilutions of Nissl stain were used, as denoted by the yellow boxes.

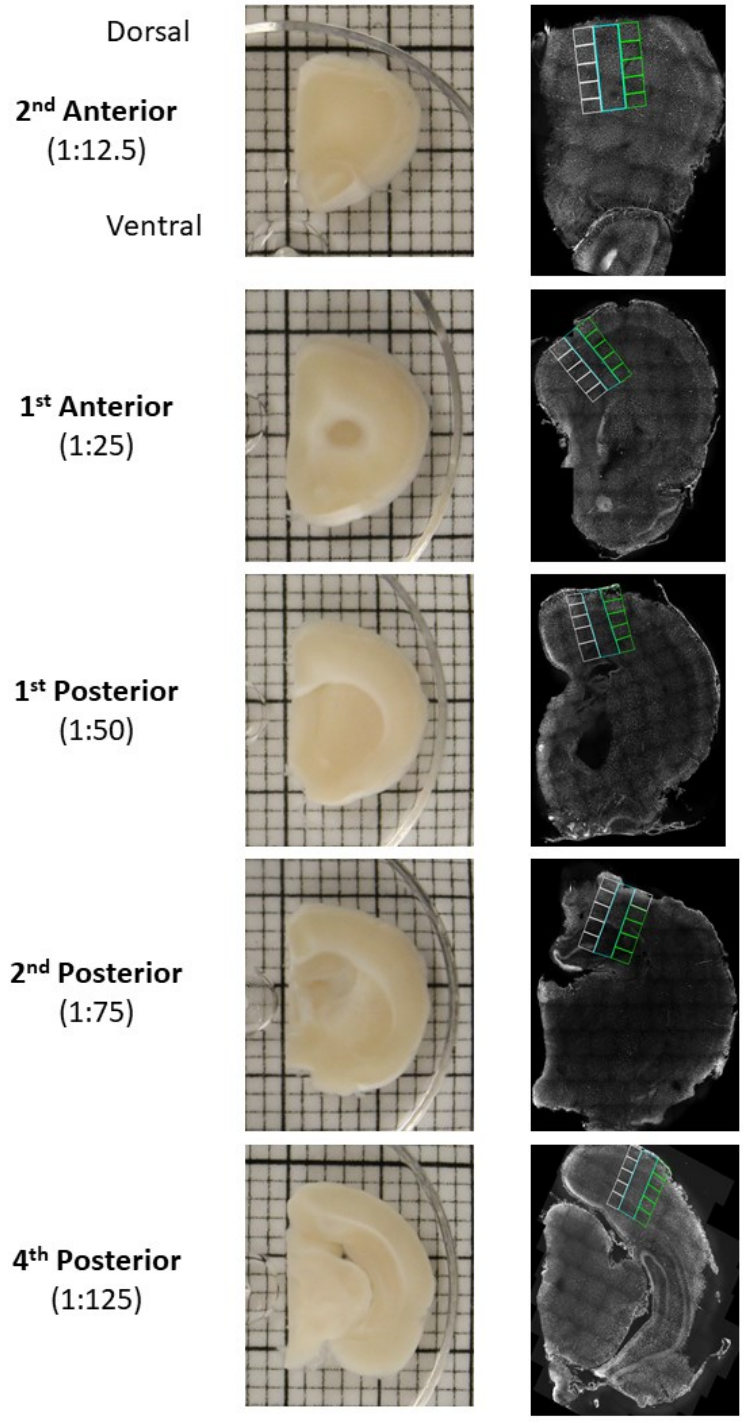

Figure 30. Fluorescent Nissl stain (530/615 nm) intensity (mean over the ROI) as a function of Nissl stain dilution tested in rat experiments. The intensity was averaged in cortical ROIs as presented by the panels at the bottom.

A. Demonstration of the signal-to-background ratio in rat brain slabs cleared with CUBIC and stained with Nissl fluorescent

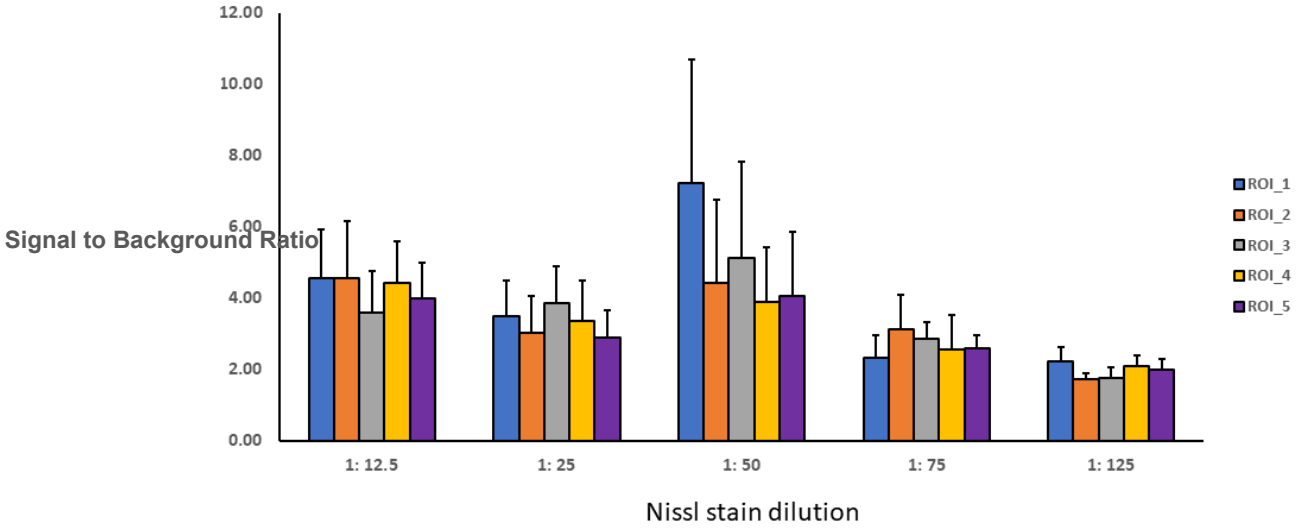

B. Scatter plot of the signal-to-background ratio in rat brain slabs cleared with CUBIC and stained with Nissl fluorescent

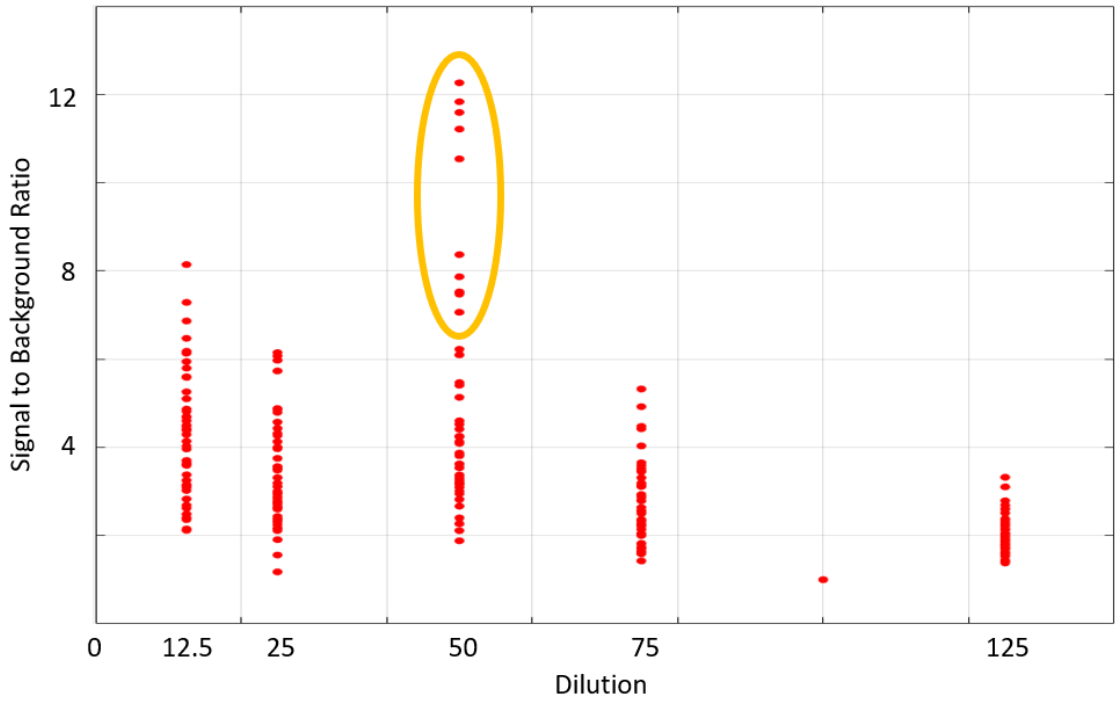

Figure 31. Fluorescent Nissl stain (530/615 nm) signal to background ratio (SBR) as a function of Nissl stain dilution tested in rat experiments. The SBR was averaged in cortical ROIs as presented in Figure 30. The upper panel (A) depicts the SBR measured with dilution 1:50 as high relative to 1:25 and 1:75. However, the lower panel (B), that presents the scatter plot of all sampled data points, shows that the SBR of the 1:50 dilution was pulled up by outliers (see the orange ellipse).

4.1.5. Comparing the CUBIC-L/R and X-CLARITY protocols as applied to 3-mm thick mouse brain slabs

Among the tissue clearing techniques, CUBIC is aqueous-based, and X-CLARITY is a tissue-transformation clearing method. As already presented in **Figure 13**, we found that the delipidation of 3-mm thick coronal slabs from the mouse brains fixed for 24 hrs took between 53 and 131 days. On average, clearing the anterior slabs took a smaller number of days compared to the posterior slabs. **Figure 32** presents the rate of delipidation of similar slabs (24 hours post-fixation, 3 mm-thick coronal slabs) using the X-CLARITY method. **Figure 33** presents the results in a graph. Within 6 hrs of electrophoretic X-clarity clearing, both the anterior and posterior slabs were delipidated completely.

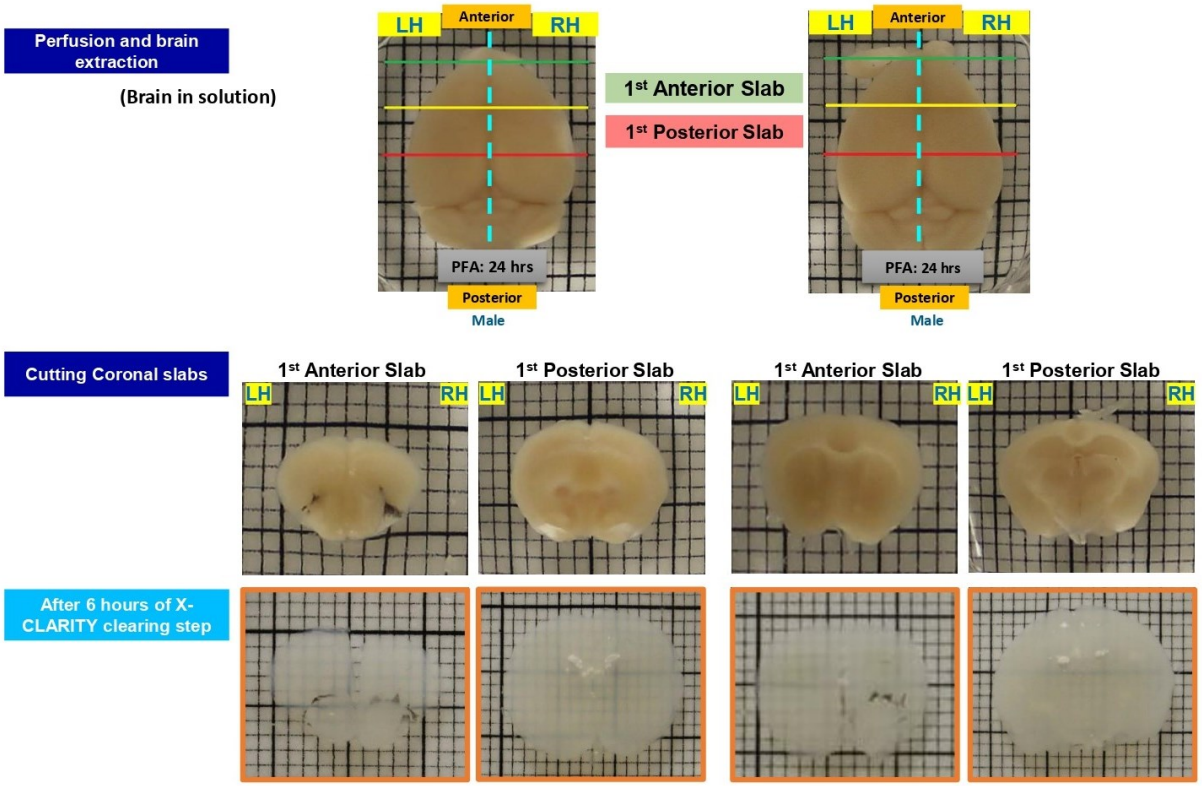

Figure 32. Demonstration of X-CLARITY tissue clearing.

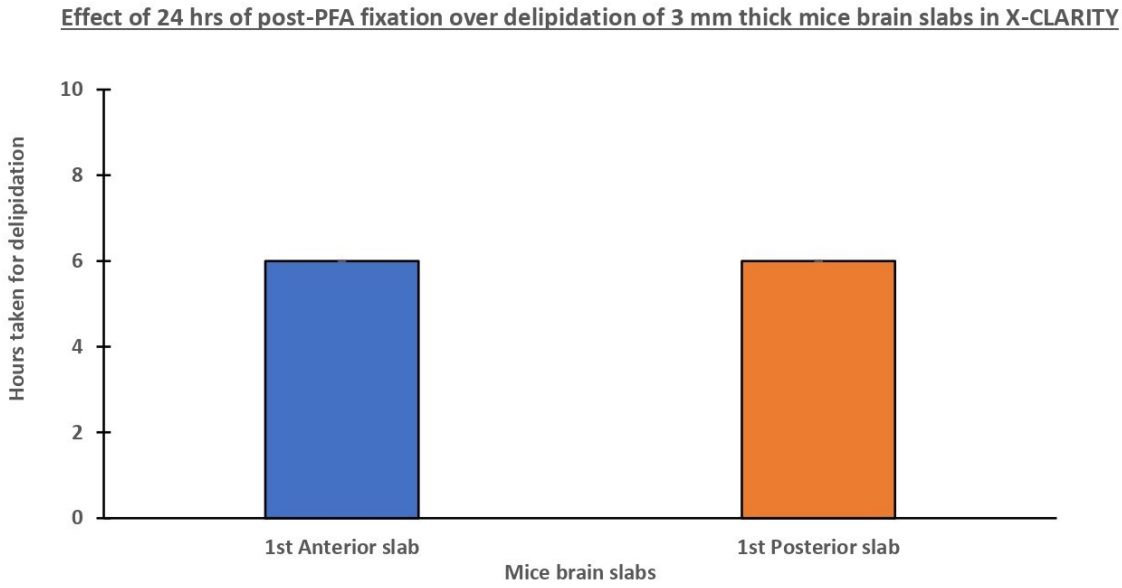

Figure 33. The duration of the electrophoretic tissue clearing of the X-CLARITY method. 3-mm thick slabs of mouse brains were used.

4.1.6 Quenching effect of RIMS in Nissl fluorescent 530/615 stained CUBIC-cleared mouse brain slabs

To evaluate the effect of quenching of RIMS - especially CUBIC-R - on NeuroTrace™ 530/615 Red Fluorescent Nissl Stain labeled CUBIC-cleared samples, we performed image acquisition of the same brain slabs one month and three months following the initial microscopy imaging. **Figure 34** presents microscopy images of an anterior slab from the left hemisphere of a mouse brain stained at a 1:100 dilution. The presented two image acquisitions were carried out 30 days apart. The intensities of these two images are shown in **Figure 35.** There is a clear decrease in fluorescence in the image taken 30 days following the initial acquisition. **Figure 36** presents similar images from a posterior slab stained with a 1:50 dilution. These two-image acquisitions were carried three months apart. **Figure 37** presents the corresponding intensities. Again, there is a clear decrease in fluorescence in the image taken 90 days following the initial acquisition.

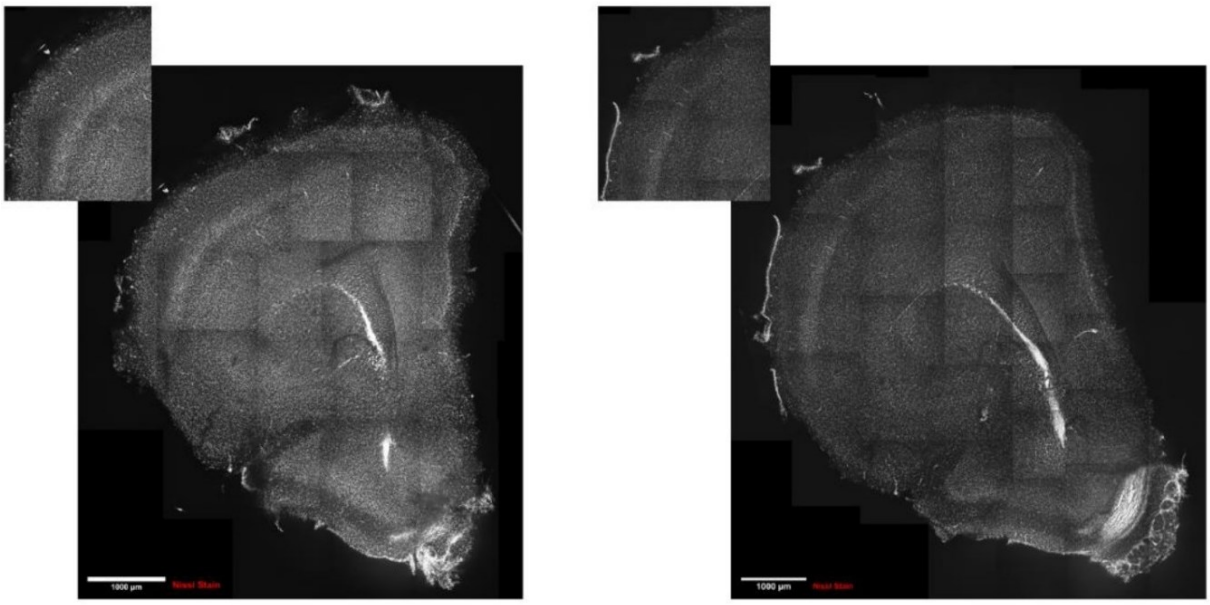

Figure 34. Demonstration of the Quenching effect of the CUBIC-R RIMS on a Nissl fluorescent 530/615 stained (1:100) CUBIC-cleared mouse brain slab. The second image (image to the *right*) acquisition was carried out 30 days after the acquisition of the first image (image to the *left*). *Scale bar: 1000 µm.*

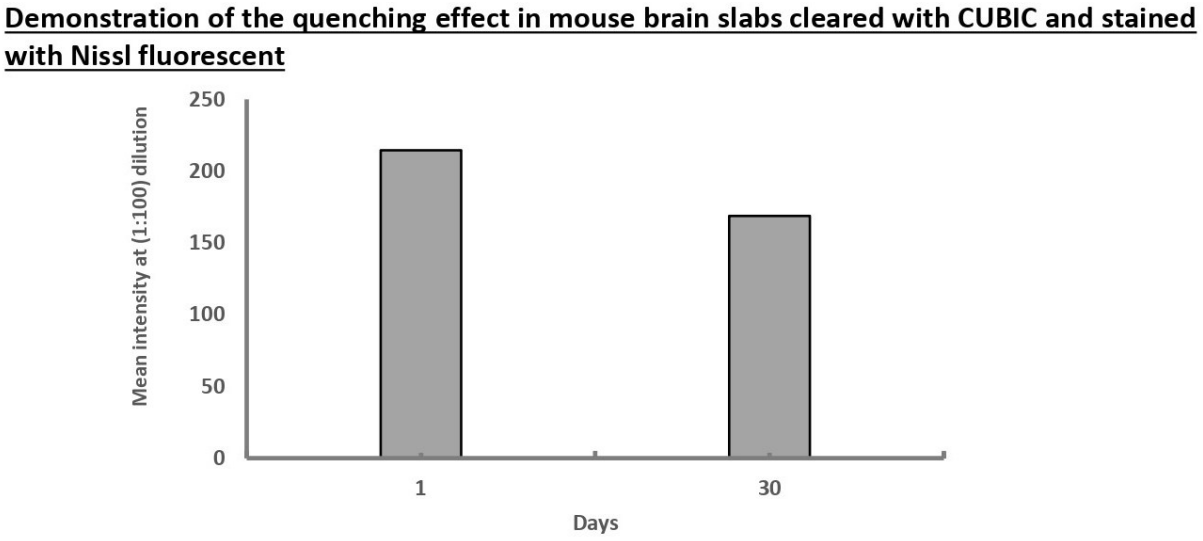

Figure 35. The mean intensity obtained in the cerebral cortex ROIs in two images acquired 30 days apart.

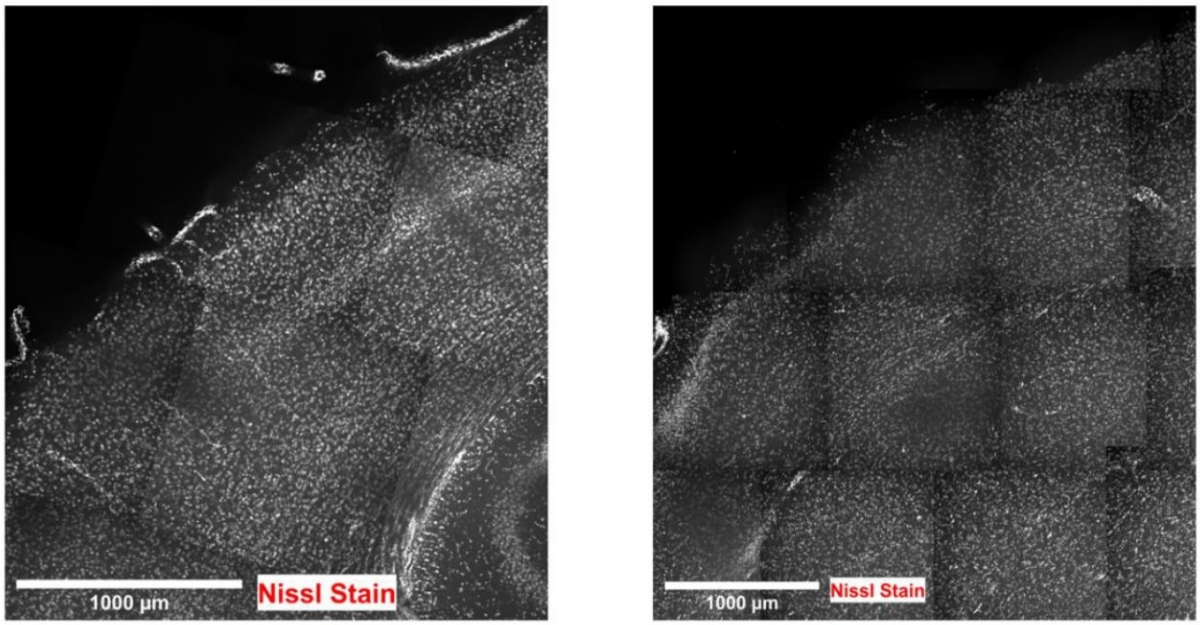

Figure 36. Demonstration of the Quenching effect of the CUBIC-R RIMS on a Nissl fluorescent 530/615 stained (1:100) CUBIC-cleared mouse brain slab. The second image (image to the *right*) acquisition was carried out 90 days after the acquisition of the first image (image to the *left*). *Scale bar: 1000 µm.*

Figure 37. The mean intensity obtained in the cerebral cortex ROIs in two images acquired 90 days apart.

4.1.7. IHC labeling in 3 mm-thick CUBIC-cleared mouse brain slabs

To check the immunostaining compatibility of the CUBIC-cleared mouse brain slabs, we performed IHC labeling to label dendrites using MAP2 antibodies. The brain slabs were incubated in primary antibody solution (anti-MAP2; dilution 1:500) in a shaker for 3 days at 4^0C and 80 rpm. Following washes, the tissue was immersed in the fluorescent secondary antibody solution (Alexa 488; dilution 1:300) for 3 days at 37^0C and 80 rpm. The slabs were then washed and subjected to counterstaining. The CUBIC-treated slabs were immersed in CUBIC-R RIMS before microscopy image acquisition. **Figure 38** presents 2D slices (upper row) and CUBIC-cleared 3 mm-thick slabs labeled with a MAP2 antibody. The 2D thin (60 micron-thick) slices demonstrated dendrites throughout cortex, although the labeling was denser in superficial layers than in deep layers (See additional 2D slices labeled with MAP2 in **Figure 43**). In contrast, the CUBIC-cleared slab had dendrites labeled only at the edges (bottom row).

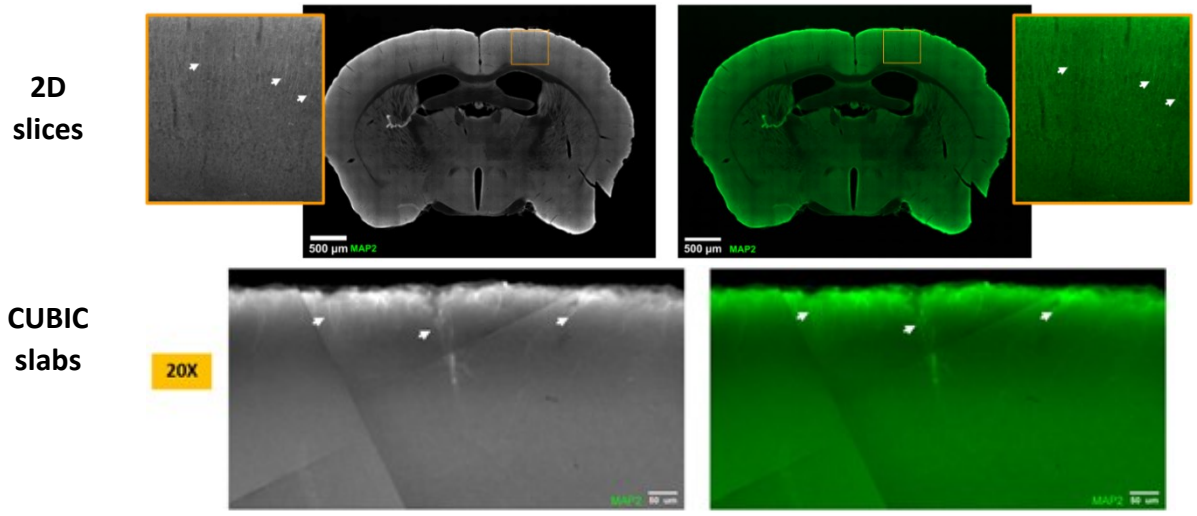

Figure 38. MAP2 antibody labeling in thin 2D slices and thick CUBUC-cleared slabs. (Top row) Confocal images of thin (60 µm) coronal sections of a mouse brain slice labeled by MAP2. See additional 2D slices labeled with MAP2 in Figure 4.1.35. (Bottom row) An image of CUBIC-cleared slab, acquired 1900 µm deep relative to the surface (20X); The MAP2 labeled dendrites were visible at the edges of the slab, but not within the interior part of the slab. The green channel represents MAP2 labels. An Opera Phenix spinning confocal microscope was used for image acquisition of CUBIC-cleared brain slabs.

In addition to the conventional CUBIC L/R used throughout this thesis, in another experiment we applied a modified CUBIC protocol (Gomez-Gaviro et al., 2017). Changing the CUBIC protocol did not overcome the problem of labeling at the edge of the slab only (**Figure 39**).

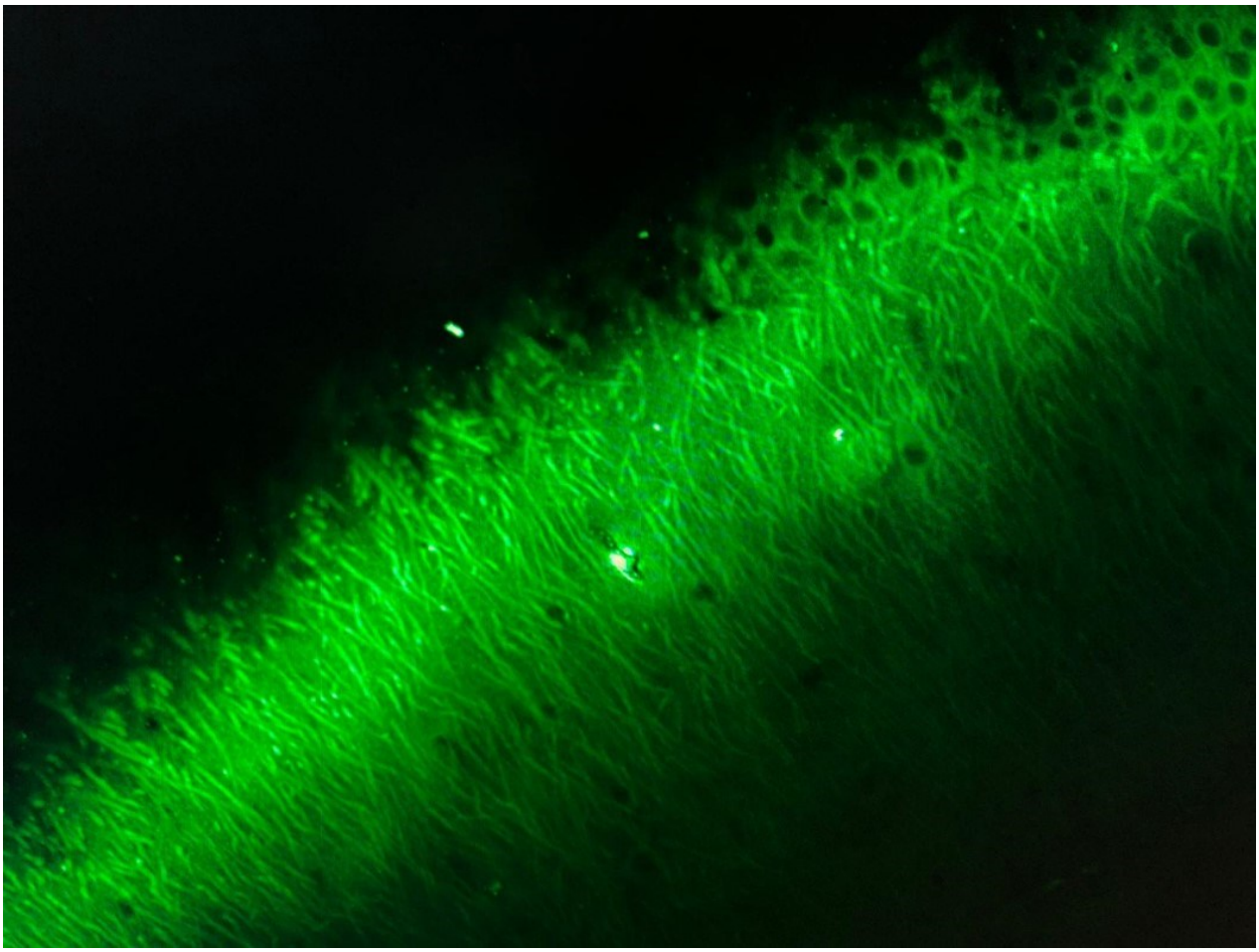

Figure 39. **MAP2 labeling of dendrites in a 2 mm thick slab cleared with a modified CUBIC protocol** (Gomez-Gaviro et al., 2017). The image was taken with an Opera Phenix microscope, at a magnification of 20X. As in the case of labeling slabs cleared with the conventional CUBIC L/R protocol, also with the modified protocol dendrites were clearly labeled at the edge of the slab, but not within its interior parts.

4.2. X-CLARITY

4.2.1. Compatibility of varying RIMS for X-CLARITY cleared samples

To evaluate the compatibility of different RIMS for X-CLARITY cleared thick brain slabs, we performed X-CLARITY clearing of 2- and 3- mm thick slabs from two mouse brains. **Figure 40** presents the cutting pattern outline for the two mouse brains. We obtained four slabs from each mouse brain. Each slab was cleared using the X-CLARITY protocol; Neurons were labeled by NeuroTrace™ 530/615 Nissl Stain at (1:50) concentration. Following PBS washing, each slab was treated with different RIMS as presented in **Figure 41.** **Figure 42** presents the standard histology images where the neuronal cells in 2D frozen slices were stained by NeuroTrace™ 530/615 Red Fluorescent Nissl stain for comparison with the labeled X-CLARITY slabs. The X-CLARITY cleared microscopy images demonstrate the compatibility and solution density behavior of each RIMS. Microscopy images with excellent image clarity were produced.

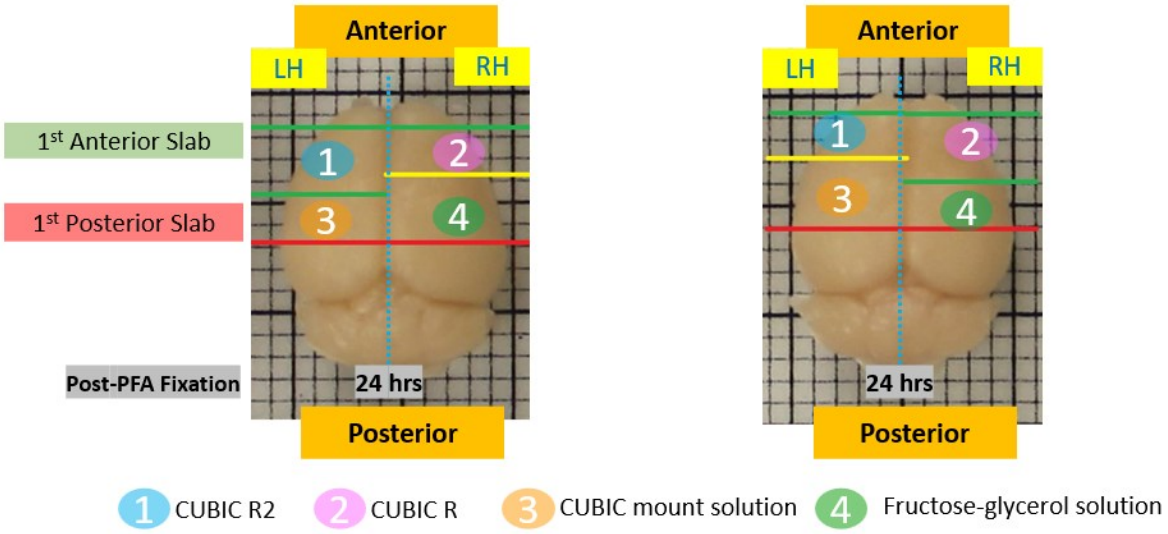

Figure 40. A scheme of the plan for cutting slabs from mouse brains for evaluating the compatibility of X-CLARITY clearing with four RIM solutions. To obtain 2- and 3-mm thick slabs, coronal sections were made at the green, yellow, and red markings. The yellow line marks the bregma. The regions between the 'yellow and green' and 'green and green' lines represent the 1st anterior slab. Similarly, the regions between the 'yellow and red' and 'green and red' lines represent the 1st posterior slab. The different RIM solutions, including CUBIC-R2, CUBIC-R, CUBIC-mount solution, and fructose-glycerol solution are denoted by the blue, magenta, orange, and green circles with indices 1, 2, 3, 4, respectively.

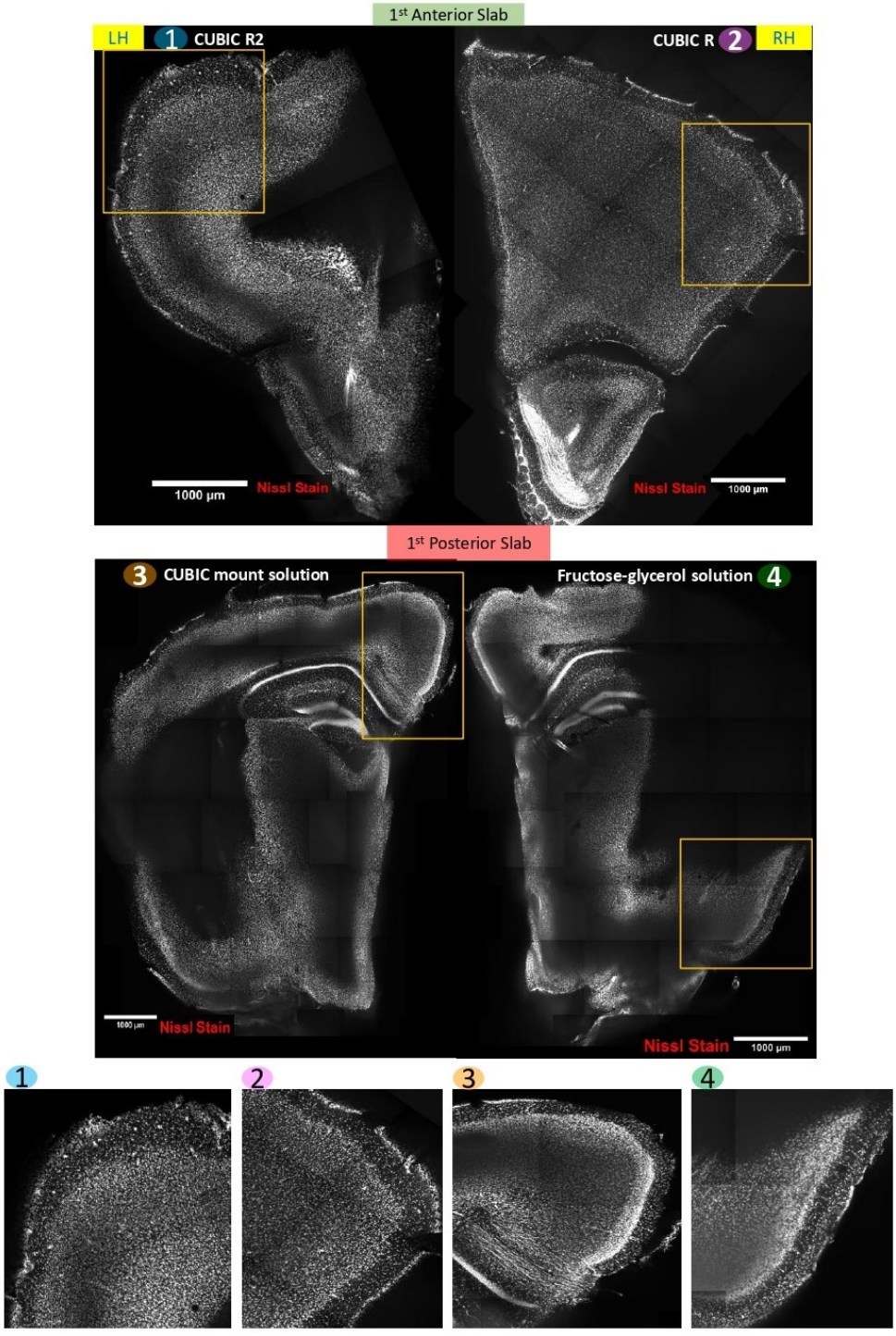

Figure 41. The effect of four RIMS on X-CLARITY cleared mouse brain slabs. The anterior left hemisphere (LH) was treated with CUBIC R2 RIMS **(*top row, left*)**, the anterior right hemisphere (RH) with CUBIC R **(*top row, right*)**, the posterior LH with CUBIC mount solution **(*middle row, left*)**, and the posterior RH with fructose-glycerol solution **(*middle row, right*)**. The **bottom row** presents magnified views of the insets. *Scale bars: 1000 µm. The cells were labeled by NeuroTrace™ 530/615 Red Fluorescent Nissl Stain.*

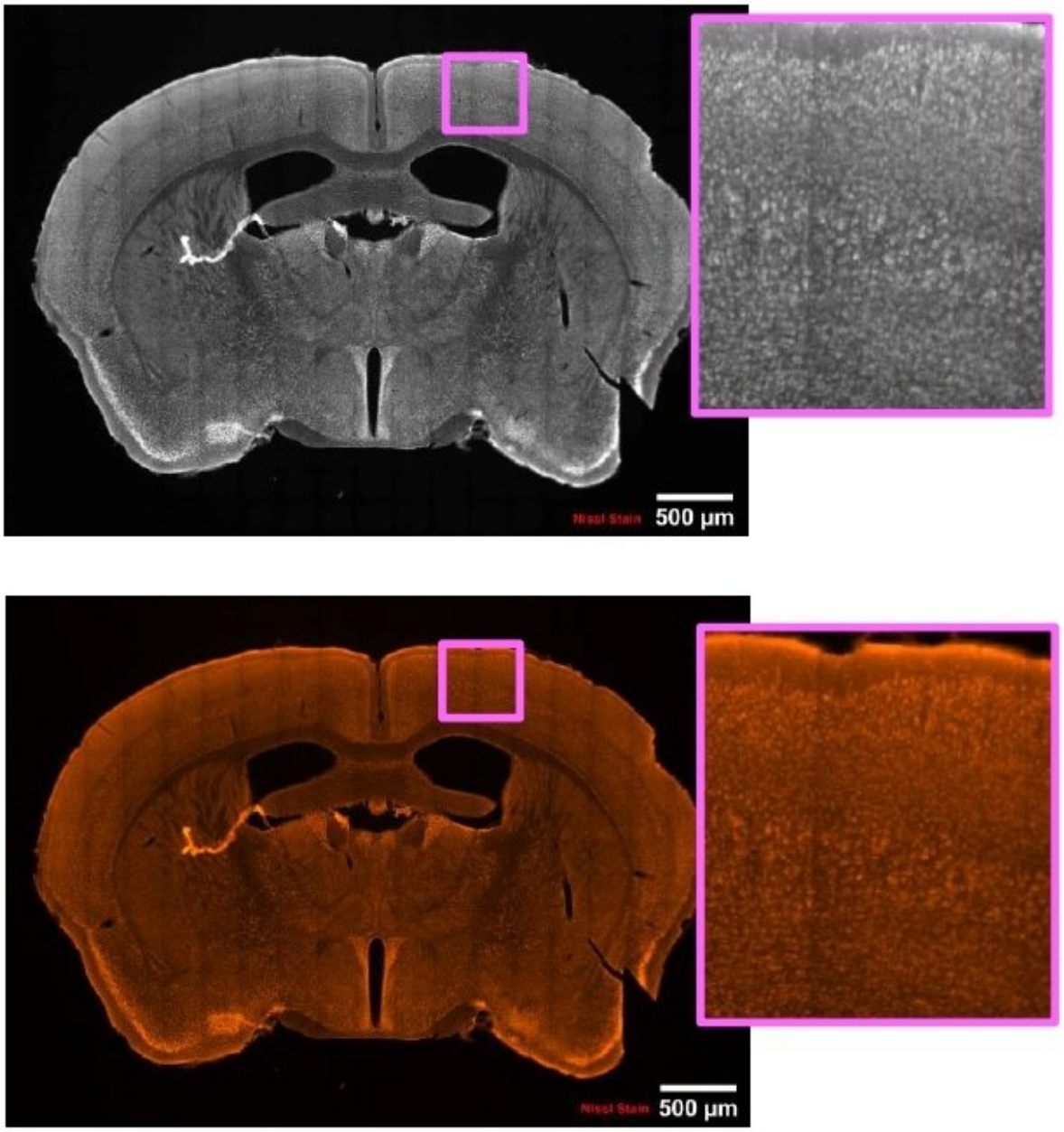

Figure 42. An image of fluorescent Nissl staining of a conventional 2D frozen section. Thin slices (60 µm) were stained with NeuroTrace™ 530/615 Red Fluorescent Nissl Stain at (1:1000) dilution. The image was acquired at 20X using a ZEISS Axio-Scan.Z1 slide scanner. Scale bar, 500 µm. The inset presents a magnified view of the square marked on the coronal image. Scale bar, 500 µm.

4.2.2. IHC labeling of 2- and 3- mm thick X-CLARITY cleared mouse brain slabs

To check the immunostaining compatibility of the X-CLARITY delipidated 2- and 3- mm thick mouse brain slabs, we carried out IHC labeling to label dendrites using the MAP2 antibody. After tissue clearing, a primary antibody incubation was performed for 2-3 days using anti-MAP2 primary antibody solution at 1:350 in a shaker at 4^0C. Then, secondary antibody incubation took place for 2-3 days, using Alexa 488 at 1:300 at 37^0C. To evaluate whether the optimized X-CLARITY clearing and immunostaining method deliver similar labeling to that obtained with standard IHC of 2D slices, we pursued standard IHC. **Figure 43** presents images of non-cleared 60 μm thin 2D slices. **Figure 44** shows microscopy images acquired from an X-CLARITY cleared mouse brain slab with the refractive index matched by CUBIC-R2. Dendrites and somas can be clearly observed in the slabs treated with CUBIC-R2. In contrast, MAP2 labeled dendrites were not visible in samples whose refractive index was matched by CUBIC-mount and fructose-glycerol solution. Hence, no images were included here.

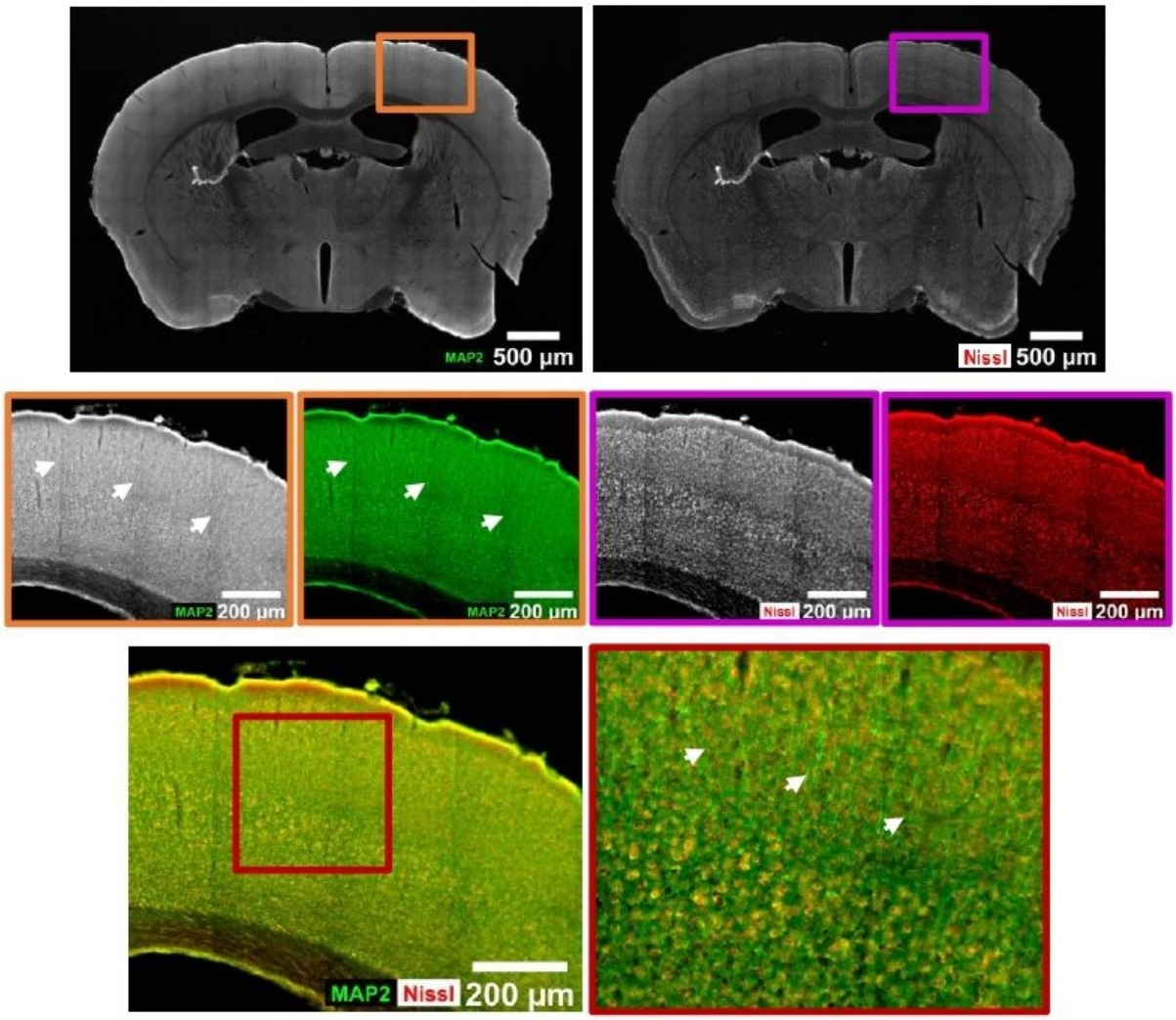

Figure 43. Images of IHC labeling with MAP2 and fluorescent Nissl staining of standard 2D frozen slices. Thin slices (60 µm) were labeled by anti-MAP2-anti-Alexa 488 (dilution 1:1000) and by NeuroTrace™ 530/615 Red Fluorescent Nissl Stain (dilution 1:1000). The images were acquired at 20X using a ZEISS Axio-Scan.Z1 slide scanner. (Top row) A coronal slice of a mouse brain labeled by anti-MAP2 (left) and Nissl fluorescent stain (right). (Middle row) Magnified views of the inset squares marked in the upper row. In each pair, the left image is in grey scale and the right image present the label. (Bottom row) The merged images of anti-MAP2-Alexa 488 and Nissl stain (left) and the expanded view of the inset square (right). *A Gaussian filter with sigma 50 was applied. The white arrows point to dendrites.*

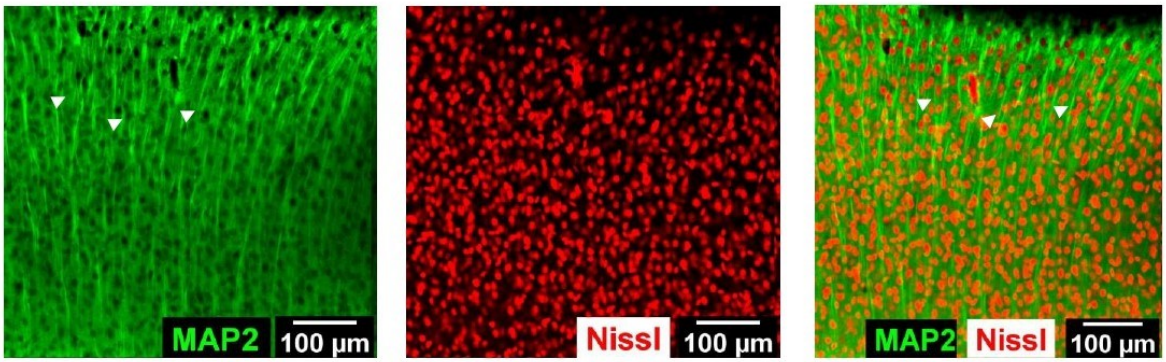

Figure 44. Opera Phenix spinning confocal microscopy images of a 2 mm-thick coronal slab of a mouse brain. (Left image) An image (10X) of an X-CLARITY cleared slab, obtained at 1000 µm depth. Dendrites are visible; the arrowheads point to specific dendrites. A Gaussian filter with sigma 20 was applied. **(Middle image)** Cell bodies labeled by NeuroTrace 530/615 red fluorescent Nissl stain. **(Right image)** The images of anti-MAP2-Alexa 488 and Nissl stain. The green and red channels represent MAP2 (1:350 dilution, GeneTex, GTX82661) and Nissl stain labels (1:50 dilution, Invitrogen, N21482), respectively.

CHAPTER 5 – DISCUSSION AND CONCLUSION

5.1. CUBIC-L & R

5.1.1. Effect of the varying post-fixation duration on delipidation of mouse brain slabs

Eunsoo Lee *et al.* reported that longer post-fixation increased the clearing time (Lee and Sun, 2016). They indicated that 2 hrs of post-fixation are sufficient for 1-2 mm thick mouse brain slabs (Lee and Sun, 2016). Our experiment with varying post-fixation with 2- and 3-mm thick brain slabs confirmed this report. With 2 hrs of post-fixation, 8-28 days and 28-30 days were required for clearing (in RT) 3-mm thick anterior brain slabs and 3-mm thick posterior slabs, respectively. Likewise, with 24 hrs of post-fixation, an average of 62-, 102-, and 123-days were required at RT for the completion of clearing by CUBIC-L of the 1st anterior-, 1st posterior-, and 2nd posterior-slabs, respectively. As the 2nd posterior slab consists of several deep brain structures with myelin, such as the caudate and putamen, these slabs took longer durations for tissue clearing. The caudate and putamen are separated by the internal capsule, a white matter tract. However, there are several strands of grey matter that cross the internal capsule between the two structures. The striatum gets its name from the white matter of the internal capsule layered with these grey matter "bridges," which gives it a striped look (Brain-striatum, see the bibliography). Likewise, sphingolipids and cholesterol comprise the majority of the brain, especially in the form of myelin. Both cholesterol and sphingolipids are functional components of the neuronal cell membrane and are incorporated in the microdomains of membrane rafts. The associated subcortical structures in white matter cause delays in tissue clearance with posterior slabs (Lipid world, see the bibliography). Still after tissue clearing, non-transparent regions were visible at the center. We found that these structures were further cleared by CUBIC-R RIMS (not shown in the thesis).

We started our optimization with only a short post-fixation, for 2 hours, because long post-fixation tends to increase the background fluorescence signal. However, the short post-fixation duration caused sample fragility. By the end of the tissue clearing, the edges first and parts of cortex later were partially or completely detached. Therefore, we changed the post-fixation to longer durations. It was clear that the tissue samples were less fragile when they were post-fixed for 24 hours relative to 2 hrs or 6 hours. **Therefore, although we confirm that the duration of clearing**

increases with increasing post-fixation duration, we recommend to post-fix rodent brains for 24 hours.

For a direct, paired comparison, we made this comparison between slabs arranged symmetrically on the two sides of the mid-sagittal plane. Comparing the slabs from the left- (24 hrs post-fixation) and right- (6 hrs post-fixation) hemispheres, 2-mm thick slabs post-fixed for 24 hrs took longer (7.5 – 28.5 days) to become highly transparent relative to slabs post-fixed for 6 hours (5 – 14.5 days; **Figure 16**). In this experiment we also confirmed - as expected - that the clearing of 2-mm thick brain slabs takes a shorter duration in comparison with 3-mm thick slabs.

The immersion of the brain slab in the CUBIC-L reagent causes the sample to swell (Gómez-Gaviro et al., 2017). It was confirmed in our experiments (**Figure: 12, 13, 15**). This effect was reduced following the CUBIC-R treatment. However, the swelling is associated with increased fragility. In conclusion, the duration for the post-fixation plays an important role in maintaining the structure of the cleared brain slabs. If the aim of the experiment is to visualize the cerebral cortex regions, we recommended post-fixing rodent brains for a minimum of 6 hrs, and ideally for 24 hrs.

5.1.2. Effect of the temperature on the delipidation rate

Mouse experiments: It has been reported that higher temperatures could be employed for accelerating tissue clearing (Yu et al., 2017). To confirm the influence of the temperature on the clearing using the CUBIC-L reagent, we performed a new set of experiments using 2-3 months aged mice and the temperature set at 37^0C or RT. Our results confirmed that the clearing induced at 37^0C was faster than that pursued at RT (**Figure 18**).

The clearing of 24 hrs post-fixed slabs incubated at RT took between 6 and 13.5 days to achieve the required transparency, relative to 5 to 13 days clearing of slabs incubated at 37^0C (**Figure 19**). Similarly, the effect we observed when clearing 6 hrs post-fixed slabs was even more pronounced. The clearing of 6 hrs post-fixed slabs at RT took 5 to 15.3 days, whereas clearing at 37^0C took 5 to 7 days (**Figure 19**). Whereas the clearing was faster at 37^0C, we expect that part of the reasons for the fragility we observed in slabs that went through short post-fixation can be attributed to the warm temperature. **We therefore recommend post-fixation for 24 hours and delipidation at 37^0C.**

Rat experiments: To verify the applicability of our recommended procedure that was based on mouse experiments also to rat brains, we performed experiments in rats. On average, clearing of the anterior slabs at 37^0C took only 3.5 – 3.75 days (**Figure 22**). Additional days were required for clearing the posterior slabs from the left hemisphere which were post-fixed for 24 hrs (**Figure 22**). Overall, **we recommend post-fixation for 24 hours and delipidation at 37^0C.** Once the slabs are clear, they should be taken out to RT; otherwise, further incubation at **37^0C** may degrade the structure of the edges of the cleared sample.

5.1.3. Effect of age on CUBIC-L delipidation

To characterize the effect of age, we applied delipidation of 2- and 3-mm thick mouse brain slabs using CUBIC-L on mice with different ages. We observed a trend of increasing delipidation time with increasing age. We therefore recommend for all studies to consider the age of animals used for tissue clearing, and wherever possible, use animals of the same age, in order to reduce variability of the results.

5.1.4. Optimization of Fluorescent Nissl stain (530/615 nm) concentration in rodent thick brain slabs: how to determine the optimal concentration in the general case?

We tested the effect of different dilutions of NeuroTrace™ 530/615 Red Fluorescent Nissl Stain on the labeling of somas in mouse cortex. For effective evaluation, we imaged the slices that were in the middle of the slab, at approximately equal distance from the anterior and posterior surfaces of the slabs. This made it possible to test the effect of dilution on the penetration of the antibodies into the slab.

For ensuring detectability of neurons, the most important feature of the imaged processed tissue is the Signal to Background Ratio (SBR). This measure is commonly estimated by eye. We developed an analysis procedure to quantify the SBR, by comparing the signal in the middle of a soma to the background in the vicinity of the same soma. We used this procedure to estimate the SBR associated with neurons that were distributed approximately homogeneously across the cortical depth. In both mice and rats, this analysis showed a trend of increased SBR with increasing Fluorescence Nissl concentration.

Based on this result, we would need to increase the concentration of the staining materials, which increases the cost significantly. But, where should one stop increasing the concentration?

We recommend evaluating the required concentration against the required results. To test whether increasing the concentration is indeed necessary, an automatic analysis can be performed, to identify the specific features of interest. **Figure 45** presents the details of an algorithm for automatic counting of the somas. Taking cell counting as an example of the feature of interest, to analyze the cost-benefit optimal concentration, one can apply such an automatic analysis and verify the results by inspection. This would include inspecting the images and identifying true positive detection, false positive and false negative (true negative is the default outcome in such an experiment). The concentration should be increased to achieve the required percentage of the true positive, false positive and false negative detection. **We recommend doing a similar evaluation in similar future studies, to analyze the cost-effectiveness of increasing stain or antibody concentration and the corresponding cost, based on the specific aims of the study.**

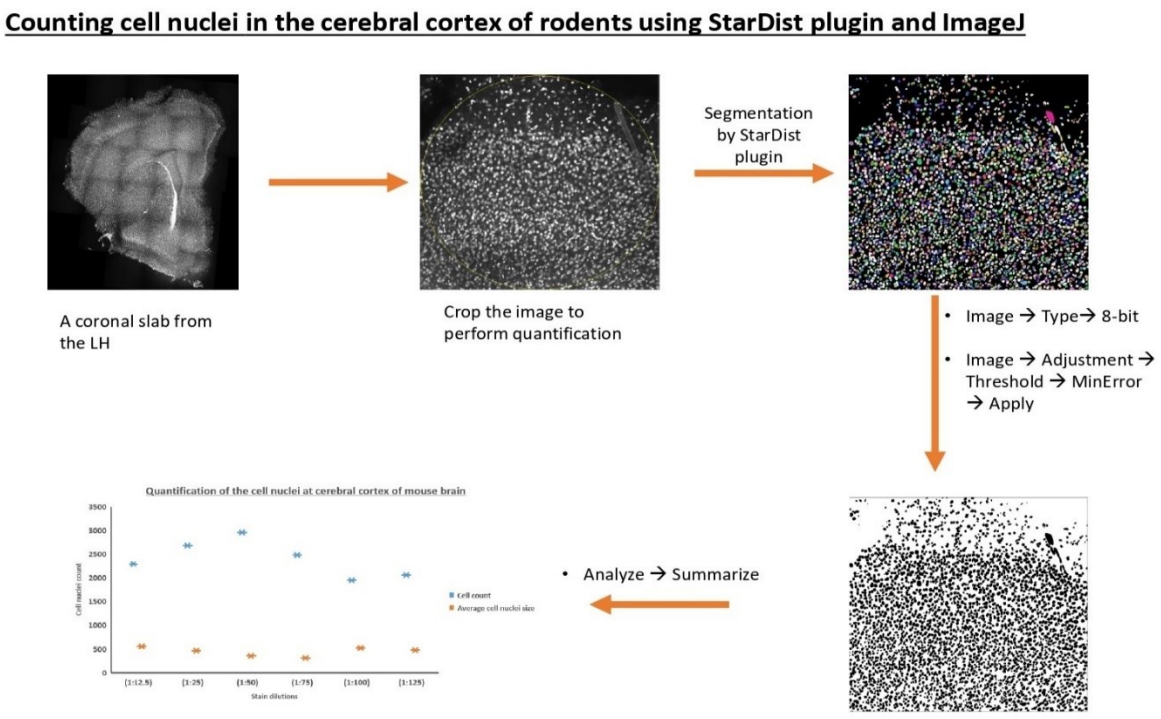

Figure 45. Counting cell nuclei in the cerebral cortex of mouse brains. The algorithm segments the cell nuclei using the StarDist plugin (Uwe 2018) for ImageJ.

5.1.5. Comparison between the CUBIC-L/R and X-CLARITY protocols

Comparing the CUBIC and X-CLARITY tissue clearing methods, we estimated the time required for the completion of delipidation of thick mouse brain slabs. We noticed that X-CLARITY took only 6 hrs to complete the delipidation of 3-mm thick slabs instead of days taken by the CUBIC procedure. The expedition of the X-CLARITY protocol mainly depends on the custom-made ETC chamber system (Lee and Sun, 2016). This system generates the regular dense current, maintains the pH of the clearing solution, removes the air bubbles, and reduces heat generation (Lee and Sun, 2016). The accessibility of ETC is mandatory for the X-CLARITY procedure. No such equipment is required for CUBIC. The CUBIC method depends on free diffusion of clearing buffers which in turn delays clearing of the sample. In conclusion, **both techniques are scalable. CUBIC is more economical but significantly slower compared to X-CLARITY**.

5.1.6 Quenching effect of RIMS in Nissl stained CUBIC-cleared mouse brain slabs

It was evident that CUBIC-R has a slow progressing quenching effect on the NeuroTrace™ 530/615 Red Fluorescent Nissl Stain. The average intensity measured in the same slab and ROI was reduced from 214 mean intensity to 168 within one month (**Figure 35)**. This 3-mm thick brain slab was stained at (1:100) concentration of Nissl fluorescent stain. Similarly, for a slab stained at (1:50), the mean intensity dropped from 321 to 272 over a 3-month duration (**Figure 37**). These results confirm the previous report on minimal quenching of fluorescence signals by the CUBIC protocol (Susaki et al., 2014). The red light transmits across the thick slabs more adequately than green laser light (Susaki et al., 2014). As a result, the red fluorescent protein is suitable to label the protein of interest with the CUBIC protocol (Susaki et al., 2014).

5.1.7. IHC labeling with the MAP2 antibody in CUBIC- cleared mouse brain slabs

CUBIC-L treatment of the thick brain slab resulted in a transparent brain. This delipidation constitutes the high permeable nature of the CUBIC-cleared sample. This should allow the penetration of macromolecules into the cleared samples. As can be observed in **Figures 38 (bottom row)** and **Figure 39**, the reagents used for the CUBIC protocol are compatible with general IHC procedures and the MAP2 antibody. However, the labeling is limited to the edge of the sample. In contrast, MAP2 clearly labeled the control 2D slices (**Figures 38 (top row)** and **Figure 43**). We hypothesize that the reason for the restriction of the labeling to the edge of the sample

is the large molecule of the MAP2 antibody that has a relatively high molecular weight of 280 kDa. Thus, it may be challenging for this molecule to penetrate even a CUBIC-cleared slab with increased porosity relative to the normal tissue.

To amplify the signal intensity of the immunostaining, Susaki et al., recommended using high concentrations, specifically 10 % Triton X-100 instead of 0.1 % which increase the antibody binding (Susaki et al., 2020). However, the limited MAP2 labeling at the edge of the sample indicates that the issue is with penetration, not necessarily in affinity.

5.2. X-CLARITY

5.2.1. Compatibility of X-CLARITY cleared samples with varying RIMS

We imaged 3 mm-thick slabs cleared with X-CLARITY using an Opera Phenix microscope. The microscope generated images with appropriate resolution to observe single labeled neuronal cells in the 2- and 3-mm thick mouse brain slabs. This Opera Phenix microscope offered 1.3 µm effective resolution in-plane at binning 1. The depth of imaging using X-CLARITY is directly proportional to the light penetration depth (Gómez-Gaviro et al., 2017). The single labeled neuronal cells by NeuroTrace™ 530/615 Red Fluorescent Nissl Stain at (1:50) concentration were visible across the Z-axis, in both 2 mm and 3 mm-thick slabs. For instance, in the cerebral cortex region, the X-CLARITY cleared slabs showed spatial distributions of neuronal cells similar to the standard histology results (**Figure 42 - Figure 44)**.

The X-CLARITY cleared samples swell during the SDS-containing delipidation; however, they return to their original size once immersed in the RIMS (Lee and Sun, 2016) (**Figure 46**). This enables the exact analysis of cellular architecture (Lee and Sun, 2016) in 3D structures that remain largely undistorted. These results show that the X-CLARITY method accelerates the clearing process with recovery of the tissue to its fundamental size (Lee and Sun, 2016).

Regarding the compatibility of the RIMS used, except for CUBIC-R, the X-CLARITY cleared brain slabs showed floaty behavior with other RIMS (meaning, the slabs floated instead of-settling at the bottom of the well). This is likely due to the highly viscous nature of sucrose or glycerol (Richardson and Lichtman, 2015). Even at the working concentration of CUBIC-R2, it has the potential to form precipitation at RT, and very easily air bubbles can be introduced (Richardson

and Lichtman, 2015). Excluding CUBIC-R, the movement of the thick cleared samples through the other three solutions during imaging resulted in uneven slices in the Z-stack (Richardson and Lichtman, 2015). This floaty and moving tendency of the thick samples can be restricted by placing RIMS-cleared agar blocks on and around the sample during image acquisition. Before microscopy imaging, all RIMS must be degassed for 30 min to remove all the air bubbles present in the

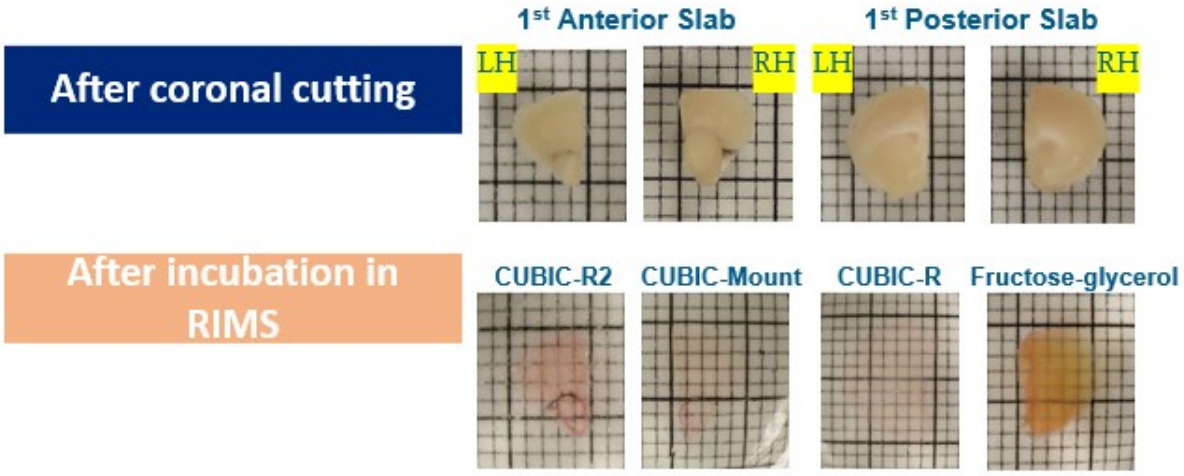

solutions.

Figure 46. Images of mouse brain blocks (2- and 3-mm thick) following the processing by RIMS. The refractive index matched slabs regained the original size. (Top row) Images taken after the coronal cutting of the mouse brain slabs. (Bottom row) Images taken once RIMS incubation completed. Scale of the slabs are 2-mm (RH-anterior slab and LH-posterior slab) and 3-mm (LH-anterior slab and RH-posterior slab). Square unit (thick lines): x: 5 mm, y: 5 mm

Even if the thick brain samples turned completely transparent in the RIMS (except for CUBIC-R), it is recommended to continue the incubation for additional 3-7 days. This will help to achieve even, complete images in z-stacks. In the two experiments, the edges of the thick samples with neuronal cells were observable but not the center regions. If we increase the incubation duration in RIMS from a minimum of 2 days to a maximum of 7 days based on the slab thickness, the problem with uneven image acquisition can be solved. Compared with DISCO tissue clearing methods, none of these RIMS causes fast quenching effect (**Figure 35, 37**) (Lee and Sun, 2016).

In conclusion, the results show that this optimized X-CLARITY protocol can be utilized for 2- and 3-mm thick mouse brain slabs and an Opera Phenix spinning disc confocal microscope. The duration for the RIM step for each RIMS needs to be optimized for better microscopy images.

5.2.2. IHC labeling of X-CLARITY cleared mouse brain slabs

It is evident that the X-CLARITY protocol is compatible with the standard immunolabeling procedure (**Figure 44)**. This is because the tissue-embedded hydrogel in the X-CLARITY treated slabs can expedite the penetration of the macromolecular-labeling components (Lee et al., 2016). Pores are formed after the removal of lipids in the brain samples (Epp et al., 2015). These pores allowed labeling with the large macromolecule of the MAP2 antibody (**Figure 44**) that did not label the interior of CUBIC-cleared slabs (**Figures 38 (bottom row) – Figure 39**). The tissue-embedded hydrogel ensures maximum preservation of the sample under study while undergoing electrophoretic clearing, staining, and microscopy imaging (Epp et al., 2015).

If we include the PRESTO approach for IHC, the passive incubation period shortens to 2-3 hrs time. Hence, the overall time required for the completion of the X-CLARITY mediated clearing and antibody labeling, refractive index matching, and imaging can be shortened to a minimum of 7 days. It may vary with the thickness of the sample under study.

In conclusion, the validated X-CLARITY method evaluated here signifies an important resource enabling future imaging of large animal brains. It provides a powerful combination of tissue clearing and IHC compatible with imaging with an Opera Phenix microscope, which can be expanded for studying neuronal connectivity, subcellular brain morphology at single-cell resolution, and three-dimensional reconstruction of the thick slab or whole-brain sample under study. The latest imaging technology including light sheets and super-resolution microscopy can increase the potential of this method.

REFERENCES

Ariel P (2017) A beginner's guide to tissue clearing. The International Journal of Biochemistry & Cell Biology 84:35–39.

Brain-striatum
https://neuroscientificallychallenged.com/posts/know-your-brain-striatum

Brochure_LL060

https://www.tcichemicals.com/assets/brochure-pdfs/Brochure_LL060_E.pdf

Chung K, Wallace J, Kim S-Y, Kalyanasundaram S, Andalman AS, Davidson TJ, Mirzabekov JJ, Zalocusky KA, Mattis J, Denisin AK, Pak S, Bernstein H, Ramakrishnan C, Grosenick L, Gradinaru V, Deisseroth K (2013) Structural and molecular interrogation of intact biological systems. Nature 497:332–337.

Dodt H-U, Leischner U, Schierloh A, Jährling N, Mauch CP, Deininger K, Deussing JM, Eder M, Zieglgänsberger W, Becker K (2007) Ultramicroscopy: three-dimensional visualization of neuronal networks in the whole mouse brain. Nat Methods 4:331–336.

Du H, Hou P, Zhang W, Li Q (2018) Advances in CLARITY-based tissue clearing and imaging. Exp Ther Med 16:1567–1576.

Epp JR, Niibori Y, (Liz) Hsiang H-L, Mercaldo V, Deisseroth K, Josselyn SA, Frankland PW (2015) Optimization of CLARITY for Clearing Whole-Brain and Other Intact Organs. eneuro 2:ENEURO.0022-15.2015.

Fluorescent tracers
https://www.thermofisher.com/ca/en/home/references/molecular-probes-the-handbook/fluo rescent-tracers-of-cell-morphology-and-fluid-flow.html

Gómez-Gaviro MV, Balaban E, Bocancea D, Lorrio MT, Pompeiano M, Desco M, Ripoll J, Vaquero JJ (2017) Optimized CUBIC protocol for three-dimensional imaging of chicken embryos at single-cell resolution. Development 144:2092–2097.

Itk-snap. ITK-SNAP - UFRC Available at: https://help.rc.ufl.edu/doc/ITK-SNAP

LaVision BioTec, UltraMicroscope Division (2017) UltraMicroscope is the most successful commercial light sheet system for high impact publications.

Lee E, Choi J, Jo Y, Kim JY, Jang YJ, Lee HM, Kim SY, Lee H-J, Cho K, Jung N, Hur EM, Jeong SJ, Moon C, Choe Y, Rhyu IJ, Kim H, Sun W (2016) ACT-PRESTO: Rapid and consistent tissue clearing and labeling method for 3-dimensional (3D) imaging. Sci Rep 6:18631.

Lee E, Sun W (2016) ACT-PRESTO: Biological Tissue Clearing and Immunolabeling Methods for Volume Imaging. JoVE:54904.

Lipid world
https://lipidworld.biomedcentral.com/track/pdf/10.1186/s12944-019-0965-z.pdf

Logos VX1901-01
https://www.atascientific.com.au/wp-content/uploads/2019/10/LogosBiosystems-X-CLARITY-product-brochure-VX1901-01.pdf LogosBiosystems X-CLARITY product brochure VX1901-01.pdf.

Logos XP1710-01
Logos XP1710-01, X-CLARITY Protocol XP1710-01.pdf

Matryba P, Kaczmarek L, Gołąb J (2019) Advances in Ex Situ Tissue Optical Clearing. Laser & Photonics Reviews 13:1800292.

Mouse anesthesia
https://www.mcgill.ca/research/files/research/110-_mouse_anesthesia_-_jan_2021.pdf

Opera_Phenix
https://resources.perkinelmer.com/lab-solutions/resources/docs/BRO_011289_01_Opera_Phenix.pdf BRO_011289_01_Opera_Phenix.pdf.

Pan C, Cai R, Quacquarelli FP, Ghasemigharagoz A, Lourbopoulos A, Matryba P, Plesnila N, Dichgans M, Hellal F, Ertürk A (2016) Shrinkage-mediated imaging of entire organs and organisms using uDISCO. Nat Methods 13:859–867.

Rat anesthesia
https://www.mcgill.ca/research/files/research/111-_rat_anesthesia_-_jan_2021.pdf

Renier N, Wu Z, Simon DJ, Yang J, Ariel P, Tessier-Lavigne M (2014) iDISCO: A Simple, Rapid Method to Immunolabel Large Tissue Samples for Volume Imaging. Cell 159:896–910.

Reveles Jensen KH, Berg RW (2017) Advances and perspectives in tissue clearing using CLARITY. Neuroscience. Available at: http://biorxiv.org/lookup/doi/10.1101/144378 [Accessed May 21, 2020].

Richardson DS, Lichtman JW (2015) Clarifying Tissue Clearing. Cell 162:246–257.

Rocha MD, Düring DN, Bethge P, Voigt FF, Hildebrand S, Helmchen F, Pfeifer A, Hahnloser RHR, Gahr M (2019) Tissue Clearing and Light Sheet Microscopy: Imaging the Unsectioned Adult Zebra Finch Brain at Cellular Resolution. Front Neuroanat 13:13.

Seo, Jinyoung, Choe, Minjin, Kim, Sung-Yon (2016) Clearing and Labeling Techniques for Large-Scale Biological Tissues. Molecules and Cells 39:439–446.

Susaki EA et al. (2020) Versatile whole-organ/body staining and imaging based on electrolyte-gel properties of biological tissues. Nat Commun 11:1982.

Susaki EA, Tainaka K, Perrin D, Kishino F, Tawara T, Watanabe TM, Yokoyama C, Onoe H, Eguchi M, Yamaguchi S, Abe T, Kiyonari H, Shimizu Y, Miyawaki A, Yokota H, Ueda HR (2014) Whole-Brain Imaging with Single-Cell Resolution Using Chemical Cocktails and Computational Analysis. Cell 157:726–739.

Susaki EA, Tainaka K, Perrin D, Yukinaga H, Kuno A, Ueda HR (2015) Advanced CUBIC protocols for whole-brain and whole-body clearing and imaging. Nat Protoc 10:1709–1727.

Tainaka K et al. (2018) Chemical Landscape for Tissue Clearing Based on Hydrophilic Reagents. Cell Reports 24:2196-2210.e9.

Tomer R, Ye L, Hsueh B, Deisseroth K (2014) Advanced CLARITY for rapid and high-resolution imaging of intact tissues. Nat Protoc 9:1682–1697.

Thermofisher Manuals Fmp21480
https://www.thermofisher.com/docum ent-connect/document-connect.html?url=https%3A%2F%2Fassets.thermofisher.com%2FTFS-Assets%2FLSG%2Fmanuals%2Fmp21480.pdf

Ueda HR, Ertürk A, Chung K, Gradinaru V, Chédotal A, Tomancak P, Keller PJ (2020) Tissue clearing and its applications in neuroscience. Nat Rev Neurosci 21:61–79.

Ultramicroscope II brochure
https://trello.com/1/cards/5e0e0cd130d34b8fbaffe556/attachments/5e0e0cef541ba98446d1e180/download/Ultramicroscope_II_brochure_Web.pdf
Ultramicroscope_II_brochure_Web.

Uwe Schmidt, Martin Weigert, Coleman Broaddus, and Gene Myers (2018). Cell Detection with Star-convex Polygons. International Conference on Medical Image Computing and Computer-Assisted Intervention (MICCAI), Granada, Spain.

Yang B, Treweek JB, Kulkarni RP, Deverman BE, Chen C-K, Lubeck E, Shah S, Cai L, Gradinaru V (2014) Single-Cell Phenotyping within Transparent Intact Tissue through Whole-Body Clearing. Cell 158:945–958.

Yu T, Qi Y, Zhu J, Xu J, Gong H, Luo Q, Zhu D (2017) Elevated-temperature-induced acceleration of PACT clearing process of mouse brain tissue. Sci Rep 7:38848.

CHAPTER 6 – APPENDIX

1) TERMINOLOGY

Slices – Tissue sections with thickness less than 1mm

Slabs – Tissue blocks with thickness greater than 1mm

Sections – Used interchangeably with slabs

2) ABBREVATIONS

3D	: Three Dimensional
ACT-PRESTO	: Active Clarity Technique-Pressure Related Efficient and Stable Transfer of macromolecules into Organs
CLARITY	: Clear Lipid-exchanged Acrylamide-hybridized Rigid Imaging/Immunostaining/In situ hybridization-compatible Tissue-hYdrogel
CT	: Computed Tomography
CUBIC	: Clear, Unobstructed Brain Imaging cocktails and Computational analysis
DW	: Distilled Water
ECM	: Extracellular Matrix
ETC	: Electrophoretic Tissue Clearing
GA	: Glutaraldehyde
GFP	: Green Fluorescent Proteins
HCS	: High Content Screening
hr	: Hour
IHC	: Immunohistochemistry
NA	: Numerical Aperture
PACT	: Passive Clarity Technique
PBS	: Phosphate-Buffered Saline
PFA	: Paraformaldehyde
RFP	: Red Fluorescent Proteins
RI	: Refractive Index
RIMS	: Refractive Index Matching Solution

RT : RT

SDS : Sodium Dodecyl Sulfate

w/v : Weight Per Volume

wt : Weight

YFP : Yellow Fluorescent Proteins

3) REAGENT AND MATERIAL INFORMATION USED

Table 2: List of reagents and materials used for tissue clearing, immunolabeling, RIM and imaging

Step		Description	Company	Cat #
Cardiac Perfusion-Fixation		16% Paraformaldehyde		
Hydrogel infusion and Polymerization		X-CLARITY™ Hydrogel Solution	Biobasic	C13103 – 1 x 1 L
		X-CLARITY™ Polymerization Initiator	Biobasic	C13104 – 1 x 2.5 g
CLARITY (Tissue Clearing Solution)		Electrophoretic Tissue Clearing Solution	Biobasic	C13001 – 12 x 1 L
		Boric acid	Sigma-Aldrich	B6768-500G
		Sodium Dodecyl Sulfate (SDS)	Sigma-Aldrich	L3771-100G
		Sodium hydroxide pellets		
CUBIC Tissue Clearing Solutions		1-methylimidazole	Sigma-Aldrich	616-47-7
		N-butyldiethanolamine		
		Triton X-100	Sigma-Aldrich	X100-500ML
		N-buthyldiethanolamine	Sigma-Aldrich	471240-500ML
Immuno-staining	Antibody Incubation Buffer	Bovine Serum Albumin (BSA)	Sigma-Aldrich	A3311-10G
		Goat Serum	Sigma-Aldrich	G9023
		0.1 % Tween 20	Sigma-Aldrich	P9416
	Primary antibody	MAP2	GTX82661	GeneTex
	Secondary antibody	Goat anti-Chicken IgG (H+L) Secondary Antibody, Alexa Fluor 488	A-11039	Invitrogen

Step		Description	Company	Cat #
Imaging (Refractive Index Matching Solution)	Nucleic Acid Stain	NeuroTrace™ 530/615 Red Fluorescent Nissl Stain - Solution in DMSO	Invitrogen	N21482
	CUBIC-R	Nicotinamide	Sigma	N3376
		Antipyrine	Sigma-Aldrich	A5882
	CUBIC-R2	Sucrose	Sigma-Aldrich	S0389-500G
		Urea	Sigma-Aldrich	51456-
		Triethanolamine	Sigma	90279
	CUBIC-mount	Sucrose	Sigma-Aldrich	S0389-500G
		Urea	Sigma-Aldrich	51456-500G
		N,N,N',N'-tetrakis(2-hydroxypropyl)ethylenediamine	Sigma-Aldrich	122262
	Fructose-Glycerol	Glycerol	Sigma-Aldrich	G5516-100ML
		Fructose	Sigma-Aldrich	F0127-100G
	Dish	Coverglass bottom dish - 24 Well plate	ibidi	82426

Adapted from Kubota *et al.,* (Kubota et al., 2017)

4) ANTIBODY AND NUCLEUS STAINS USED

Table 3: List of antibody and nucleus stains used in cleared tissue

Antibody	Catalog number	Company
MAP2	GTX82661	GeneTex
Goat anti-Chicken IgG (H+L) Secondary Antibody, Alexa Fluor 488	A-11039	Invitrogen
Stain	**Catalog number**	**Company**
NeuroTrace™ 530/615 Red Fluorescent Nissl Stain - Solution in DMSO	N21482	Invitrogen

Adapted from Kubota *et al.,* (Kubota et al., 2017)

5) CUBIC SOLUTIONS USED

Table 4: List of CUBIC solutions used

Name	Key ingredients
CUBIC-P	1-methylimidazole,
CUBIC-L	N-buthyldiethanolamine, Triton X-100
CUBIC-R	Nicotinamide, Antipyrine

Adapted from Kubota *et al.,* (Kubota et al., 2017)

6) EXTENDED EXPERIMENTAL PROCEDURE

6.1 Standard Immunohistochemistry Protocol (Shi et al., 2008)

6.1.1 Steps:

1) **Acclimatization:** Before starting the IHC protocol, all coronal thin slices of 30 µm were set at RT for 20 minutes and washed with 1X PBS. Repeat the washing step two more times. In 24-well plate, each well can hold a maximum of 6 slices.
2) **Permeabilization Step:** Then, permeabilize the slices using 2 ml of 0.3% PBST in each well and incubate for RT for one hour.
3) **Blocking Buffer:** After the permeabilization step, 2 ml of bovine serum albumin (1%) add in each well. It is incubated at RT for 15 min. This step can be repeated one more time.
   Note: In the case of high background, use donkey serum instead of BSA.
4) **Primary Antibody Labeling:** Slices are incubated in the primary antibody at (1: 1000) dilutions (1ml/well) at 4^0C overnight. The primary antibody solution containing the primary antibody from the stock solution is diluted in 1% BSA.
5) **PBST washing:** For washing of slices, use 1% bovine serum albumin prepared in 0.3% PBST where 2ml added per well and incubated for 10 min at RT. Repeat it 3 more times.
6) **Secondary Antibody labeling:** Incubate sections with secondary antibody at (1:1000) dilutions at RT for 2 hours under dark. The secondary antibody solution containing the secondary antibody from stock solution is diluted in 1% BSA.
7) **PBST washing:** For washing of slices, use 1% bovine serum albumin prepared in 0.3% PBST where 2ml was added per well and incubated for 10 min at RT. Repeat it 3 more times.
8) **Nissl Stain:** Incubate slices with Nissl stain at (1:100) dilutions at RT for 1 hour under dark where 1 ml per well. The neuronal Nissl body staining fluorescent Nissl stain solution containing stain from stock solution is diluted in 1X PBS.
9) **PBS washing:** For washing of slices, use 1X PBS where 2ml added per well and incubated for 10 min at RT. Repeat it 2 more times under dark.
10) **Mounting of slices on silica gel coated microscope slide:** Mount the 30µm tissue sections onto glass slides and dry overnight at RT using slide box.
11) **Anti-fade mounting medium and coverslip mounting:** Swiftly rinse the microscope slide using 0.01X PBS followed by saline. Then, tap the edges of the slide on a paper towel to remove excess solution, then place it on a flat surface. Apply 3-4 drops of mounting medium at the left side of the slide having slices. Place the coverslip in a tilting position over the slide by touching the mounting medium and then, slowly lower the coverslip. Using thumb, slightly apply pressure and squeeze away the air bubbles, if any. Using Kim wipe, the excess mounting medium can be removed by touching the sides of the slide. Dry overnight. Neatly clean the slide before microscopy imaging.

6.2 Perfusion Protocol

6.2.1. Mouse: Perfusion using 1X PBS and 4% PFA Solutions

6.2.1.1. Details to be noted down before perfusion:

i. Experiment started on: __ __ __ __/ __ __ __ / __ __ (yyyy/mmm/dd)
ii. Mouse Cage Number :
iii. Date of birth : __ __ __ __/ __ __ __ / __ __ (yyyy/mmm/dd)
iv. Sex (M/F) : _____
v. Age : _____ Months, ____ Days
vi. Weight : ___ g

6.2.1.2. Experimental solution preparation:

i. 15 mL of 1X PBS, pH 7.4
ii. 20 mL of 4% PFA, pH 7 – 7.5
Note: *Store 1X PBS and 4% PFA solutions into the fridge (4^0C) or in an ice tank until ready to begin the perfusion.*
iii. 45 ml of 4% PFA (to hold brain after the extraction)

6.2.1.3. Animal sacrifice and brain collection

i. Prepare 3x the normal dose of anesthetic cocktail (Ketamine/Xylazine/Acepromazine) based on the age, the sex, and the weight of the animal
Note: *Anesthetic cocktail dose: 1 ml of ketamine 100mg/kg, 0.5 ml of xylazine 10mg/kg, 0.3 ml of acepromazine 3mg/kg* (Mouse anesthesia, see the bibliography)
ii. Inject intraperitoneally
iii. After injection,
    a. Wait until the animal is adequately anesthetized.
    b. Test this by pinching the toes of the paws.
        - If the animal still twitches, wait longer before beginning the perfusion.
        - If the animal no longer twitches, they are ready to be perfused.
iv. Begin the perfusion with
Δ Critical step *Cooling of PBS and 4% (wt/vol) PFA on ice is important for successful perfusion. Muscle stiffness after perfusion is a good indicator of successful perfusion. Residual blood in the mouse brain increases autofluorescence, especially in the green-laser excitation. The pH value of PFA is also crucial for efficient clearing and lower autofluorescence. Over-fixation causes both lower clearing efficiency and autofluorescence.*
        - PBS (at 3 mL/min)

- Once the beaker containing 15 ml of PBS is nearly empty, pause the machine, and place the tube into the 4% PFA beaker.

▪ 4% PFA (at 3 mL/min)

- Once the beaker containing 20 ml of PFA is almost empty, pause the machine.

v. Then, remove the needle from the animal's heart and place that end of the tube in the sink.

vi. Move the other end of the tube into a beaker of DW.

- Run the machine with water through the tubes to rinse it.

vii. Carefully remove the brain from the skull of the animal.

viii. Transfer the brain into the 4% PFA in 1X PBS and store it in an ice tank.

ix. After brain extraction, place the brain on a grid paper and align it (parallel) to the respective markings. Then, take photos of the whole brain with and without 1X PBS solution. Refer to the below figures which spot the brain slab without and with the 1X PBS respectively (**Figure 47**).

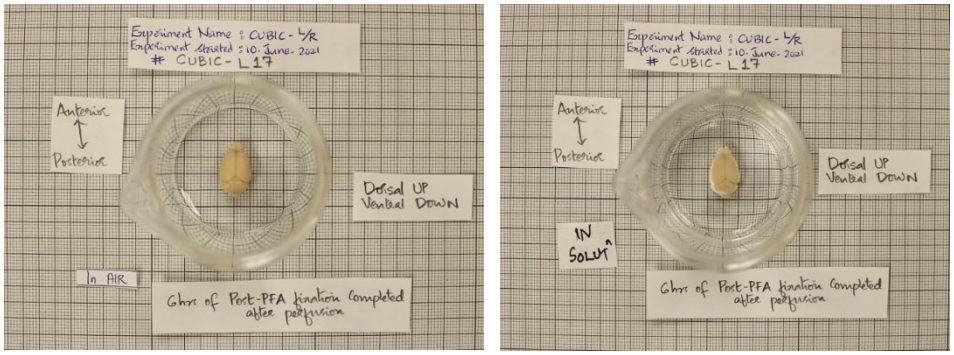

Figure 47. The placing of the mouse brain without PBS (left) and with PBS solution (right) while taking photos was demonstrated.

6.2.1.4. Brain Fixation and PBS washing

i. Incubate the brain in 4% PFA at 4^0C for 24 hours.

Note: After incubation, use the pipette to remove PFA and discard it into the PFA waste bottle.

ii. Rinse the brain using PBS for 24 hours.

iii. After 24 hours, the brain is ready to be used for the experiment.

6.2.2. Mouse: Perfusion using 1X PBS, 4% PFA, and CUBIC-P solutions

6.2.2.1. Details to be noted down before perfusion:

i. Experiment started on: __ __ __ __/ __ __ __ / __ __ (yyyy/mmm/dd)

ii. Mouse Cage Number :
iii. Date of birth : __ __ __ __/ __ __ __ / __ __ (yyyy/mmm/dd)
iv. Sex (M/F) : _____
v. Age : _____ Months, ____ Days
vi. Weight : ___ g

6.2.2.2 Experimental Solution Preparation:

i. 30 mL of 1X PBS, pH 7.4
ii. 20 mL of 4% PFA, pH 7 – 7.5

Note: *Store 1X PBS and 4% PFA solutions into the fridge (4^0C) or in an ice tank until ready to begin the perfusion.*

Note: *Check and confirm the pH of the PFA (~ 7.4) before the start of the experiment.*

iii. 100 ml of CUPIC-P solution(Tainaka et al., 2018)

Note: *Before the experiment, degas the CUBIC-P reagent with a vacuum desiccator for ~30 min at ~0.1 MPa and stored at RT*(Susaki et al., 2015)*.*

iv. 5 ml of CUBIC-L

Note: *CUBIC-L was used to start the delipidation step directly after the extraction of the brain without 4% PFA post-fixation.*

6.2.2.3. Animal sacrifice and brain collection

i. Prepare 3x the normal dose of anesthetic cocktail (Ketamine/Xylazine/Acepromazine) based on the age, the sex, and the weight of the animal (Mouse anesthesia, see the bibliography)

Note: *Anesthetic cocktail dose* (Mouse anesthesia, see the bibliography)*: 1 ml of ketamine 100mg/kg, 0.5 ml of xylazine 10mg/kg, 0.3 ml of acepromazine 3mg/kg*

ii. Inject intraperitoneally
iii. After injection,
    a. Wait until the animal is adequately anesthetized.
    b. Test this by pinching the toes of the paws.
        - If the animal still twitches, wait longer before beginning the perfusion.
        - If the animal no longer twitches, they are ready to be perfused.
iv. Begin the perfusion with

Δ Critical step(Susaki et al., 2015) *Cooling of PBS and 4% (wt/vol) PFA on ice is important for successful perfusion. Muscle stiffness after perfusion is a good indicator of successful perfusion. Residual blood in the mouse brain increases autofluorescence, especially in the green-laser excitation. The pH value of PFA is also crucial for efficient clearing and lower autofluorescence. Over-fixation causes both lower clearing efficiency and autofluorescence.*

- PBS (at 3 mL/min(Susaki et al., 2015))

- Once the beaker containing 15 ml of PBS is nearly empty, pause the machine, and place the tube into the 4% PFA beaker.

- 4% PFA (at 3 mL/min)
  - Once the beaker containing 20 ml of PFA is almost empty, pause the machine and move the tube into the 1X PBS beaker.
- PBS (at 3 mL/min)
  - Once the beaker containing 15 ml of PBS is nearly empty, pause the machine, and place the tube into the CUBIC-P beaker.
- CUBIC-P (at 3 mL/min(Tainaka et al., 2018))
  - The transcardiac perfusion of 100 mL of CUBIC-P from the left ventricle was performed. At the end of the perfusion, pause the machine.

v. Then, remove the needle from the animal's heart and place that end of the tube in the sink.

vi. Move the other end of the tube into a beaker of DW.
  - Run the machine with DW through the tubes to rinse it.

vii. Carefully remove the brain from the skull of the animal.

viii. Transfer the extracted brain directly into the 5ml of CUBIC-L solution(Gómez-Gaviro et al., 2017; Tainaka et al., 2018).

ix. After brain extraction, place the brain on a grid paper and align it (parallel) to the respective markings. Then, take photos of the whole brain with and without PBS solution.

6.2.3. Rat: <u>Perfusion using 1X PBS and 4% PFA Solutions</u>

6.2.3.1. Details to be noted down before perfusion:

i. Experiment started on : __ __ __ __/ __ __ __ / __ __ (yyyy/mmm/dd)
ii. Rat Cage Number :
iii. Date of birth : __ __ __ __/ __ __ __ / __ __ (yyyy/mmm/dd)
iv. Sex (M/F) : _____
v. Age : _____ Months, ____ Days
vi. Weight : ___ g

6.2.3.2. Experimental Solution Preparation:

i. 150 mL of 1X PBS, pH 7.4
ii. 150 mL of 4% PFA, pH 7 – 7.5

Note: *Store 1X PBS and 4% PFA solutions into the fridge (4^0C) or in an ice tank until ready to begin the perfusion.*

iii. 45 ml of 4% PFA (to hold brain after extraction)

6.2.3.3. Animal sacrifice and brain collection

i. Prepare 3x the normal dose of anesthetic cocktail (Ketamine/Xylazine/Acepromazine) based on the age, the sex, and the weight of the animal

Note: *Anesthetic cocktail dose* (Rat anesthesia, see the bibliography)*: 1 ml of ketamine 100mg/kg, 0.5 ml of xylazine 10mg/kg, 0.3 ml of acepromazine 3mg/kg*

ii. Inject intraperitoneally

iii. After injection,

a. Wait until the animal is adequately anesthetized.

b. Test this by pinching the toes of the paws.

- If the animal still twitches, wait longer before beginning the perfusion.
- If the animal no longer twitches, they are ready to be perfused.

iv. Begin the perfusion with

Δ Critical step *Cooling of PBS and 4% (wt/vol) PFA on ice is important for successful perfusion. Muscle stiffness after perfusion is a good indicator of successful perfusion. Residual blood in the mouse brain increases autofluorescence, especially in the green-laser excitation. The pH value of PFA is also crucial for efficient clearing and lower autofluorescence. Over-fixation causes both lower clearing efficiency and autofluorescence.*

- PBS (at 15 mL/min)
  - Once the beaker containing 150 ml of PBS is nearly empty, pause the machine, and place the tube into the 4% PFA beaker.
- 4% PFA (at 15 mL/min)
  - Once the beaker containing 150 ml of PFA is almost empty, pause the machine.

v. Then, remove the needle from the animal's heart and place that end of the tube in the sink.

vi. Move the other end of the tube into a beaker of DW.

- Run the machine with water through the tubes to rinse it.

vii. Carefully remove the brain from the skull of the animal.

viii. Transfer the brain into the 4% PFA in 1X PBS and store it in an ice tank.

ix. After brain extraction, place the brain on a grid paper and align it (parallel) to the respective markings. Then, take photos of the whole brain with and without PBS solution. Refer to the below images which spot the brain slab without and with 1X PBS respectively (**Figure 48**).

6.2.3.4. Brain Fixation and PBS washing

i. Incubate the brain in 4% PFA at 4^0C for 24 hours.

Note: Use the pipette to remove PFA and discard it into the PFA waste bottle.

ii. Rinse the brain using PBS for 24 hours.

iii. After 24 hours, the brain is ready to begin the experiment.

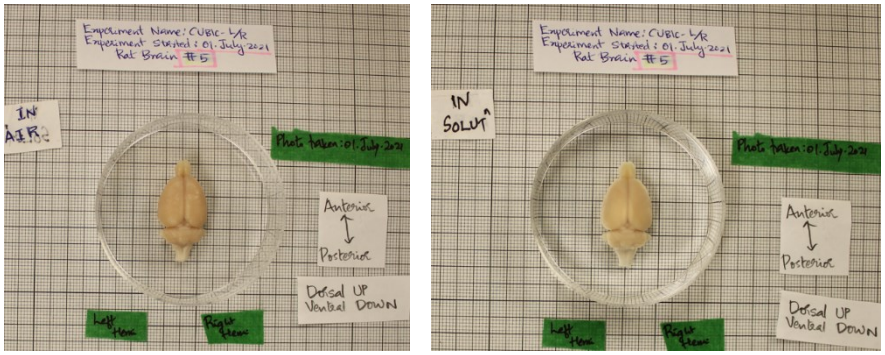

Figure 48: The placing of the rat brain without PBS (Right) and with PBS solution (Left) while taking photos was demonstrated.

6.3 CUBIC Tissue Clearing Protocol

6.3.1. Using 'CUBIC – L' and 'CUBIC – R' protocol

6.3.1.1. Experimental Precautions:

1. The experiment must perform under the fume hood.
2. As N-butyldiethanolamine is known to cause skin corrosion and serious eye damage, always wear double gloves and tightly fitting safety goggles. Always wear a lab coat.
3. As N-butyldiethanolamine is known to cause corrosion to metals, use only plastic or glass vessels.
4. While performing the experiment, the experimenter must spread 'the disposable incontinence blue pads' in the fume hood to prevent contamination due to the spillage.
5. At the end of the experiment, deposit the used blue pads into a yellow box specified for hazardous waste for the final disposal.

6.3.1.2. Pre-treatment with 50 % CUBIC-L:

6. Recommended to prepare 50 % CUBIC-L just before the experiment. If prepare it beforehand, store it at RT, and never store it at 4^0C as it will form crystals.
7. Incubate each brain slab of thickness 2- or 3-mm in 5 ml of 50 % CUBIC-L for 24 hours on a shaker at RT.
8. Next day, take a photo of the brain slabs using the same 50 % CUBIC-L and make sure the camera is parallel to the table and to align the grid so that it is parallel to the camera.

   Note: *Place the brain on the grid and make sure it is aligned (parallel) to the grid. Mark anterior and posterior of the brain with essential experiment details.*
9. Use a pasteur pipette to get all the solution out of the jar.

6.3.1.3. Treatment with CUBIC-L: Delipidation Step

10. Transfer each brain slab into 5 ml of CUBIC-L solution.

11. Incubate the brain slabs at RT with gentle shaking (40 rpm).
12. Then, refresh the CUBIC-L solution every three consecutive days until the brain slabs become completely transparent. This indicates the delipidation is completed.

    Note: *The number of days required to complete the delipidation varies for 2- or 3-mm thick slabs from anterior to posterior of the brain. For instance, the first slab from the anterior of the brain may be cleared within 4 – 12 days. But for other brain slabs towards the posterior, the period of incubation for delipidation may get extended. Thus, if the white matter is not transparent enough after the 12th day of the delipidation step, then extend the period of delipidation incubation furthermore*(Susaki et al., 2015)*. Check each brain slab every third day, then decide whether to continue the same step or not. The duration taken for delipidation is correlated to the sex, and age of the experimental animal.*
13. Take a photo of the brain slabs every 3rd day using the same CUBIC-L solution and make sure that the camera is parallel to the table and to align the grid so that it is parallel to the camera.

    Note: *Place the brain on the grid and make sure it is aligned (parallel) to the grid. Mark anterior and posterior of the brain with essential experiment details.*
14. Use a pasteur pipette to get all the solution out of the jar.

6.3.1.4. Washing Step (Total 1 day):

15. Once the delipidation is completed, rinse each brain slab in 45 ml of 1X PBS for 15 min with gentle shaking (40 rpm) at RT.
16. Repeat the previous step 7 more times (~ 1.45 hours), using new PBS each time. Use a pasteur pipette to get all the solution out of the jar.
17. Lastly, refresh the PBS (45 ml) and incubate each brain slab for the remaining 22 hours with gentle shaking (40 rpm) at RT.
18. Next day, initially take the photo of the brain slab without the solution, then take the second photo with the 1X PBS solution.
    - If the brain slab moves, re-adjust the position using the plastic forceps. Use the camera lens and zoom in if it is hard to see the edges of the brain.
      - ***Note:*** *To re-adjust the position of the brain slab, use only plastic forceps as N-butyldiethanolamine is corrosive to metals and also, the brain slabs are getting more fragile and softer in texture as it is progressing in delipidation*(Susaki et al., 2015)*.*
    - Make sure that the camera is parallel to the table and to align the grid so that it is parallel to the camera.
      - ***Note:*** *Place the brain on the grid and make sure it is aligned (parallel) to the grid. Mark anterior and posterior of the brain with essential experiment details.*

Δ Critical step *Complete removal of CUBIC-L during the washing step is crucial for final clearing efficiency*(Susaki et al., 2015)*. The absence of soapy bubbles means the removal of CUBIC-L is complete. Thus, the sample is ready for the next step.*

6.3.1.5a. Immunohistochemistry:

19. Primary antibody incubation: Incubate the cleared 2-3 mm thick brain samples for 2-3 days in primary antibody solution at 40C with gentle shaking. For the MAP2 antibody, we had checked two dilutions of (1:350) and (1:500) to optimize the best dilution for 3-mm thick mice brain samples.
20. Washing step (2 hrs/mm tissue thickness): Rinse the primary antibody labeled sample in 20ml of 1X PBST for 6 hr with gentle shaking (40 rpm) at RT where refresh the 1X PBST every hour. After this, incubate the brain slabs at RT overnight with refreshed 1X PBS.
21. Secondary antibody incubation: On the next day, incubate the washed brain slabs for 2-3 days in secondary antibody solution at RT with gentle shaking. In the secondary antibody solution, we had used (1:300) dilution of Alex Fluorophore 488.

    Note: *Since Alex Fluorophore 488 is light sensitive, wrapped aluminum foil around the jars to ensure that the brain slabs are properly shielded from light duration incubation in RT.*
22. Washing step (2 hrs/mm tissue thickness): Rinse the secondary antibody labeled sample in 20ml of 1X PBST for 6 hr with gentle shaking (40 rpm) at RT where refresh the 1X PBST every hour. After this, incubate the brain slabs at RT overnight with refreshed 1X PBS.
23. Counter nuclear staining: After the completion of the IHC, the thoroughly washed 2-3 mm thick brain slab was stained again with fluorescent nuclear staining dye for 3 days with gentle shaking in RT under dark. This counterstaining is performed using NeuroTrace™ 530/615 red fluorescent Nissl stain at (1:50) dilution(Yang et al., 2014).
24. Washing step: The counter-stained brain slab was washed for 6 hr in 1X PBS with gentle shaking in RT. Refresh the 1X PBS every 1 hour. The slab containing the jar was covered with aluminum foil to protect the dyes from light exposure. Repeat this step two more times. After this, incubate the brain slabs at RT overnight with refreshed 1X PBS.

6.3.1.5b. Counter Nuclear Staining:

25. After the washing step, the 2-3 mm thick one hemisphere brain slab(s) was stained by NeuroTrace™ 530/615 Red Fluorescent Nissl Stain for 2-3 days.
    - **E.g:** To prepare (1:50) dilution, use 30 µl Nissl Stain from the stock and is then mixed with 1470 µl of 1X PBS solution. This 1500 µl total volume is good for 3-mm thick one hemisphere brain slab.
    - Similarly, for the coronal 3-mm thick slab, a total of 3000 µl is required for that 60 µl Nissl stain from the stock have thoroughly mixed with 2940 µl of 1X PBS solution.
26. Then, incubate the brain slab at RT with gentle shaking (40 rpm).

Note: *Since NeuroTrace™ 530/615 Red Fluorescence Nissl Stain is light sensitive, wrap aluminum foil around the jars to ensure that the brain slabs are properly shielded from light.*

Note: *Careful handling is required after the delipidation step as the brain slabs are fragile in nature*.

27. Use a pasteur pipette to get all the solution out of the jar.

6.3.1.6. Washing Step (Total 1 day):

28. After the Nissl staining step, rinse the brain slabs in 1X PBS for 15 min with gentle shaking at RT (Brochure_LL060, see the bibliography; Susaki et al., 2015).

    Note: *Cover the sample with aluminum foil to protect it from the light.*

29. Repeat 'step f' for 7 more times (~ 1.45 hours), using new PBS each time. Use a pasteur pipette to get all the solution out of the jar.
30. Lastly, refresh the PBS (45 ml) and incubate the brain slabs for the remaining 22 hours with gentle shaking (40 rpm) at RT.
31. On the next day, take a photo of the brain slab using the new PBS solution and make sure that the camera is parallel to the table and align the grid so that it is parallel to the camera.

    Note: *Place the brain slab on the grid and make sure it is aligned (parallel) to the grid. Mark anterior and posterior of the brain slab with essential experiment details.*

32. Use a pasteur pipette to get all the solutions out.

6.3.1.7. Pre-treatment with 50 % CUBIC-R+ and degassing(Susaki et al., 2015) of the sample:

33. Recommended to prepare 50 % CUBIC-R just before the experiment. If prepare beforehand, store at RT and never stored at 4^0C as it will form crystals.
34. Incubate each brain slabs of thickness 2- or 3-mm in 2 ml of 50 % CUBIC-R for 24 hours with gentle shaking at RT.

    Note: *Cover the sample with aluminum foil to protect it from the light.*

    Note: *Since the delipidated brains are fragile, careful handling is required.*

    Note: *Place brain on the grid and make sure it is aligned (parallel) to the grid. Mark anterior and posterior of the brain slab with essential experiment details.*

35. Optional step: Using a vacuum desiccator or any degassing apparatus, degas the sample with a minimum volume of 50% CUBIC-R+.
    i. Take 5 ml of 50% CUBIC-R in a 50 ml conical tube and transfer the sample.
    ii. After connecting to the degassing apparatus, wait for 16 – 24 hours
    iii. Check whether the sample sinks to the bottom

    Note: *If the sample sinks, stop the degassing step. This is a sign of complete immersion. Please closely watch the sample while degassing.*

6.3.1.8. Treatment with CUBIC-R+: RI matching

36. After 24 hours with 50% CUBIC-R+ incubation, transfer each brain into 2 ml of CUBIC-R+.
37. Incubate at RT for 1 day with gentle shaking.

38. On the next day, refresh CUBIC-R+ and continue incubation for another 24 hours with gentle shaking at RT. Now, the sample is ready for microscopic imaging sessions.
39. Take the photo of the brain slab using the same CUBIC-R+ solution and make sure that the camera is parallel to the table and align the grid so that it is parallel to the camera.

Note: *Place the brain slab on the grid and make sure it is aligned (parallel) to the grid. Mark anterior and posterior of the brain slab with essential experiment details.*

• ***Pause Point*** *The brain slabs can be left in CUBIC-R+ for up to 1 week at RT. Further immersion increases the final transparency, but it also causes swelling of the sample. After imaging, the sample can be washed with PBS/0.01% (wt/vol) sodium azide, completely immersed in 30% (wt/vol) sucrose in PBS/0.01% (wt/vol) sodium azide and stored in O.C.T. compound at −80 °C. To continue the imaging, thaw the samples gradually at RT and wash them with PBS at least twice, with each wash for 1 h, to remove sucrose and O.C.T. compound. The sample will now be ready for the imaging.*

6.3.2. Using 'CUBIC-P', 'CUBIC – L' and 'CUBIC – R' protocol

6.3.2.1. Experimental Precautions:

1. The experiment must perform under the fume hood.
2. As N-butyldiethanolamine is known to cause skin corrosion (https://www.sigmaaldrich.com/CA/en/sds/aldrich/471240) and serious eye damage, always wear double gloves and tightly fitting safety goggles. Always wear a lab coat.
3. As N-butyldiethanolamine is known to cause corrosion to metals, use only plastic or glass vessels.
4. While performing the experiment, the experimenter must spread 'the disposable incontinence blue pads' in the fume hood to prevent contamination due to the spillage.
5. At the end of the experiment, deposit the used blue pads into a yellow box specified for hazardous waste for the final disposal.

6.3.2.2. Treatment with CUBIC-L: <u>Delipidation Step</u>

6. After the extraction of the brain, directly transfer each brain slab into 5 ml of CUBIC-L solution without any 4% PFA post-fixation step(Tainaka et al., 2018).
7. Incubate the brain slabs at RT with gentle shaking (40 rpm).
8. Then, refresh the CUBIC-L solution every three consecutive days until the brain slabs become completely transparent. This indicates the delipidation is completed.

Note: *The number of days required to complete the delipidation varies for 2- or 3-mm thick slabs from anterior to posterior of the brain. For instance, the first slab from the anterior of the brain may be cleared within 4 – 12 days. But for other brain slabs towards the posterior, the period of incubation for delipidation may get extended. Thus, if the white matter is not transparent enough after the 12th day of the delipidation step, then extend*

the period of delipidation incubation furthermore(Susaki et al., 2015). *Check each brain slab every third day, then decide whether to continue the same step or not. The duration taken for delipidation is correlated to the sex, and age of the experimental animal.*

9. Take photos of the brain slabs every 3rd day using the same CUBIC-L solution and make sure that the camera is parallel to the table and to align the grid so that it is parallel to the camera.

   Note: *Place the brain on the grid and make sure it is aligned (parallel) to the grid. Mark anterior and posterior of the brain with essential experiment details.*

10. Use a pasteur pipette to remove solutions from the jar.

6.3.2.3. Washing Step (Total 1 day):

11. Once the delipidation is completed, rinse each brain slab in 45 ml of 1X PBS for 15 min with gentle shaking (40 rpm) at RT (Brochure_LL060, see the bibliography; Susaki et al., 2015).
12. Repeat the previous step 7 more times (~ 1.45 hours), using new PBS each time. Use a pasteur pipette to get all the solution out of the jar.
13. Lastly, refresh the PBS (45 ml) and incubate each brain slab for the remaining 22 hours with gentle shaking (40 rpm) at RT.
14. Next day, take photos of the brain slabs with and without 1X PBS solution.
    - If the brain slab moves, re-adjust the position using the plastic forceps. Use the camera lens and zoom in if it is hard to see the edges of the brain.
      - ***Note:*** *To re-adjust the position of the brain slab, use only plastic forceps as N-butyldiethanolamine is corrosive to metals and also, the brain slabs are getting more fragile and soft texture as it is progressing in delipidation*(Susaki et al., 2015).
    - Make sure that the camera is parallel to the table and to align the grid so that it is parallel to the camera.
      - ***Note:*** *Place the brain on the grid and make sure it is aligned (parallel) to the grid. Mark anterior and posterior of the brain with essential experiment details.*

Δ CRITICAL STEP *Complete removal of CUBIC-L during the washing step is crucial for final clearing efficiency. The absence of soapy bubbles means the removal of CUBIC-L is complete. Thus, the sample is ready for the next step.*

6.3.2.4a. Immunohistochemistry:

15. **Primary antibody incubation**: Incubate the cleared 2-3 mm thick brain samples for 2-3 days in primary antibody solution at 4^0C with gentle shaking. For the MAP2 antibody, we had checked two dilutions of (1:350) and (1:500) to optimize the best dilution for 3-mm thick mice brain samples.
16. **Washing step** (2 hrs/mm tissue thickness): Rinse the primary antibody labeled sample in 20ml of 1X PBST for 6 hr with gentle shaking (40 rpm) at RT where refresh the 1X PBST every hour. After this, incubate the brain slabs at RT overnight with refreshed 1X PBS.
17. **Secondary antibody incubation**: On the next day, incubate the washed brain slabs for 2-3 days in secondary antibody solution at RT with gentle shaking. In the secondary antibody solution, we had used (1:300) dilution of Alex Fluorophore 488.

    Note: *Since Alex Fluorophore 488 is light sensitive, wrapped aluminum foil around the jars to ensure that the brain slabs are properly shielded from light duration incubation in RT.*
18. **Washing step** (2 hrs/mm tissue thickness): Rinse the secondary antibody labeled sample in 20ml of 1X PBST for 6 hr with gentle shaking (40 rpm) at RT where refresh the 1X PBST every hour. After this, incubate the brain slabs at RT overnight with refreshed 1X PBS.
19. **Counter nuclear staining:** After the completion of the IHC, the thoroughly washed 2-3 mm thick brain slab was stained again with fluorescent nuclear staining dye for 3 days with gentle shaking in RT under dark. This counterstaining is performed using NeuroTrace™ 530/615 red fluorescent Nissl stain at (1:50) dilution(Yang et al., 2014).
20. **Washing step**: The counter-stained brain slab was washed for 6 hr in 1X PBS with gentle shaking in RT. Refresh the 1X PBS every 1 hour. The slab containing the jar was covered with aluminum foil to protect the dyes from light exposure. Repeat this step two more times. After this, incubate the brain slabs at RT overnight with refreshed 1X PBS.

6.3.2.4b. Counter nuclear staining:

21. After the washing step, the 2-3 mm thick one hemisphere brain slab(s) was stained by NeuroTrace™ 530/615 Red Fluorescent Nissl Stain for 2-3 days.
    - **E.g:** To prepare (1:50) dilution, use 30 µl Nissl Stain from the stock and is then mixed with 1470 µl of 1X PBS solution. This 1500 µl total volume is good for 3-mm thick one hemisphere brain slab.
    - Similarly, for the coronal 3-mm thick slab, a total of 3000 µl is required whereas 60 µl Nissl stain from the stock have thoroughly mixed with 2940 µl of 1X PBS solution.
22. Then, incubate the brain slab at RT with gentle shaking (40 rpm).

    Note: *Since NeuroTrace™ 530/615 Red Fluorescence Nissl Stain is light sensitive, wrap aluminum foil around the jars to ensure that the brain slabs are properly shielded from light.*

    Note: *Careful handling is required after the delipidation step as the brain slabs are fragile in nature*.

23. Use a pasteur pipette to remove all solutions from the jar.

6.3.2.5. Washing Step (Total 1 day):

24. After the Nissl staining step, rinse the brain slabs in 1X PBS for 15 min with gentle shaking at RT.

    Note: *Cover the sample with aluminum foil to protect it from the light.*

25. Repeat 'step f' for 7 more times (~ 1.45 hours), using new PBS each time. Use a pasteur pipette to get all the solution out of the jar.
26. Lastly, refresh the PBS (45 ml) and incubate the brain slabs for the remaining 22 hours with gentle shaking (40 rpm) at RT.
27. On the next day, take photos of the brain slab using the new PBS solution and make sure that the camera is parallel to the table and to align the grid so that it is parallel to the camera.

    Note: *Place the brain slab on the grid and make sure it is aligned (parallel) to the grid. Mark anterior and posterior of the brain slab with essential experiment details.*

28. Use a pasteur pipette to get all the solutions out.

6.3.2.6. Pre-treatment with 50 % CUBIC-R+ (Tainaka et al., 2018) and degassing (Susaki et al., 2015) of the sample:

29. Recommended to prepare 50 % CUBIC-R just before the experiment. If prepare beforehand, store at RT and never stored at 40C as it will form crystals.
30. Incubate each brain slabs of thickness 2- or 3-mm in 2 ml of 50 % CUBIC-R for 24 hours with gentle shaking at RT.

    Note: *Cover the sample with aluminum foil to protect it from the light.*

    Note: *Since the delipidated brains are fragile, careful handling is required.*

    Note: *Place brain on the grid and make sure it is aligned (parallel) to the grid. Mark anterior and posterior of the brain slab with essential experiment details.*

31. Optional step: Using a vacuum desiccator or any degassing apparatus, degas the sample with a minimum volume of 50% CUBIC-R+.
    i. Take 5 ml of 50% CUBIC-R in a 50 ml conical tube and transfer the sample.
    ii. After connecting to the degassing apparatus, wait for 16 – 24 hours
    iii. Check whether the sample sinks to the bottom

    Note: *If the sample sinks, stop the degassing step. This is a sign of complete immersion. Please closely watch the sample while degassing.*

6.3.2.7. Treatment with CUBIC-R+: RI matching

32. After 24 hours with 50% CUBIC-R+ incubation, transfer each brain into 2 ml of CUBIC-R+.
33. Incubate at RT for 1 day with gentle shaking.

34. On the next day, refresh CUBIC-R+ and continue incubation for another 24 hours with gentle shaking at RT. Now, the sample is ready for microscopic imaging sessions.

Figure 49. Home-screen of X-CLARITY polymerization system. (Image courtesy of (Logos VX1901-01, see the bibliography))

35. Take the photo of the brain slab using the same CUBIC-R+ solution and make sure that the camera is parallel to the table and align the grid so that it is parallel to the camera.
    Note: *Place the brain slab on the grid and make sure it is aligned (parallel) to the grid. Mark anterior and posterior of the brain slab with essential experiment details.*

6.4. X-CLARITY Tissue Clearing Protocol

6.4.1.Hydrogel infusion and Polymerization

1) Add one part 25% (w/v) X-CLARITY polymerization Initiator to 100 parts X-CLARITY Hydrogel Solution. Mix thoroughly.
   Note: X-CLARITY polymerization Initiator (VA-044) can be stored at -20^{0}C and X-CLARITY Hydrogel Solution at 4^{0}C
2) Incubate the sample (for e.g., the whole brain or the sliced sectioned) in hydrogel-initiator solution at 4^{0}C for 24 hours. Use enough solution to submerge samples

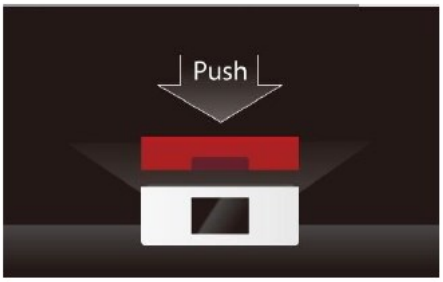

Figure 50. Activation of vacuum in polymerization system. Push on the lid by hand until it vanished (Image courtesy of (Logos VX1901-01, see the bibliography))

3) **Polymerization System Setup**: Once the polymerization system is switched ON, set the parameters on the touch screen as shown in **Figure 50.**
4) **Sample loading & starting a RUN**: Open the cover of the system, place the 50 ml conical tube having submerged samples with loosened caps in the appropriate heat blocks and then, close the lid.

Figure 51. Polymerization completed status displayed.
(Image courtesy of (Logos VX1901-01, see the bibliography)

5) Press the RUN on the touch home-screen of the polymerization system. Thus, **Figure 51** appeared on the home-screen indicating the activation of the vacuum pump initiated. After generating a seal between the lid and the chamber, **Figure 6.4.1.b** disappears.
6) After 3 hours, the initiated polymerization end with a beep sound, and it is displayed on the home-screen as shown in **Figure 6.4.1.c**. After 5 minutes, the system released the vacuum seal.
7) Then, open the lid and observe the sticky nature of (hydrogel: initiator) solution over the sample.
8) Shake samples gently for 1 minute after polymerization.
9) **Reservoir, Pump, and Electrophoretic Chamber Set up:** While polymerization reaction happens, wash reservoir with DW for half an hour.
10) Check the connection: Reservoir → Pump → Electrophoretic Chamber → back to the reservoir
11) Fill the reservoir with 600 ml of DW and start pumping into the 'electrophoretic chamber' by selecting CCW (to fill the chamber), then press the 'start/stop' button.
12) After half an hour washing step, stop the pump and drain the electrophoretic chamber' by selecting CW (to drain the chamber) on the pump, then press the 'start/stop' button.
13) Remove any traces of DW from the chamber using a pasteur pipette.
14) Replace the reservoir with 800 ml of clearing buffer which is the reliable volume for 4 hours of tissue clearing for one mouse whole brain or for 2-3 mm thick-sliced mouse brain slabs.

15) Then, half of the electrophoretic chamber fills with the buffer.
16) Before transferring into the electrophoretic chamber, wash the polymerized sample initially with 3 ml of DW for 1 min. Repeat this for 3 times. Then, washed the sample using 20 ml of 1X PBS 3 times with gentle manual shaking at RT to remove excess hydrogel.

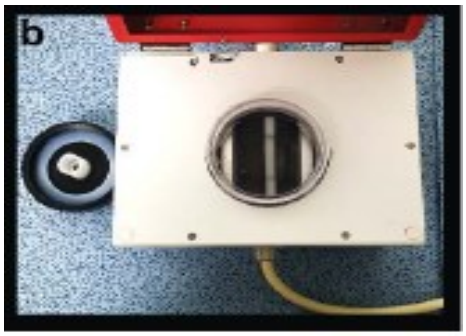

Figure 52. An image of ETC chamber (Image courtesy of (Logos VX1901-01, see the bibliography)

17) **Tissue clearing**: Transfer the washed polymerized samples into the sample holder and then, keep the tissue container in the ETC chamber as shown in Figure 3.
18) By starting the pump, the ETC chamber is filled with a clearing solution (100 ml).
19) After observing the dripping of clearing buffer back into the reservoir, press the RUN/STOP button on ETC Controller

Note: While re-using the clearing buffer (example: for 3rd time), check the pH. If it is showed a pH of 8.5, then good for re-use.

20) ETC controller needs to set up where current is at 1.5 A (is ideal for mouse brain), temperature at 37^{0}C, pumping rate at 30 – 50 rpm, duration from 4 to 6 hrs (would vary upon the age of the mice). Then, start the tissue-clearing step.
Note: If a new sample is cleared for the first time, check the delipidation progression of the sample on every 2 (for 2-mm thick slabs) or 3 (3-mm thick slabs) hours which is essential step to estimate the time required for clearing to be completed.

21) **Washing Step:** After the tissue clearing completion, rinse the X-CLARITY cleared sample in 50ml of 1X PBS for 2.5 hr with gentle shaking (40 rpm) at RT. Repeat this step 2 or more times, using new PBS each time.
Note: During PBS washing step, the transparency of the tissue will be lost. But it will regain after it is incubated in RIMS.
Note: Make sure the complete removal of SDS, i.e., To check this, briefly shake the washed PBS solution without the sample and there is no soapy bubble formation. Now, the sample is ready to start following antibody labeling and/or the Nissl staining.

22) Lastly, refresh the 1X PBS and incubate overnight with gentle shaking (40 rpm) at RT. On the next day, take a photo of the cleared-whole/sliced section(s) of the brain with and without PBS and make sure that the camera is parallel to the table and to align the grid so that it is parallel to the camera.
23) **Immunohistochemistry: Primary antibody incubation**: Incubate the cleared 3-mm thick brain samples for 3 days in primary antibody solution at 4^0C with gentle shaking. For the MAP2 antibody, we had checked two dilutions of (1:350) and (1:500) to optimize the best dilution for 3-mm thick mice brain samples.
24) **Immunohistochemistry: Washing step** (2 hrs/mm tissue thickness): Rinse the primary antibody labeled sample in 20ml of 1X PBST for 6 hr with gentle shaking (40 rpm) at RT where refresh the 1X PBST every hour. After this, incubate the brain slabs at RT overnight with refreshed 1X PBS.
25) **Immunohistochemistry: Secondary antibody incubation**: On the next day, incubate the washed brain slabs for 3 days in secondary antibody solution at RT with gentle shaking. In the secondary antibody solution, we had used (1:300) dilution of Alex Fluorophore 488.
    Note: Since Alex Fluorophore 488 is light sensitive, wrapped aluminum foil around the jars to ensure that the brain slabs are properly shielded from light duration incubation in RT.
26) **Immunohistochemistry: Washing step** (2 hrs/mm tissue thickness): Rinse the secondary antibody labeled sample in 20ml of 1X PBST for 6 hr with gentle shaking (40 rpm) at RT where refresh the 1X PBST every hour. After this, incubate the brain slabs at RT overnight with refreshed 1X PBS.
27) **Counter nuclear staining:** After the completion of the IHC, the thoroughly washed 3-mm thick brain slab was stained again with fluorescent nuclear staining dye for 3 days with gentle shaking in RT under dark. This counterstaining is performed using NeuroTrace™ 530/615 red fluorescent Nissl stain at (1:50) dilution (Yang et al., 2014).
28) **Counter nuclear staining**: **Washing step**: The counter-stained brain slab was washed for 6 hr in 1X PBS with gentle shaking in RT. Refresh the 1X PBS every 1 hour. The slab containing the jar was covered with aluminum foil to protect the dyes from light exposure. Repeat this step two more times. After this, incubate the brain slabs at RT overnight with refreshed 1X PBS.
29) **Refractive index matching step:** On the next day, incubate each brain slab in 2 ml of 50% RIMS for 24 hours at RT with gentle shaking. After 24 hours, refresh the slabs with 100% RIMS and then, incubate overnight or until the samples regain its complete transparency in dark with gentle shaking. Once the sample gained complete optical clearing, i.e., completely transparent, it is ready for imaging. Before taking for imaging, the RIMS must refresh without any air bubbles at least 24 hours before.
30) Only after imaging is completed, take the photo of brain slabs incubated in RIMS.